

Electronic Thesis and Dissertation Repository

---

8-23-2021 9:30 AM

## The Effects of Silver Nanoparticles on Soybean (Glycine max) Growth and Nodulation

Paul J. Boersma, *The University of Western Ontario*

Supervisor: Macfie, Sheila M., *The University of Western Ontario*

A thesis submitted in partial fulfillment of the requirements for the Master of Science degree in Biology

© Paul J. Boersma 2021

Follow this and additional works at: <https://ir.lib.uwo.ca/etd>



Part of the [Biology Commons](#)

---

### Recommended Citation

Boersma, Paul J., "The Effects of Silver Nanoparticles on Soybean (Glycine max) Growth and Nodulation" (2021). *Electronic Thesis and Dissertation Repository*. 8069.

<https://ir.lib.uwo.ca/etd/8069>

This Dissertation/Thesis is brought to you for free and open access by Scholarship@Western. It has been accepted for inclusion in Electronic Thesis and Dissertation Repository by an authorized administrator of Scholarship@Western. For more information, please contact [wlsadmin@uwo.ca](mailto:wlsadmin@uwo.ca).

## Abstract

Due to their antimicrobial properties, silver nanoparticles (AgNPs) have become popular in consumer and industrial products, leading to increasing concentrations in agricultural fields and other environments. Exposure to AgNPs could be detrimental to plants, microbes, and their symbiotic relationships. When subjected to 10 µg/mL AgNPs in a 96-well plate, growth of *Bradyrhizobium japonicum* USDA 110 was halted. In hydroponic culture with 2.5 µg/mL AgNPs, biomass of inoculated *Glycine max* (L.) Merr. was 50% of control. Axenic plants were unaffected by this dose with 30 nm AgNPs, but growth was inhibited with the same dose of 16 nm AgNPs, indicating that AgNPs inhibit both nodulation and growth. Nodules treated with 2.5 µg/mL AgNPs appeared absent of bacteroids, and plants given 0.5-2.5 µg/mL AgNPs had 40-65% decreased nitrogen fixation. In conclusion, I determined AgNPs not only interfere with plant-microbe relations but also with general plant and bacterial growth. As a consequence, we should be mindful of not releasing AgNPs to the environment and agricultural land.

## Keywords

AgNPs, silver nanoparticles, nanoparticles, soybeans, *Glycine max*, *Bradyrhizobium japonicum*, nodules, symbiosis, antimicrobial

## Summary for Lay Audience

It has been known for thousands of years that silver can kill bacteria. Hence, human use of silverware. In recent years, silver in the form of nanoparticles (very small particles, about 500 hundred thousand times smaller than a grain of salt) has gained popularity. These tiny particles possess properties different from bulk silver. One of these properties is a greater ability to kill bacteria. This enhanced ability comes from high surface area, small size, and increased release of toxic silver ions. As their popularity increases, we see more use of silver nanoparticles (AgNPs) in consumer products and industry. This includes their incorporation into clothes, soaps, and other materials. Through production, use, washing, and disposal, AgNPs are released into the environment. They first enter wastewater but are not fully removed at water treatment facilities. They enter agricultural soil when sludges (biosolids) are used as fertilizers. While crop fertilization is important, this addition of antimicrobial silver could lead to problems with plant-microbe relationships. Specifically, the soybean-nitrogen fixing bacteria relationship could be harmed. My goal was to determine the potential toxicity of AgNPs to soybean, its nitrogen-fixing bacterial partner *Bradyrhizobium japonicum*, and their symbiotic relationship. I found decreased mass of soybeans as the concentration of AgNPs increased. I also found that smaller AgNPs (16 nm average diameter) were more harmful to plants compared to larger AgNPs (30 nm average diameter). High concentrations of AgNPs also inhibited growth of the nitrogen-fixing bacteria. Nodules in the plant root are the 'house' in which bacteria fix nitrogen. Nodule mass and the amount of nitrogen fixed decreased with increasing concentrations of AgNPs. All these results point towards AgNPs harming the nitrogen-fixing relationship and reducing soybean crop yield. Using electron microscopy, I showed that AgNPs are taken up and transported throughout the plants; however, I found that AgNPs in soybean tissues could not be detected using Raman spectroscopy. In conclusion, AgNPs inhibited bacterial growth, plant growth, and development of functional nodules. As a consequence we need to be careful in our use of AgNPs and control or prevent their release into wastewater and their subsequent addition to agricultural fields.

## Co-Authorship Statement

Dr. Sheila M. Macfie and I will be co-authors of the manuscript that arises from this thesis. The experimental design was developed by both Dr. Macfie and me. While performing the experiment was mainly my job, Dr. Macfie provided input and training during the process. Analyzing the data was done mainly by myself with added input from Dr. Macfie. Interpretation of the data was done by both Dr. Macfie and me, while writing the manuscript will be done by mainly me with editing done by Dr. Macfie.

## Acknowledgments

Thanks to Dr. Krzysztof Szczyglowski, a research scientist at the London Research and Development Centre, Agriculture and Agri-Food Canada (AAFC) in London ON, for providing the *Bradyrhizobium japonicum* USDA 110 axenic cultures. Thanks to Dr. Kangfu Yu from the Science and Technology Branch, Harrow Research and Development Centre of AAFC for providing the soybeans seeds used in this project. Thanks to Elzbieta Myscich, a lab technician in Biology at the University of Western Ontario, for help with culturing and quantifying bacterial colonies. Thanks to PhD candidate Danielle McRae and Dr. François Lagurné-Labarthe (from the Lagurné-Labarthe Nanofab lab at the University of Western Ontario) for help with Raman spectroscopy. Thanks to Dr. Hobson, Department of Biology at the University of Western Ontario, for use of the microbalance. Thanks to Reza Khazaei and Dr. Richard Gardiner (both from the Biotron Integrated Microscopy Facility at the University of Western Ontario) for help with sample preparation and collection of transmission electron microscope images. Also, a large thanks to my supervisor for the endless help she provided with this thesis, including data interpretation, edits, training and many more aspects.

# Table of Contents

Abstract.....	ii
Summary for Lay Audience.....	iii
Co-Authorship Statement.....	iv
Acknowledgments.....	v
Table of Contents.....	vi
List of Figures.....	x
List of Appendices.....	xi
1 Introduction to Nanoparticles.....	1
1.1 Nanoparticles in Consumer Products.....	2
1.2 Nanoparticles in Industry.....	3
1.2.1 Nanoparticles in Medicine.....	5
1.2.2 Nanoparticles in Plant Research and Environmental Remediation.....	6
1.2.3 Raman Spectroscopy and Silver Nanoparticles.....	6
1.3 Release of Silver Nanoparticles into the Environment.....	8
1.4 Silver Nanoparticles' Antimicrobial Effects.....	11
1.4.1 Antimicrobial Mechanisms.....	13
1.5 Silver Nanoparticles' Effects on Plant Growth.....	14
1.5.1 Movement of Silver Nanoparticles within Plants.....	15
1.5.2 Effects on Growth.....	16
1.6 Overview of Silver Nanoparticle-Specific Effects on Plant Cells.....	19
1.6.1 Oxidative Stress.....	19
1.6.2 Genotoxicity.....	20
1.7 Silver Nanoparticles' Effects on Plant and Bacterial Interactions: Emphasis on <i>Fabaceae-Bradyrhizobium</i> .....	21
1.8 Rationale and Objectives.....	23

1.8.1	Rationale .....	23
1.8.2	Objectives .....	24
2	Materials and Methods .....	24
2.1	Study Organisms .....	24
2.2	Experimental Treatments and Conditions .....	25
2.2.1	Synthesis, Preparation and Confirmation of Silver Nanoparticles .....	25
2.2.2	Concentration, Confirmation and Size of Silver Nanoparticles .....	26
2.2.3	Bacterial Growth .....	26
2.2.4	Hydroponic Setup and Soybean Growth Conditions .....	28
2.3	Raman Spectroscopy .....	30
2.4	Toxicity of Silver Nanoparticles to Bacterial Cultures .....	30
2.5	Uptake and Location of Silver Within Soybeans .....	31
2.5.1	Inductively Coupled Plasma Mass Spectrometry .....	31
2.5.2	Desorption of Plaque from Root Surface .....	31
2.5.3	Transmission Electron Microscopy .....	32
2.6	Toxicity of Silver Nanoparticles to Soybeans .....	33
2.6.1	Phytotoxicity to Soybean .....	33
2.6.2	Carbon and Nitrogen Analysis .....	34
2.7	Nodule Assessment .....	34
2.8	Data Analysis .....	35
3	Results and Discussion .....	35
3.1	Raman Measurements and Maps .....	35
3.2	Silver Nanoparticle Effects on <i>Bradyrhizobium japonicum</i> USDA 110 .....	44
3.3	Location of Silver Within Soybeans .....	44
3.4	Location of Silver Within Soybeans .....	46
3.5	Silver Nanoparticle Effects on the Mass and Health of Soybeans .....	52

3.6 Nodulation, Nitrogen Fixation and Bacteroid Health .....	58
3.7 Changes to Nitrogen and Carbon .....	64
4 Limitations, Future Directions and Conclusions.....	66
4.1 Limitations and Future Directions .....	66
4.2 Conclusions.....	68
References.....	70
Appendices.....	85
Curriculum Vitae .....	87



## List of Tables

Table 1.1: General uses of nanoparticles in consumer products*.....	4
Table 1.2: General uses of nanoparticles in industry.....	4
Table 2.1: Transmission electron microscope images showing nanoparticles used for testing.. .....	27
Table 2.2: Growth media. ....	28

# List of Figures

Figure 3.1: Raman spectroscopy of control soybean root cross section showing a xylem cell within the stele. .... 37

Figure 3.2: Raman spectrum associated with glass. .... 39

Figure 3.4 Growth of *Bradyrhizobium japonicum* USDA 110 in response to AgNPs. .... 45

Figure 3.5: Electron micrographs of root cross sections..... 49

Figure 3.6 Silver was taken up by and translocated within the plants..... 50

Figure 3.6 Silver was taken up by and translocated within the plants..... 51

Figure 3.6 Silver was taken up by and translocated within the plants..... 51

Figure 3.7 Dry biomass of roots, stems and leaves for inoculated and non-inoculated plants treated with AgNPs. .... 54

Figure 3.8: Top growth, total biomass for inoculated and non-inoculated plants given both 16 nm and 30 nm AgNPs, as well as the chlorophyll fluorescence and leaf area for plants subjected to 30 nm AgNPs..... 56

Figure 3.9: Total nodule biomass of inoculated plants given both 16 nm and 30 nm AgNPs, along with normalized nitrogen fixation and total fixation of nitrogen..... 59

Figure 3.10: TEM images of healthy and AgNP-treated nodules..... 63

Figure 3.11: Nitrogen and carbon percentages along with nitrogen total mass and carbon to nitrogen ratios. .... 65

## List of Appendices

Appendix A: Standard curve for <i>Bradyrhizobium japonicum</i> USDA 110 cell density.....	85
Appendix B: VISUAL MINTEQ model of availability of selected nutrients within the full-N solution.....	86

# 1 Introduction to Nanoparticles

It has been known for thousands of years that silver has antimicrobial properties, hence human use of silver in silverware. In recent years, silver, in the form of nanoparticles (AgNPs), has gained popularity, as these tiny particles possess properties different from their bulk counterpart. For example, they have enhanced antimicrobial activity, which is attributed to their high surface area, small size and increased release of toxic silver ions (reviewed in Kocak and Karasu, 2018). The increased popularity of AgNPs is manifest in a greater use of silver in consumer products and industry, typically through AgNP incorporation into clothes, soaps and other materials.

Nanotechnology is on the rise. As of 2018 the global market was an estimated US \$45-50 billion, and projected to increase by 13% per year between 2019 to 2025 (Global Nanotechnology Market, 2018). The market value of nanotechnology is predicted to rise above US \$125 billion by 2024 (Global Nanotechnology Market, 2018). This increased value will be paralleled by an increase in the numbers and types of nanoproducts and their uses. While the economic benefits of nanotechnology to numerous industries are many (see sections 1.1 and 1.2), the potential risks associated with the use of nanoparticles are less well understood. Through production, use, washing, and disposal, there is increased release of silver into the environment (Whiteley et al. 2013). Silver is not a targeted contaminant at wastewater treatment facilities, and it may inadvertently be added to agricultural fields through the use of sludge and biosolids as fertilizers. Trace amounts of silver in fertilizers applied to agricultural fields could lead to problems with crop production and plant-microbe relationships. In this thesis I will explore the phytotoxicity of AgNPs, both in terms of direct toxicity to a common crop plant and its symbiotic bacterium as well as indirect toxicity via disruption of the plant-microbe symbiosis.

There are many kinds of nanoparticles, ranging from ones made of metals, to plastics, organics, and more. A nanoparticle is anything within the 1- 100 nm range, and one nanometer is a millionth of a millimeter. Due to this extremely small size these

nanoparticles have similar physical characteristics, and theoretically should be able to enter pores of plant cells if they are small enough to do so. Yet this small size also means they have a small volume to surface area ratio, typically allowing them to be more reactive than their bulk counterpart. Although they have similarities, the various molecules or elements that nanoparticles are made of or attached to give rise to inherently different chemical properties, such as differences in reactivity, colour, and various other properties. The chemical differences mean they can be used in various applications.

## 1.1 Nanoparticles in Consumer Products

Silver nanoparticles are frequently incorporated into consumer products such as sportswear, bandages and cleaning products (Danish Ecological Consumer Council, 2021). As reviewed by Vance et al. (2015), AgNPs can be suspended in liquids (which can then be aerosolised), woven into solids, adhered to surfaces or aggregated, but the most common types of incorporation tend to be surface-bound and suspended AgNPs.

The Project on Emerging Nanotechnologies, Consumer Products Inventory (CPI) revealed a steady increase in the number of products containing nanoparticles by the early 2000's (Maynard and Michelson, 2005). There were just 54 listed products in 2005; this number rose to 1814 by 2013. Although the CPI has not been updated since 2014, other product inventories show the steady rise in AgNP-containing products continuing. For example, the Nanodatabase (a global inventory of nanoparticle-containing consumer products maintained by the Danish Ecological Council and Danish Consumer Council) catalogues a further increase from 1208 products in 2012, all the way to 5169 products by July 2021 (Danish Ecological Consumer Council, 2021).

The CPI has eight categories of consumer products that incorporate nanoparticles (the number of products in each category is in parentheses): children's goods (84), appliances (162), electronics and computers (261), food and beverage (228), automotive (584), home and garden (881) and health and fitness (3169). Health and fitness represent 61% of the products in the inventory, and includes products such as clothing, shampoos, and cosmetics. Home and garden is the next largest category at 17% of all products, and

includes products with nanoparticles added such as furnishings, cleaning materials, paints and more. This wide array of products probably does not cover the whole scope, and one can find examples of nanoparticle incorporation in other places.

Nanoparticles are most commonly used in consumer products to take advantage of their antimicrobial properties. Interestingly, even without antimicrobial abilities, titanium and titanium dioxide are the second most abundant nanoparticles behind silver (Danish Ecological Consumer Council, 2021). A great example of the wide variety of uses for titanium dioxide nanoparticles is their incorporation into food products, which has been cleared for use in Europe; these nanoparticles are typically added to products to improve colour (EPCD, 1994). Peters et al. (2014) found that 24 items out of 27 (including chewing gum, toothpaste, hard and soft candy, pastry and chocolate) contained titanium dioxide nanoparticles, with concentrations reaching as high as 5 mg/g in some chewing gum and toothpaste. As of April 2020, the Nanodatabase (<http://nanodb.dk/en/search-database/>) included 5169 products that likely contain nanoparticles with 3628 containing nanoparticles of unspecified or unknown composition; silver is in 552 (36%) of the other 1541 products, titanium/titanium dioxide is in 335 products (22%) and carbon nanotubes/carbon/carbon black are in third place being in 223 (15%) of nanoparticle-containing products.

## 1.2 Nanoparticles in Industry

Nanoparticles are added to products for a variety of reasons, which is reflected in the wide range of products containing nanoparticles. Tables 1.1 and 1.2 provide a general overview of nanoparticle uses. Nanoparticles are not only used in commercial products and at least eight industries but are also being tested for new purposes. Like most nanoparticles, silver at the nanoscale differs from its bulk form, and unique chemical and physical properties arise (Calderón-Jiménez et al. 2017).

Table 1.1: General uses of nanoparticles in consumer products\*.

<u>Action/Purpose of Nanoparticle</u>	<u>Main Types of Nanoparticles</u>	<u>Products</u>
Goods for Kids (antimicrobial)	Mainly AgNPs	toys, clothes, pacifiers, blankets, carriages, etc.
Protective Coatings	SiO <sub>2</sub> and TiO <sub>2</sub>	bike pedals/chain, tools, tape, etc.
Cosmetics	Ag, TiO <sub>2</sub> , ZnO SiO <sub>2</sub> & more	UV protection, molecular carriers for moisturizing etc.
Health and Fitness	Ag, Au, Mg, Ca, Cu & more	"Immune boosts", supplements, creams, shampoos, etc.
Electronics	Gallium nitride	hair driers, lights, processors, chargers, cameras, etc.
Home and Garden (antimicrobial)	Mainly AgNPs	wipes, sprays, pillows, washing machines, biocides, etc.
Automotive	Mainly SiO <sub>2</sub> & TiO <sub>2</sub>	polish, paints, wax, weather proofing, etc.

\*Information obtained from Vance et al. (2015) and the Nano database (Danish Ecological Consumer Council, 2021)

Table 1.2: General uses of nanoparticles in industry.

<u>Industry</u>	<u>Main Types of Nanoparticles</u>	<u>Purpose/Use</u>	<u>Reference</u>
Medical	AgNP, AuNP, FeO and more	cancer treatments, antifungal or antibacterial, drug delivery & more	Ruenraroengsak et al. (2019) Devi and Bhimba (2014) Lombardo et al. (2019)
Material Analysis	AgNP, AuNP and more	detection of substance through enhanced Raman signals (e.g., mold, aging of art, etc.)	Anghelone et al. (2015) Kozachuk et al. (2018)
Energy	SiNPs, FeS <sub>2</sub> and more	solar power, hydrogen generation, and likely many other uses	Wipperman et al. (2013) Callejas et al. (2014)
Other	Various nanoparticles	biotech, manufacturing, photonics and many more materials and items	Tartaj et al. (2005) Pulci et al. (2018) Hamad et al. (2013)

Silver nanoparticles have various uses, and a number of their properties can be exploited. The colour of AgNPs can change based on their shape, carrier solvent, size, and concentration (González et al. 2014). This trait can be harnessed for various optical uses

and analyses. These changes in colour are mainly due to plasmon resonance, which occurs due to the resonance of electrons on the surface of a noble metal. The electromagnetic and conductive properties of nanoparticles act to enhance the signals that are generated the surrounding bonds, which is further explained in section 1.2.3.

Plasmon resonance is unique to the noble metals, and each metal has unique features. In addition to affecting colour, plasmon resonance can be employed in technology (section 1.2.1), diagnostics for healthcare (section 1.2.2), and plant research (section 1.2.3).

The technology, electronics, and computer industry fields have advanced due to discoveries of nanoparticle use. As reviewed in Velavan and Myvizhi (2015), the use of various shapes of nanoparticles has the potential to help us create smaller computer components therefore boosting memory per unit area of the processor, leading to overall increases in processing speeds, memory, and other valuable technological features.

### 1.2.1 Nanoparticles in Medicine

Nanoparticles and on-going development of nanoparticle-involved technologies are being used or investigated for drug delivery and medicinal treatments. For example, gold nanostars (star-shaped gold nanoparticles), which are coated with zinc oxide nanoparticles (ZnOPs) in pores of a macroporous silica nanolayer conjugated with an antibody, have the potential to kill drug-resistant lines of cancer cells (Ruenraroengsak et al. 2019). The nanocompound enters the cancer cell due to conjugation with an antibody, and once inside the cell the porous layer then releases ZnONPs. Cell viability decreased by up to 85% in known drug-resistant lines treated with gold nanostars (Ruenraroengsak et al. 2019).

Nanoparticles offer more than just drug delivery or disease treatments but also diagnostics for pharmacological and other fields of research. For example, nanoparticles can be combined to create label-free biosensors as shown by Ryu et al. (2010), who used silicon nanowire coated with gold nanoparticles hybridized to a probe specific to breast cancer. Detection of the electrical flow in their nanowire allowed for detection of a complimentary DNA sequence specific to cancer cells that is typically found at concentrations around one picomole.



## 1.2.2 Nanoparticles in Plant Research and Environmental Remediation

Nanotechnology is also being developed for agricultural purposes. The use of silica-silver nanoparticles as an anti-fungal treatment was tested by Park et al. (2006), whose study showed success against powdery mildew when the nanoparticles were sprayed at moderately low concentrations on green squash plants. With the use of magnets, González-Melendi et al. (2008) showed that ferromagnetic nanoparticles moved through plant vascular systems to the location of the magnet. Development of these types of applications could mean the ability to conjugate pesticides, drugs or other materials onto the surface of nanoparticles to target specific tissues by ferromagnetic forces, which could possibly be introduced into fields such as agriculture, medicine and biology. Similar to using nanoparticles for drug delivery, incorporation of nitrogen, phosphorus and potassium in chitosan (a chitin polymer, either partially or fully deacetylated) nanoparticles is a viable option for slow-release fertilizers (Corradini et al. 2010).

Another interesting use of magnetic nanoparticles comes in the field of environmental remediation. Calí et al. (2018) used ferromagnetic nanoparticles with a phosphate-based coating that has a high affinity to bind uranium to its surface; then, with the use of magnets and attraction of the ferromagnetic nanoparticles, they removed uranium (bound to the nanoparticles) from contaminated water at a rate that was almost double (2333 mg U/g Fe) of the next highest (1250 mg U/g Fe) previously reported method. Adsorption properties of charged nanoparticles can also be utilized in filtration for treatment of wastewater and brackish water, which can be combined with the antimicrobial effects of the nanoparticles to remedy multiple problems using a single filter (reviewed in Kanchi, 2014 and Das et al. 2019). This includes the removal or detection of toxic metals, such as cadmium, copper, nickel and lead in water (Das et al. 2019).

## 1.2.3 Raman Spectroscopy and Silver Nanoparticles

Nanoparticles (specifically gold and silver) hold many different properties, but none as unique as the fact that these particles can be used to enhance or amplify Raman signals.

These signals are the vibrations of a bond that has been excited by monowavelength lasers. The signals are measured using a CCD (charged coupled device) and can be used to assess the chemical composition within materials, including biological tissues, because different bond types in a molecule emit unique Raman signals. Signal amplification mainly occurs because noble metals enhance the electromagnetic field around them, as reviewed by Eustisa and El-Sayed (2006). Due to this enhancement phenomenon, silver and gold nanoparticles hold a special role in Raman spectroscopy studies because they can increase the intensity of bond-specific signals, allowing lower detection limits, tagging, and other various uses. The typical silver resonance is 400-500 nm (10-100 nm particles sizes) whereas it is 525-600 nm (5-100 nm sizes) for gold (<https://www.sigmaaldrich.com/technical-documents/articles/materials-science/nanomaterials/gold-nanoparticles.html>). The choice of metal to use depends on the excitation wavelength to be used. When using Raman spectroscopy, one of the largest problems is fluorescence from both the sample and the medium on which the sample is mounted. Fluorescence can be decreased by using longer wavelengths, such as 785 nm instead of 532 nm. This makes gold a slightly more attractive element than silver for plasmonic resonance, since resonance can be achieved with lower strength lasers, resulting in decreased sample fluorescence.

Raman spectroscopy is used to characterize molecular bonding and the information that can be derived from the molecular bonds, such as the molecular makeup of a sample (Delhaye and Dhamelincourt, 1975). In Raman spectroscopy, a mono-wavelength laser is applied to the sample, exciting molecular bonds and causing them to vibrate. These vibrations occur at unique wavelengths, which gives information on the identity of the bond being excited. Wavelengths of excited bonds can differ depending on the wavelength of the excitation laser, this is accounted for by the Raman shift ( $\text{cm}^{-1}$ ), which is a way of normalizing data for any mono-wavelength excitation laser so that each bond has an associated Raman shift value (e.g., the shift for a C=C bond is  $1600 \text{ cm}^{-1}$ ) (Zoubir, 2012). Since AgNPs enhance molecular signals, it is theoretically possible that you could detect and possibly localize silver in plants based on which signals are enhanced. For example, Raman spectra showing that the signal from lignin is enhanced in the

nanoparticle-treated versus control plants would indicate the nanoparticles are close to lignin-containing cells or tissues.

Noble metals have the ability to enhance the electromagnetic field around them to amplify the Raman signal (refer to section 1.3.1 for a more detailed explanation of Raman spectroscopy) of any molecules near their surface (Eustisa and El-Sayed, 2006). This enhancement comes from the scattering of electrons on the surface of the metal, which amplify the signal of the adjacent molecules, this is known as plasmon resonance (reviewed in Stockman, 2006). The amplification depends also on the shape of the particle, with rough edges giving increased enhancement of the surface electromagnetic field (Hao et al. 2004).

This characteristic has led to the creation of labelled nanoprobe for *in vivo* imaging and quantification. For example, one can use a gold nanostar attached to a ‘Raman label’, held apart by a placeholder that is removed when bound to a target miRNA sequence. The nanostar then enhances the label’s signal due to the contact between the label and the target (Strobbia et al. 2019). The label can be detected using SERS (surface-enhanced Raman scattering) for live imaging of intact tissues on the scale of the whole leaf (Strobbia et al. 2019).

Although gold and silver hold many interesting properties for industry and science, currently the most attractive feature is their antimicrobial ability (see section 1.4.1). In particular, AgNPs are best known for being antimicrobial (Kim et al. 2007), which explains why they are frequently used.

### 1.3 Release of Silver Nanoparticles into the Environment

With the steady increase in the use of nanoparticles and products containing nanoparticles, an increase in nanoparticles being released to the environment will surely follow. Although nanoparticles currently are not held to any specific regulations under the toxic substances control act (USEPA, 2021), and nanoparticles have received some regulatory attention, strict guidelines have not yet been established. In 2011, the Canada-U.S. Regulatory Cooperation Council was created in order to help with economic

stability and productivity in certain fields (agriculture, environmental, health and personal care products, workplace chemicals, transportation and some cross-sectoral issues) as well as to establish regulatory transparencies between the two countries. This Council assists with the oversight and regulation of nanoparticles in industry and production (Government of Canada, 2017). The United States Environmental Protection Agency (EPA) has not yet set specific limits to the production or release of nanoparticles (USEPA, 2018a).

As reviewed in a report from the Finnish Institute of Occupational Health (2017), nanoparticles can be released from materials into the environment through multiple avenues including industrial releases (e.g., wastewater, aerosol and solid waste), accidental spills, decomposition (e.g., leaching from landfill sites) and destruction (e.g., incineration releases nanoparticles to the atmosphere, then they settle on fields). In addition, because nanoparticles such as AgNP are weakly bound to textiles, during and after use AgNPs and silver ions are released from many products and enter the environment. As an example, socks advertised as being antibacterial, can have up to 1350  $\mu\text{g}$  Ag/g, and soaking the socks four times for 24 hours released 1845  $\mu\text{g}$  of total silver, and after three, one-hour washes up to 1020  $\mu\text{g}$  of total silver was released (Benn and Westernhoff, 2008). As another example, washing liquids such as shampoo have 0.8-3.9  $\mu\text{g}/\text{L}$  of AgNPs within them (Mitrano et al. 2014). Use of these types of materials releases AgNPs into our wastewater and sewage systems, and our environment.

Biosolids (treated sewage sludge) most likely will be the largest significant source of AgNPs to agricultural fields. Schlich et al. (2013) determined that 90% of AgNPs were not removed after wastewater treatment – they remained in the sludge – and the USEPA (2018b) measured Ag concentrations ranging from 1.94 to 856 mg/kg dry weight in sludge. These numbers may seem high but, due to their small size, silver nanoparticles would not be easily filtered out of the sludge. According to the USEPA (2018b), 47% of biosolids that are generated in the United States are used as fertilizer for agricultural or other lands, indicating use of biosolids in agricultural is common practice. Further, an audit of the USEPA in 2018 revealed that biosolids are tested for only nine out of a known 361 pollutants: arsenic, cadmium, copper, lead, mercury, molybdenum, nickel,

selenium and zinc. Silver and other contaminants are not being monitored or tested for, meaning there is no established safety threshold. Blaser et al. (2008) used a model to predict the amount of silver in sewage sludge expected to be added to European Union agricultural fields in 2010 and found that an intermediate estimate (50% of sludge produced used on fields) would be 140 tonnes per year. Addition of low concentrations of silver into fields could become damaging to the health of humans and other consumers due to accumulation in the soil over time, especially since soil has been known to be a sink for AgNPs (Zhai et al. 2016).

Another source of AgNP contamination to agricultural fields is through polluted air from waste incineration of products containing AgNPs; suspended nanoparticles settle onto the fields. Blaser et al. (2008) estimated that in 2010 there would be 13 tonnes of AgNP per year entering the atmosphere, mainly from waste incineration. In contrast, Gottschalk et al. (2009) predicted only 0.9 tonnes per year entering the atmosphere and into the fields from production and consumption of products that contain nanoparticles, and none from waste incineration. More recent estimates of environment levels of nanoparticles have not been published. Despite the uncertainty about the actual amounts, the risk of increasing environmental contamination is real.

Nanoparticles can bioaccumulate. They bioaccumulate readily (only mercury bioaccumulates more) in saltwater environments, with phytoplankton having 10000-70000  $\times$  more silver than the surrounding water (Luoma, 2008). In addition, silver is retained in the top layers of the soil (Kim et al. 2010), therefore silver could accumulate in agricultural fields, leading to progressively higher silver levels, which could become a serious problem. Not only is silver retained in the rooting zone, but humic acid also has the potential to transform silver ions ( $\text{Ag}^+$ ) into AgNPs (Maurer et al. 2012 and Akaighe et al. 2011). Other researchers have found that organic matter (Yin et al. 2012), superoxides (Jones et al. 2011) and  $\text{Ag}^+$  near parent AgNP can create AgNPs (Glover et al. 2011), all leading to AgNPs forming or re-forming in soil. Gottschalk et al. (2009) predicted soil concentrations of nano-Ag would be 7  $\mu\text{g}/\text{kg}$  of soil by 2012 in the United States. Although no recent studies have been done to confirm concentrations have reached these levels, it is highly possibly it did, given the rising number of products

containing AgNPs. Levels of AgNPs are expected to stay on their rising trajectory, and rise each year by 0.001 mg/kg, meaning the maximum threshold for safety could be reached within 50 years in Germany, under their current regulations (Schlich et al. 2013).

## 1.4 Silver Nanoparticles' Antimicrobial Effects

Although most nanoparticles are not explicitly known to be toxic, toxicity to microbes is what makes silver by far the most popular type of nanoparticle used. Adding AgNPs to a product can increase its bacterial resistance; they are typically incorporated into clothing, soaps, and food packaging (Das et al. 2019). Because of this, silver's properties and the mechanics of its antimicrobial action are a popular research topic.

AgNPs are useful and effective at controlling, or completely inhibiting, growth of numerous bacterial species. Kim et al. (2007) showed that AgNPs inhibited two bacterial species (*Escherichia coli* and *Staphylococcus aureus*) and a yeast (*Bovine mastitis*) equally compared to a positive control (Itraconazol and Gentamycin, respectively). They also found that minimal inhibitory concentrations (MIC) can be quite low and can vary among species. Using an average size of 13.4 nm particle, they determined that the MIC for yeasts is somewhere between 6.6-13.2 nM. *E. coli* has a MIC in the 3.3 nM-6.6 nM range, while *S. aureus* was more tolerant with an MIC of 33 nM, the highest used concentration. *E. coli* growth has also been shown to be completely inhibited at a moderately high AgNP concentration of 10 µg/mL, sized 5 nm on average (Li et al. 2010). As reviewed in Moreno-Garrido et al. (2015), AgNPs are also toxic to various species of marine microalgae, including both fresh and saltwater species.

As the popularity of AgNPs in industrial and household products increases, their concomitant increased release into the environment could severely affect ecosystems, starting with bacteria. Silver nanoparticles can be detrimental to the health and survival of various microorganisms, while hardly impacting others at all. Gordienko et al. (2019) determined that *S. aureus* was more resistant to AgNPs, while *Bacillus cereus* was more resistant to silver ions. Kim et al. (2007) found that *E. coli* (ATCC43890), yeast (ATCC19636) and *S. aureus* were inhibited at 3.3, 6.6 and 33 nM quantities of AgNPs,

respectively. The symbiotic genera responsible for nitrogen fixation in root nodules, *Bradyrhizobium* and *Rhizobium* (explained in further detail in section 1.7), showed no adverse effects when soil was treated with AgNPs or other various metal-NPs (Shah et al. 2014). The authors did not determine several key factors, such as the ability of the plant and bacteria to form symbioses and the health of bacteroids within the root nodules. In addition, when sensitivity to AgNPs is tested at the genus level, species-specific differences within the genus may be missed. This could mean that certain species in the community have decreasing abundance while others are increasing, leading to no net change in genus abundance. This is possibly the case for *Bradyrhizobium*, in which some species are sensitive to and inhibited by AgNPs, such as *Bradyrhizobium canariense* (another plant-associated bacterium) (Kumar et al. 2011). The previous result lends evidence to the thought that to have an overall no net change in genus abundance within a community some species must increase in abundance. This difference in the way individual species react to AgNPs will lead to a change in the community of the soil microbiome.

Changes in the microbial community in response to the addition of silver nanoparticles have been documented. Hänsch and Emmerling (2010) showed that addition of 3.2 µg Ag/kg soil decreased microbe biomass by 15%, and 32 µg Ag/kg soil decreased biomass by 27%. Zhai et al. (2016) also reported decreases in Shannon's index of diversity, which quantifies community diversity using species richness and evenness, when AgNPs were added to soil; decreases in microbial diversity occurred over the entire range of tested concentrations from 0.0067 mg/L - 0.708 mg/L, depending on the shape of nanoparticle; the highest concentrations (0.307 - 0.708 mg/L) of all shapes resulted in decreased diversity. In another study in which cucumber (*Cucumis sativus*) was grown in soil, microbial diversity as measured using Sobs (single alpha diversity) index, an index of species richness in a community, decreased at all classification levels when AgNPs (20 nm at 100 mg/kg soil) were added; conversely, in unamended soil microbial richness increased at all but the phylum level when AgNPs were added (Zhang et al. 2020). They also showed that adding AgNPs not only changes the richness but also the composition of the community, as large changes in relative abundance of particular taxonomic groups within the soil samples, which could also partially be from the changes to metabolites in

the soil, were seen. Zhang et al. (2020) also reported that communities from unamended soil, Ag-treated soil, soil with cucumber, and Ag-treated soil with cucumber all had vastly different microbial communities, and cucumber biomass decreased in Ag-treated soil. All these effects depend on certain factors such as soil type, shape, size, nanoparticle coating, and other physical/chemical factors (see section 1.4.2).

#### 1.4.1 Antimicrobial Mechanisms

The mechanisms of AgNP toxicity have received attention from researchers lately due to the promise of AgNPs as a new antimicrobial agent. There seem to be two sources of toxicity: the silver ions released from AgNPs, which appears to be the main effect, and chemical reactions at the particle surface. For example, Kim et al. (2007) determined from electron spin resonance data that free radicals/reactive oxygen species (ROS) were released from the surface of AgNPs. I speculate this is a result of silver ions around nanoparticles reacting with organic molecules after entering the bacterial cells, and possibly also interacting with the external cell membrane.

Nanoparticles can cause many deleterious effects to cells due to the following mechanisms of toxicity. Sondi and Salopek-Sondi (2004) used scanning electron microscope (SEM) images to show that 12 nm particles at 50 ug/mL could form pits in the walls of the cells of *E. coli* and cause death. In addition, Carlson et al. (2008) showed that AgNPs caused up to a 50% decrease in mitochondrial membrane potential and a 90% decrease in cell viability. Similarly, when treated with AgNPs, *E. coli* had almost 250% higher leakage of reduced sugars and 45% higher leakage of proteins, which can both be assumed to be from membrane and cell wall damage (Li et al. 2010).

While AgNPs have varied effects on different species of bacteria, toxic effects can also change with varied sizes, shapes, and coatings. In almost all cases, smaller nanoparticles tend to be more toxic, while in other cases larger ones seem to be more toxic (Martinez-Castanon, 2008). For example, Carlson et al. (2008) found that at 25 ug/mL, as particle size went from 55 to 30 or 15 nm, the mitochondrial membrane potential of macrophages dropped by 25% and 30%, respectively, indicating greater damage by smaller particles.



Not only does nanoparticle diameter and composition determine their relative toxicity to bacterial species but their surrounding environment, including soil composition, also matters. As seen by Grün et al. (2019), toxicity varied depending on the type of soil and duration of exposure. During the first day of exposure, bacterial phyla (Actinobacteria, Acidobacteria, alpha-Proteobacteria, Bacteroidetes and beta-Proteobacteria) in sand experienced the least toxicity (compared to those in clay and loamy soil), but after 14 or 28 days AgNPs in sand were significantly more toxic (depending on phyla) to microbes than they were in loamy soil, likely due to the presence of increased organic matter. Grün et al. (2019) also showed that the chemical speciation of silver changed over time; the amount of pure silver decreased steadily over time,  $\text{AgNO}_3$  concentrations reached a maximum on day 14 then decreased; this was accompanied by a rise in  $\text{NO}_3$  and an increase in  $\text{Ag-COOH}$ . These data indicate shifts in the chemical speciation of silver over time. After 90 days there were significant differences in the community of microbes in sandy versus loamy soil and between sandy versus clayey soils, with sand having communities that varied the most from the control (Grün et al. 2019). This was also reported by Schlich and Hund-Rinke (2015) who found AgNPs in a low pH soil with high sand content were the most inhibitory to microbial activity. Schlich and Hund-Rinke (2015) also found that the toxicity after 50 days of chemical transformations was the same as that of unchanged nanoparticles, indicating no loss of toxicity in some treatments despite altered chemical speciation.

## 1.5 Silver Nanoparticles' Effects on Plant Growth

With an increase in the use of silver and its release to the environment, silver will accumulate in agricultural fields. This is especially true given that some agricultural products include AgNPs, as seen with the previously mentioned fertilizer example in section 1.2.2.

As reviewed in Dietz and Herth (2011), there are five main ways that nanoparticles, in general, can cause phytotoxicity: chemical effects of ions, mechanical injury due to shape and size, catalytic effect, binding of proteins to particle surface, and particle-induced changes to the environment such as pH. These effects are likely to have an impact on

many key crop species, as reviewed by Yan and Chen (2019) decreased biomass has been reported for crops (rice - *Oryza sativa* L., wheat - *Triticum aestivum* L., peas - *Pisum sativum*, Onion - *Allium cepa*, Mustard - *Brassica* sp., Cucumber – *Cucumis sativus*, see their paper for more examples) and plants in general (bryophyte (*Physcomitrella patens*), *Arabidopsis thaliana*, and others such as *Lemna minor* L.).

### 1.5.1 Movement of Silver Nanoparticles within Plants

Plant roots constantly take up water along with dissolved ions, compounds and substances that are present in the soil pore water. Particulate matter will travel in the bulk flow of water to the root, but it does not get taken up by the plants due to its size or other physical factors that prevent it from crossing the cell membrane. Even if some of the solutes in the water are potentially toxic, specific plant defenses can exclude or deal with these substances. A good example of a soil contaminant for which most plant species have a defense mechanism is cadmium, which enters the cell via calcium channels and is then transported into the vacuole for safe storage (Seregin and Ivanov, 2001). AgNPs seem to have no specific site of entry into plant cells, and no defense mechanism to deal with AgNPs has yet been found in plants. The period of time during which AgNPs have been accumulating in the environment would likely not be long enough for the evolution of specific plant defense mechanisms, and due to the apparent absence of such mechanisms, one can presume that natural nanoparticles (e.g., ash, soot, mineral particles found in air or water) that pre-date anthropogenic industrial activity are not phytotoxic.

AgNPs for the most part seem to enter cells through physical openings. As reviewed by Tripathi et al. (2017a), AgNPs can permeate the plant cell wall network, which acts like a sieve. Smaller AgNPs tend to accumulate more in plants than larger AgNPs (reviewed in Yan and Chen, 2019). AgNPs up to 40 nm have been shown to enter plant cells, likely through pores in cell membranes (reviewed in Ma et al. 2010). Larger particles could subsequently gain access to the cell via the induction of larger holes after damage caused by smaller AgNPs (Navarro et al. 2008). AgNPs could also gain entry into the symplast when lateral roots are forming and breaking through the endodermis and cortex as well as through wounds and root tips. Once in the cytosol, the nanoparticles can be transported

cell to cell via plasmodesmata (reviewed in Ma et al. 2010) and movement through the xylem facilitates long distance translocation (Aslani et al. 2014).

Not only have AgNPs been shown to be taken up and transported to leaves and other organs (Dietz and Herth, 2011; Ma et al. 2010; Geisler-Lee et al, 2014), the same has been found for many other types of nanoparticles. For example, 45 nm NaYbEr<sub>4</sub> [ytterbium (Yb), erbium (Er)]-NPs are visible within plant tissue via luminescence and were found to accumulate initially in the velamen of the aerial roots in orchids (Hischemöller et al. 2009). Over time, these NaYbEr<sub>4</sub>-NPs reached the central root cylinder and spread to the rest of the plant, with NaYbEr<sub>4</sub>-NPs luminescence being detected in the leaves and stem within 6 days.

### 1.5.2 Effects on Growth

As diverse as nanoparticles are, with different sizes, shapes, compositions and more, one can assume that the effects on plants are just as diverse, and they certainly are. Hao et al. (2019) reported that 150 mg/L of 150 nm mesoporous carbon nanoparticles (MCN) decreased root elongation by 21% and shoot length by 29% in rice. However, 80 nm MCN at the same concentration decreased root length by 70% and shoot height by 57% (Hao et al. 2019). Canas et al. (2009) found that up to 1,750 mg/L of carbon nanotubes had inconsistent effects on root growth of different species over 48 hours. Specifically, tomato (*Solanum lycopersicum* L.) had decreased root elongation, carrot (*Daucus carota*) was unaffected, and root elongation increased in onion (*Allium cepa* L.). Silica nanoparticles can also be toxic, which Slomberg and Schoenfisch (2012) attributed to their high surface area and unique surface properties that could favour binding of essential elements causing nutrient deficiency.

Nanoparticles are phytotoxic at higher concentrations, yet some plants seem to benefit from low doses of AgNPs. This may be due to hormesis, which is a phenomenon seen for many toxins for which the low-dose response is stimulation, and a high-dose response is growth inhibition. Jasim et al. (2017) found that AgNPs at 1 mg/mL increased the root and shoot length of fenugreek (*Trigonella foenum-graecum* L.) seedlings by 100%, and wet weight by 200%. In Arabidopsis subjected to 100 µM AgNPs, there was a 33%

increase of free amino acid concentration in the leaves compared to control, but AgNPs did not have this effect in the roots (Wen et al. 2016). Despite these few reports of beneficial effects of low doses of AgNPs, the majority of reports in the literature indicate that AgNPs are detrimental to plant health and growth.

Roots of soybean and rice (*Oryza sativa*) exposed to AgNPs had 70% and 55% decreased biomass, respectively, as well as 400% and 200% increased leaf ROS, respectively (Li et al. 2017). Pea plants (*Pisium sativum*) also had a decreasing dry weight per plant with increasing concentrations of AgNPs above 1000  $\mu\text{M}$  (Tripathi et al. 2017b). Mustard (*Brassica* sp) plants given 1 mM AgNPs had shorter shoot (5% decrease) and root length (10% decrease) as well as reduced fresh weight of shoots by 11% and root weight by 28% (Vishwakarma et al. 2017). In a study using soil, wheat had a 5 cm decrease in shoot height, relative to control, when subjected to 20 mg/kg AgNPs and a 10 cm decrease when subjected to 200 mg/kg; root length also decreased but only at 2000 mg/kg (Yang et al. 2018). Yang et al. (2018) also found that the number of grains and length of spikes decreased by five grains per pot and 1 cm on average when exposed to 200 mg/kg, while the average 100-grain weight decreased only by about 1 g on average at 2000 mg/kg. Bell peppers (*Capsicum annuum* L.) grown with AgNPs also had 20-40% decreased stem weight (Vinković et al. 2017). Decreases in overall biomass tend to, but do not always, reduce the amount of fruit/crop production by plants (Shackleton, 2002).

The influence of Ag<sub>2</sub>Sulphur-nanoparticles (Ag<sub>2</sub>S-NPs), a slight variation from using typical AgNPs, was tested on wheat growth. According to (Kampe et al. 2018), Ag<sub>2</sub>S-NP is the most likely silver nanoparticle to be found in sewage sludge as AgNPs typically transform into Ag<sub>2</sub>S-NPs. Shoot fresh biomass decreased by 0.1 g when plants were treated with 10  $\mu\text{g}/\text{mL}$  of Ag<sub>2</sub>S-NPs (Wang et al. 2017). Although Ag<sub>2</sub>S-NPs are toxic, it seems to not be as toxic as pure or citrate-AgNPs (Pure AgNPs with citrate caps for stabilizing). This can be seen with wheat subjected to 6  $\mu\text{g}/\text{mL}$  of Ag<sub>2</sub>S-NPs, which had a 30% decrease in root and 10% decrease in shoot weight, and AgNP-treated plants had lower biomass with 85% decrease for roots and a 60% decrease for shoots (Wang et al. 2015). Wang et al. (2015) also showed that cow pea plants (*Vigna unguiculata*) subjected to Ag<sub>2</sub>S-NPs at 6  $\mu\text{g}/\text{mL}$  had decreases relative to control in all the following: root

biomass by 50%, 30 % for shoots and 10% for leaves. Cucumbers also had decreased growth in response to 10  $\mu\text{g/mL}$   $\text{Ag}_2\text{S-NPs}$ , but in this case both root and shoot had decreased fresh weight, root fresh weight had a 45% decrease while shoots had a 15% decrease (Wang et al. 2017). Bell peppers had decreased root weight by 25%, 45%, 25% and 24% when grown in 0.01, 0.1, 0.05 and 0.5  $\mu\text{g/mL}$  AgNPs, respectively, but interestingly plants given 1  $\mu\text{g/mL}$  AgNPs were not significantly different from the control (Vinković et al. 2017).

Crop species are not the only types of plants to have a negative reaction to up to 10  $\mu\text{g/mL}$  of  $\text{Ag}_2\text{S-NPs}$ . Al-Huqail et al. (2018) showed that *Lupinus termis* L. had 40% shorter roots and about 20% shorter shoots when subjected to concentrations of AgNPs at 0.5  $\mu\text{g/mL}$ . They also observed a 25% decrease in overall dry biomass in plants given 0.3  $\mu\text{g/mL}$  of AgNPs and a 60% decrease for 0.5  $\mu\text{g/mL}$  of AgNPs. An interesting relationship occurred in common duckweed (*Lemma minor*) where growth rates of plants treated with AgNPs did not have typical response to increasing doses (Pereira et al. 2018). With 0.05, 0.13 or 2  $\mu\text{g/mL}$  of citrate-AgNPs growth rates were 25% to 30% lower than the control, but 0.32 and 0.8  $\mu\text{g/mL}$  of citrate-AgNPs had no effect on plant growth rate and then at the highest dose of 2  $\mu\text{g/mL}$  of citrate-AgNPs the growth rate was reduced by ~30%. A similar pattern occurred in response to nanoparticles coated with PVP (polyvinylpyrrolidone, which is a large polymer consisting of the monomer n-vinylpyrrolidone); at 0.05  $\mu\text{g/mL}$  plant growth rate was ~40% lower, 0.13 and 0.32  $\mu\text{g/mL}$  had no effect on growth rate, and 0.8 and 2  $\mu\text{g/mL}$  of PVP-coated nanoparticles decreased growth rates by ~40% and 45%, respectively (Pereira et al. 2018). This is interesting, considering that with these two examples of coated nanoparticles there is a non-linear relationship between dose and response. The uncoated particles in contrast had a linear relationship. The non-linear pattern for coated particles points towards a hormesis-like response at low concentrations. Similar patterns are very likely to be found for other types of nanoparticles. Effects will depend on the coating, species of plant and most likely many other factors such as location of nanoparticles in plants, size, shape, type of soil, pH, and others.

## 1.6 Overview of Silver Nanoparticle-Specific Effects on Plant Cells

Nanoparticles entering cells can have a number of effects, from indirect effects of ion discharge to direct binding to proteins and other molecules, leading mainly to oxidative stress and genotoxicity.

### 1.6.1 Oxidative Stress

Exposure to AgNPs results in oxidative stress and oxidative responses from the plant. Malondialdehyde is a result of ROS-induced peroxidation of membranes and hydrogen peroxide is a potent ROS that also damages other cellular components. It has been suggested that ROS are generated from the surface of AgNPs (Kim et al. 2007), yet oxidative stress could also be the result of the release of toxic Ag<sup>+</sup> ions. Li et al. (2017) showed in soybean that exposure to AgNPs from 1 to 30 µg/mL resulted in at least 2 to 4 times more malondialdehyde and 1.5 to 5 times more hydrogen peroxide. Their results were similar for rice except that ROS were produced only at the highest doses of AgNPs. ROS content of *Allium cepa* roots also increased after exposure to 25 µM AgNPs, with ROS concentrations increasing further with up to 75 µM AgNPs, indicating steadily increasing production of ROS with increased AgNP concentrations (Cvjetko et al. 2017). Another plant that has been tested for ROS stress after exposure to AgNPs is potato (*Solanum tuberosum* L.), which had 4 times more ROS in plants given 10 µg/mL AgNPs when compared to control, and 10 times more ROS in plants treated with 20 µg/mL (Bagherzadeh Homae and Ehsanpour, 2016). Pereira et al. (2018) found that levels of glutathione-S-transferase activity (an enzyme that is involved with ROS detoxification) increased to 200% of the control when plants were subjected to 0.8 µg/mL AgNPs. They also reported that glutathione peroxidase activity reached more than 500% of control in plants treated with up to 0.8 µg/mL AgNPs. Oxidative stress is manifest by damage to membranes and inhibited mitochondrial metabolism. This could lead to problems for nitrogen fixation by *B. japonicum* inside nodules since they rely on the nodule membrane (which is non-permeable to oxygen) to keep their environment close to anoxic. Nitrogen fixation relies on an oxygen-free environment due to oxygen binding mainly with the Fe-

protein of the enzyme nitrogenase, thus inhibiting nitrogen fixation (Gallon 1981). If oxygen were to enter the nodules via AgNP-damaged nodule membranes, then the nitrogen-fixing bacteroid form of *B. japonicum* would have drastic metabolic problems.

### 1.6.2 Genotoxicity

Silver nanoparticles have genotoxic properties, causing damage to the DNA of the plant cells, most likely through ROS damage or physical binding of the AgNP to genetic components. When Abdelsalam et al. (2018) exposed root tips of wheat to AgNPs (using concentrations of 10, 20, 40, or 50  $\mu\text{g}/\text{mL}$  for 8, 16 and 24 hours) they found many types of chromosomal aberrations; increased concentrations increased damage and thus few cells divided and underwent mitosis as a result. Kumari et al. (2009) found that  $< 100$  nm AgNPs at 25-100  $\mu\text{g}/\text{mL}$  inhibited cell division and lowered the mitotic index. Similarly, *Vicia faba* root tips had various chromosomal aberrations and a decreased mitotic index when grown with 60 nm AgNPs at 25, 50 and 100 mg/L but not at 12.5 mg/L (Patolla et al. 2012). At even lower concentrations of AgNPs, the root tips of *Allium cepa* also had increased chromosomal aberrations and decreases to their mitotic and meiotic indices when exposed to AgNPs (5, 10 and 20  $\mu\text{g}/\text{mL}$  for four hours); yet interestingly, the researchers found that biosynthesized nanoparticles were less toxic than chemically synthesized particles (Saha and Dutta Gupta, 2017). Another group who studied *A. cepa* and 70 nm AgNPs reported a decrease in mitotic index at 5 mg/L, significant changes to the micronucleus at 20 mg/L and nuclear aberrations 40 mg/L (Panda et al. 2011). Interestingly, *A. cepa* has been shown to withstand 100  $\mu\text{M}$  of AgNPs without a reduction in dry mass or plant length even though there were more DNA breakages, seen by the increase in tail DNA (Cvjetko et al. 2017).

With so much information on DNA damage from AgNP its clear that they (or at least the  $\text{Ag}^+$  ions) can enter plant cells and be detrimental to the health of plants. Damaging crop DNA will lead to poor harvests as they will likely lead to detrimental effects on plant growth.

## 1.7 Silver Nanoparticles' Effects on Plant and Bacterial Interactions: Emphasis on *Fabaceae-Bradyrhizobium*

Soybean is an important agricultural crop; in 2006, the United States alone produced 3.2 billion bushels of soybeans, grown on 74.6 million acres (USDA, 2007). Plant roots not only take up water and nutrients but hold symbiotic relationships with bacteria and fungi, and the soil around the roots houses the root microbiome – a complex community of microbes both good and bad. Soybean health and that of their symbiotic rhizobia, as well as their relationship, might be compromised by the presence of AgNPs in soil.

Although AgNPs affect certain microbial species more than others, one can expect drastic changes in the microbiome due to interacting toxic effects. For example, the effects of AgNPs on plants (see section 1.5 for complete list) include accumulation of the nanoparticles within plasmodesmata (Geisler-Lee et al. 2014) and subsequent blocking of signaling conduits. This could lead to interruptions of the signals between the plant and the microbes that are essential for root nodulation. Blocking of plasmodesmata could also inhibit nutrient and sugar movement from the plant to the bacteroids within its nodules, and the transport of nitrogen from the nodule to the plant. If AgNPs block plasmodesmata, it could have negative effects on the nutrient levels in the plant. Blocked plasmodesmata could stop, or at least slow, the bulk flow of water and nutrient ions from the roots, which was shown by Robards and Clarkson (1976). This blockage could occur in other regions of the plant as well. Asli and Neumann (2009) showed that 20 nm titanium dioxide particles in hydroponic solution decreased the transpiration rate of plants by a little over 20% compared to controls, and root hydraulic conductivity decreased by 7% compared to control. Silver nanoparticles of the same diameter would most likely have the same effect, as they have already been seen to block plasmodesmata in *Arabidopsis* plants (Giesler-Lee et al. 2014). Another effect from the blockage of the plasmodesmata is inhibition of some transcription factors (Wayne, 2019), which could result in slowing plant growth and possibly other processes such as nodulation.

The nodulation process is initiated by the release of flavonoids from plant roots. When encountered by appropriate bacteria (e.g., *Bradyrhizobium* spp.), the bacteria release



nodulation factors (Cohn et al. 1998). Upon receiving the nodulation factor signal, a plant root hair binds with a rhizobial cell, activating the underlying cortical cells (Gage, 2004). Next, continued growth of the root hair includes curling due to the presence of the nodulation factor and then a microcolony of rhizobia grow in the curl, cytoplasmic bridges (PITs) form within the cortical cells and infection thread initiation begins (Gage, 2004). After this event, the bacteria will eventually grow within the infection thread into the cortical cells and be released from the infection thread into the nodule primordium, which were derived from the inner and middle cortex along with the pericycle cells (Gage, 2004). The interior of the nodule is an oxygen-free environment in which the bacteria undergo metabolic and physical changes to become bacteroids. This changed physical form with a different metabolism than that of the bacterial form is the one that fixes nitrogen within the nodule. The oxygen-free environment is essential because oxygen prevents nitrogen-fixation, a process completed by the bacteroids after they have colonized the nodule. These bacteroids fix and provide nitrogen in exchange for sugars from the plant. This symbiotic relationship benefits both plant and bacteria as well as farmers who can reduce the cost of fertilization. Peoples and Craswell (1992) showed that symbiotic nitrogen fixation can account for up to 97% of a soybean's total nitrogen, proving that soybeans can almost fully rely on this relationship for this nutrient.

As was discussed above, the responses of plants to AgNP-treatment are not always linear and some researchers report different responses at low and high doses relative to intermediate doses (see section 1.5.2). A similar pattern has been reported for nodulation. At a fairly high concentration of 50  $\mu\text{g}/\text{mL}$ , roots of cowpea (*Vigna unguiculata*) had double the number of nodules compared to the control plants (Pallavi et al. 2016); however, plants given 70  $\mu\text{g}/\text{mL}$  had the same number of nodules as the control plants. Given the antimicrobial properties of AgNPs, one would expect that plant given even higher concentrations would have fewer nodules than control plants.

When quantifying nitrogen fixation, the nodule number is not a good measure of total nitrogen fixed, or even the rate of fixation, as one large nodule can fix as much nitrogen as many small nodules. The actual fixation process can be measured through an acetylene reduction assay (ARA) rather than direct measurement of the activity of nitrogenase. The

latter is a delicate process that is ruined by exposure of the nitrogen-fixing enzyme to oxygen (Gallon 1981). To my knowledge nobody has developed a protocol for direct measurement of nitrogenase activity. An ARA takes advantage of the fact that the enzyme (nitrogen reductase) can catalyze more than one reaction. This enzyme can convert  $C_2H_2$  (acetylene), which is given to the plant in a closed environment, to  $C_2H_4$  (ethylene), which can then be measured using gas chromatography, as a proxy to nitrogen fixed from the atmosphere. This measurement is much more reliable than measuring nodule weight since nodules could still develop but not fix any nitrogen if they have unhealthy bacteroids within the nodules.

High concentrations of nano- $CeO_2$  have been shown to reduce nitrogen fixation by 50% (Priester et al. 2012). Similarly, when faba bean (*Vicia faba*) were exposed to AgNP in soil, nodulation was delayed and nitrogenase activity decreased, along with a 65% decrease in nodule weight and an 80% decrease in nodule number (Abd-Alla et al. 2016). The effect of AgNPs on soybean nodules would most likely be similar to that of the closely related faba bean. Although the sensitivity of the soybean's symbiotic relationship to AgNPs has not yet been tested, the genus *Bradyrhizobium* is typically tolerant to AgNPs (Shah et al. 2014). However, it is not known if the *Bradyrhizobium* bacteroids respond in the same way to AgNPs as do the free-living bacteria in the soil. Due to the ROS-induced membrane damage resulting from AgNP-treatment (see section 1.4.2), oxygen may leak into the nodule interior. Since the bacteroids have evolved in the oxygen-free environment of the nodule, the bacteroids might be expected to be more sensitive to AgNPs than the parent bacteria.

## 1.8 Rationale and Objectives

### 1.8.1 Rationale

Due to release of nanoparticles, specifically AgNPs into the environment from various sources (e.g., sewage sludge, leaking from landfills, incineration, etc.) and their antimicrobial properties, we should be concerned about the effects that AgNPs will have on plant-microbe relationships.

## 1.8.2 Objectives

1. To assess uptake and accumulation of silver nanoparticles within soybeans by;
  - A. Determining if Raman spectra of molecular bonds can assess AgNP uptake or location of AgNP accumulation in plant roots.
  - B. Confirming the subcellular presence of AgNPs in root cells using transmission electron microscopy.
  - C. Quantifying the concentration of silver in shoots, roots and on root surfaces, the latter using chemical desorption of Ag<sup>+</sup> from the root surface.
2. To assess the toxic effects of AgNPs on soybeans, *Bradyrhizobium japonicum* and their symbiotic relationship by;
  - D. Quantifying growth of *B. japonicum* USDA 110 in liquid culture, measured using spectrophotometric optical density
  - E. Studying growth of inoculated and non-inoculated plants, measured as dry biomass, photosynthetic efficiency, and select nutrient concentration (carbon and nitrogen).
  - F. Assessing nodule biomass and morphology (using transmission electron microscopy), and nitrogen-fixing activity (using an acetylene reduction assay).

## 2 Materials and Methods

### 2.1 Study Organisms

Soybeans (*Glycine max* (L.) Merr.) cv SO9-C3X were grown from seeds provided by Environmental Sciences Western Field Station. A culture of *Bradyrhizobium japonicum* USDA110 was obtained from the London Research and Development Centre – Agriculture and Agri-Food Canada.

## 2.2 Experimental Treatments and Conditions

### 2.2.1 Synthesis, Preparation and Confirmation of Silver Nanoparticles

Synthesis of AgSNPs was based on the protocol described in Bastús et al. (2014) for citrate-stabilized AgSNPs. First, 200 mL of sodium citrate (5 mM) and tannic acid (0.1 mM) were boiled (110-115 °C) with vigorous stirring, for 15 minutes. After boiling, 2 mL of aqueous silver nitrate (25 mM) was added to the solution, resulting in immediate production of silver nanoparticles. Sodium citrate ( $\text{Na}_3\text{C}_6\text{H}_5\text{O}_7$ ), silver nitrate ( $\text{AgNO}_3$ ) and tannic acid ( $\text{C}_{76}\text{H}_{52}\text{O}_{46}$ ) were purchased from Sigma Aldrich.

The size of the AgSNP particles was controlled by the tannic acid concentration, with 0.1 mM tannic acid resulting in  $\sim 10 \pm 5$  nm particles (Bastús et al. 2014). This reaction took place in a two-neck round-bottomed flask held within an oil bath for even heating. The flask was topped with a condenser to ensure no solvent loss. Larger particle sizes can be generated by using higher concentrations of tannic acid, but also by stepwise growth reactions (Bastús et al. 2014); both were attempted for obtaining larger particles. A concentration of 0.1 mM tannic acid resulted in  $\sim 16 \pm 2.5$  nm particles, which was confirmed by TEM (transmission electron microscope) imaging. Stepwise growth was attempted by using particles made with 0.1 mM tannic acid. Solution was brought to 90 °C, then 100  $\mu\text{L}$  of sodium citrate (25 mM), tannic acid (2.5 mM) and 1 mL silver nitrate (25 mM) were added sequentially 1 minute apart to increase the size of the particles. My particles were  $30 \pm 2.7$  nm (stepwise growth) for the first batch and  $16 \pm 2.5$  nm for the second batch. For the larger first batch I used the stepwise growth method, this was mainly done because stock solutions for creating the smaller size had been made and thus this technique was easier. Both methods for achieving larger particles could have worked equally well.

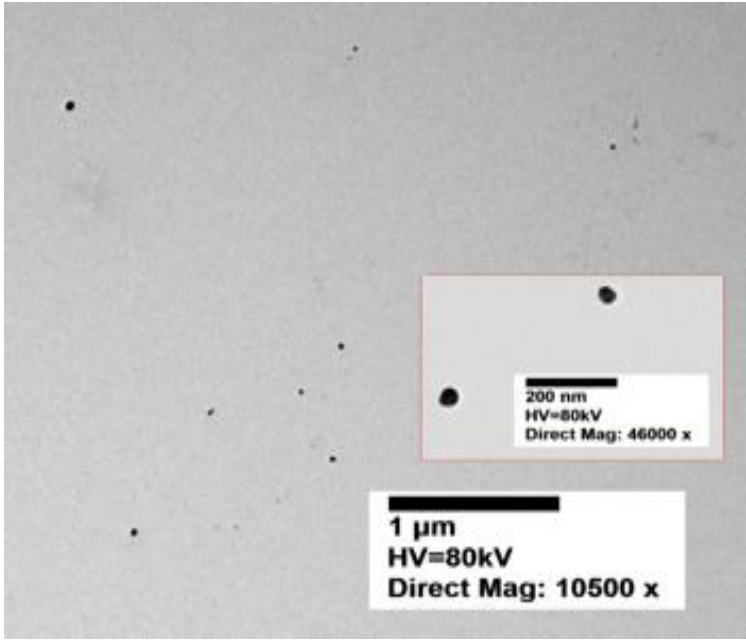
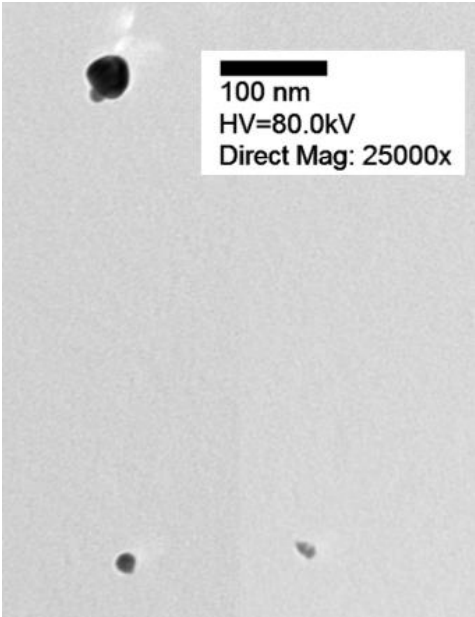
## 2.2.2 Concentration, Confirmation and Size of Silver Nanoparticles

After synthesis, nanoparticles were collected using a centrifuge; reaction products were spun at  $18000 \times g$ , the supernatant was removed, and the pellet of nanoparticles was re-suspended in RO (reverse osmosis) water. Several batches of small particles were pooled to accumulate a greater number of particles of uniform concentration and size range, and the same was done for batches of larger particles. TEM imaging was done in conjunction with ImageJ to confirm both shapes and sizes of the nanoparticle batches, and to determine both range and averages of size. The average  $\pm$  standard deviation for particles in the first batch were  $30 \pm 2.7$  nm, and particles in the second batch were  $16 \pm 2.5$  nm (see Table 2.1). Concentrations (mass per mL) were calculated using a microscale balance by the methods of Shang and Gao (2015). To do this, 600  $\mu$ L of suspension containing silver nanoparticles was weighed, before and after evaporation of the solvent. Concentration of each batch of silver nanoparticles was also assessed showing batch one (30 nm) had a concentration of 3.35 mg/mL and batch two (16 nm) had a concentration of 2.20 mg/mL. For the remainder of this section, the first batch will be called 30 nm or the larger nanoparticles, while the second batch will be referred to as 16 nm or the smaller nanoparticles.

## 2.2.3 Bacterial Growth

Axenic cultures of *B. japonicum* were grown in Petri plates on HEPES-MES (HM) agar growth medium supplemented with chloramphenicol (see Table 2.2). This was done to kill other bacteria; *B. japonicum* USDA 110 is not affected by this antibiotic (Cole and Elkan, 1973). Cultures were incubated for two days at 28 °C and then the process was repeated twice to ensure cells were active and a pure culture. They were then transferred to liquid HM medium for both testing and inoculation. Liquid culture was grown for 2-3 days then used to start another liquid culture to ensure the experimental culture was in the log growth phase and no dead cells disrupted the optical density reading. Liquid cultures were grown at 22 °C to assess growth when exposed to AgNPs.

**Table 2.1: Transmission electron microscope images showing nanoparticles used for testing growth and symbiosis of soybeans and *B. japonicum***

Size	Representative TEM Image
30 ± 2.7 nm; N=12	
16 ± 2.5 nm; N =11	

**Table 2.2: Growth media.**

**Modified Hoagland's Nutrient solutions (Hoagland and Arnon, 1950) and bacterial medium used for growing full nitrogen (axenic) plants, low nitrogen (inoculated) plants, and *B. japonicum*, respectively.**

Full Nitrogen Solution (mM)	Low Nitrogen Solution (mM)	HM Growth Medium (g/L)
K <sub>2</sub> HPO <sub>4</sub> (0.05)	K <sub>2</sub> HPO <sub>4</sub> (0.05)	Na <sub>2</sub> HPO <sub>4</sub> (0.125)
MgSO <sub>4</sub> (0.15)	MgSO <sub>4</sub> (0.15)	Na <sub>2</sub> SO <sub>4</sub> (0.25)
KNO <sub>3</sub> (0.1)	KNO <sub>3</sub> (0.1)	NH <sub>4</sub> Cl (0.32)
K <sub>2</sub> SO <sub>4</sub> (0.1)	K <sub>2</sub> SO <sub>4</sub> (0.1)	MgSO <sub>4</sub> •7H <sub>2</sub> O (0.18)
CaSO <sub>4</sub> (0.4)	CaSO <sub>4</sub> (0.4)	Yeast extract (0.25)
NH <sub>4</sub> NO <sub>3</sub> (2.9)	MnCl <sub>2</sub> •4H <sub>2</sub> O (0.0005)	L – Arabinose (1)
MnCl <sub>2</sub> •4H <sub>2</sub> O (0.0005)	H <sub>3</sub> BO <sub>3</sub> (0.0015)	Na-Gluconate (1)
H <sub>3</sub> BO <sub>3</sub> (0.0015)	ZnSO <sub>4</sub> •7H <sub>2</sub> O (0.0000125)	FeCl <sub>3</sub> (0.004)
ZnSO <sub>4</sub> •7H <sub>2</sub> O (0.0000125)	CuSO <sub>4</sub> •5H <sub>2</sub> O (0.0000375)	CaCl <sub>2</sub> (0.001)
CuSO <sub>4</sub> •5H <sub>2</sub> O (0.0000375)	Na <sub>2</sub> MoO <sub>4</sub> •2H <sub>2</sub> O (0.00024775)	HEPES (1.3)
Na <sub>2</sub> MoO <sub>4</sub> •2H <sub>2</sub> O (0.00024775)	FeCl <sub>3</sub> •6H <sub>2</sub> O (0.0025)	MES (1.1)
FeCl <sub>3</sub> •6H <sub>2</sub> O (0.0025)	Na <sub>2</sub> EDTA (0.00275)	2 % Agar (20)
Na <sub>2</sub> EDTA (0.00275)		chloramphenicol (0.03)

Axenic cultures were also transferred to 30% glycerol in a 1:3 liquid culture to glycerol ratio and stored at -80 °C for future use, if required.

## 2.2.4 Hydroponic Setup and Soybean Growth Conditions

A sufficient number of seeds was germinated to select seedlings that were an approximate equal size for experimentation. Seeds were coated in a copper-based

antimicrobial coating, so there was no need to surface-sterilize the seeds, but the coating was removed prior to inoculation. Seeds were germinated in a Petri dish on filter paper (VWR 314) moistened with RO water and placed in the dark at ~22 °C. After 2-3 days, germinated seedlings of equal size were selected for one of two bacterial treatments: non-inoculated and inoculated. Seeds that were meant to grow axenically were placed in sand that had been sterilized in an autoclave at 121 °C for 20 minutes, allowed to cool, then saturated with modified Hoagland's nutrient solution (see Table 2.2). Roots of these seedlings developed no nodules. In order to get inoculated plants, I generated bacterial inoculum cultures. Liquid cultures were started in 5 mL of HM growth medium (Table 2.2) within sterile 15 mL Falcon tubes and kept on a shaker to ensure sufficient oxygen for growth. Liquid culture was then grown until the optical density reached 0.5-0.6 (which translated to  $1 \times 10^8$  to  $2 \times 10^8$  cells per mL, see Appendix A). After seeds had germinated and the radicle was 4-5 cm long, roughly 25-30 seeds per Petri dish were submerged in inoculum for 20 minutes. The seeds were then placed in sand that had been saturated with low (<0.1 mM) nitrogen nutrient solution (see Table 2.2) because higher levels of available nitrogen will inhibit nodulation (Streeter et al. 1985), and an additional 100  $\mu$ L of the inoculum was placed on the seeds.  $1 \times 10^9$  bacterial cells per mL in suspension has been shown to be sufficient for inoculating at least 25 soybean plants (each weighing 12 g or less) with *B. japonicum* (Ralston and Imsande, 1983), but I found that  $1 \times 10^8$  cells per mL was sufficient to produce nodules on roots of every seedling.

Sand was moistened with RO water as needed to compensate for evaporation and transpiration, and seedlings were grown for 2-3 days until all were approximately 4 cm tall. Seedlings were then transferred into hydroponic jars containing AgNPs in  $\frac{1}{4}$  strength low nitrogen (for inoculated seedlings) or  $\frac{1}{4}$  strength full nitrogen (for axenic seedlings, see Table 2.2) nutrient solution. Using  $\frac{1}{4}$  strength solution was based on preliminary experiments in which the root nodules formed on healthy plants grown in this modified Hoagland's medium. The concentrations of AgNPs were 0, 0.5, 1, or 2.5  $\mu$ g/mL. Jars were covered with aluminum foil to minimize microbial/algal growth and the solutions were aerated to ensure proper oxygen levels. Nutrient solutions, including ones with AgNPs, were changed every 3 days to ensure adequate nutrient supply. Plants were 21 days old at harvest: 3 days in Petri dishes, 4 days in sand and 14 days in nutrient solution.



## 2.3

### 2.3 Raman Spectroscopy

Raman spectroscopy (Xplora Plus Microspectrometers from HORIBA, equipped with 1200 grooves per mm grating) was conducted to determine if silver binds to and alters the signals of common plant cell molecules (e.g., cellulose and lignin). Root tips of plants exposed to 0, 0.5, 1 or 2.5  $\mu\text{g/mL}$  AgNPs and tips exposed to a very high concentration (2 mg/mL for 2 hours) were taken and thinly sliced into cross sections by hand using a razor. These cross-sections were placed on thin microscope cover slips and wetted with RO water. Preliminary tests determined that a glass cover over the sample interfered with the readings and readings could not be obtained without a drop of water on the sample. Readings were taken from multiple areas within each cross section, but only the area around the vascular tissue produced signals. Recordings were taken using a 785 nm laser applied at 4.9 mW focused on the sample with a 50 $\times$  objective having 0.75 NA (numerical aperture) with a nitrogen cooled CCD (charge-coupled device) detector. The laser spot size was roughly one micron, and the grating was 600  $\text{g mm}^{-1}$ . I acquired 12 by 12 point maps giving a total of 144 Raman spectra for each map, using 10 second acquisition for each point. Three regions were chosen: red was 1045 – 1165  $\text{cm}^{-1}$ , blue was 1238 – 1522  $\text{cm}^{-1}$ , and lastly green was 1549 – 1702  $\text{cm}^{-1}$ . The peak at 1045 – 1165  $\text{cm}^{-1}$  is indicative of cellulose or glucomannan, 1238 – 1522  $\text{cm}^{-1}$  indicates cellulose and 1238 – 1522  $\text{cm}^{-1}$  indicates lignin (Gierlinger and Schwanninger, 2006), this is further described in section 3.1. In addition, Lab Spec 6 software was used for baseline corrections of each of the map modes that were integrated into the overlapped map image of all three regions. Spectra were collected from xylem cells because Giesler-Lee et al. (2014) determined that silver moved throughout the plant via xylem.

### 2.4 Toxicity of Silver Nanoparticles to Bacterial Cultures

Liquid cultures were grown with 0 or 10  $\mu\text{g/mL}$  of AgNPs (16 nm size). To assess the antibacterial ability of AgNPs, 0.1 mL of liquid culture was placed in each of the wells of a 96-well plate. The 96-well method was chosen to ensure no bacteria were removed each time a reading was taken, which can cause inflation of optical densities. It also ensures a sterile environment and decreases the amount of AgNP needed. Growth was estimated by

measuring optical density of the culture via a spectrophotometer (600 nm) at the same time each day for 4 days. Optical density was converted to cell counts using a standard curve (Appendix A) that had been created by plotting optical density against actual cell count (using a hemocytometer).

## 2.5 Uptake and Location of Silver Within Soybeans

### 2.5.1 Inductively Coupled Plasma Mass Spectrometry

Acid digestion of plants followed the methods of Shute and Macfie (2006). First, leaves from each plant were placed in a brown paper bag and dried to constant mass in an oven at 60 °C. Aboveground stems and full root systems, with nodules removed, were separately dried in brown paper bags, and also dried to constant mass in the oven at 60 °C. Using the oven-dried samples for each plant, leaves, roots and stems were separately ground into a fine powder. Then ~0.1 grams of each were put into separate test tubes and digested using 1 mL OmniTrace® nitric acid. Reagent blanks (just nitric acid) and samples were digested at room temperature overnight and then the nitric acid was boiled until the orange-tinted fumes turned clear. One hundred and twenty-one digested samples were filtered using filter paper (VWR 415) and sent to the University of Western Ontario Biotron Analytical Lab (London ON) (plant root, stem and leaves concentrations). Each concentration 0 – 2.5 µg/mL had n = 10, this is due to 5 non-inoculated and 5 inoculated plants being pooled in order to gain better power. However, the 10 µg/mL treatment had only n = 3 due to not having enough AgNPs to prepare more replicates.. The National Institute of Standards and Materials did not have standard reference materials (SRM) with certified concentrations of silver within a plant matrix; therefore, no SRM was used to determine the efficiency of the acid digestion procedure for extracting silver from the plant samples.

### 2.5.2 Desorption of Silver from Root Surface

Roots were chemically desorbed to determine how much silver accumulated on the root surface, compared to how much silver was inside the roots. Twenty soybean plants were

grown as described in section 2.2.3. There were 5 controls (0  $\mu\text{g}$  AgNP /mL) and 15 treated plants (2.5  $\mu\text{g}$  AgNP /mL). Of the treated plants, 5 sets of roots were not desorbed so as to measure total silver associated with the roots, 5 sets were desorbed for the recommended time of 5 minutes, and the remaining 5 set were desorbed for a longer time (10 minutes).

Plants were harvested after 21 days of growth, which includes 14 days within the experimental treatment. Roots were separated from the shoots then rinsed with RO water. Control plants were not desorbed, but treated plants were soaked in Clorox bleach (200 mg/L, 50 mL, 5 or 8 minutes) then ammonium hydroxide (2.8%  $\text{NH}_3 \cdot \text{H}_2\text{O}$ , 50 mL, 1 or 2 minutes) and then a final rinse with RO water (50 mL, 1 or 2 minutes) following the methods of Zhang et al. (2019). All plants were then put into labelled paper bags and dried in the oven at 60 °C for at least 3 days. Plants were then ground into a powder, weighed, and digested in nitric acid for ICP-MS analysis (see previous section 2.5.1, Inductively Coupled Plasma Mass Spectrometry). Including two blanks and 20 plant samples, 22 total digested samples were sent to the Trent University Water Quality Lab (Peterborough ON) for ICP-MS (inductively coupled plasma mass spectrometry) analysis for silver, with a sample size of  $n = 5$  for each treatment. The amount of silver on the root surface was calculated by subtracting the amount in desorbed roots from the total amount in the corresponding non-desorbed roots.

### 2.5.3 Transmission Electron Microscopy

AgNPs were located and confirmed at a subcellular level using transmission electron microscopy (TEM) equipped with EDAX (energy-dispersive X-ray spectroscopy) (Philips 420 Transmission Microscope). On harvest day, 0.5 mm sections of a root tip, nodule, tap root and stem (epicotyl) were cut by hand from each plant and subsequently fixed with 2% glutaraldehyde and 3% paraformaldehyde in 0.1 M cacodylate buffer. Samples were then dehydrated with a graded ethanol series (50%, 70%, 90%, 95%, and then 100% for three times, each for 10 minutes, stained with (and some without) osmium tetroxide (which stains cell membranes only) and embedded in Spur's plastic. Embedded samples were then trimmed and cut on a microtome (Reichert-Jung Ultracut E) using a

diamond knife, to achieve cross-sections 70 nm thick. Based on my previous work (Boersma, 2019), attention was focused on plasmodesmata and extracellular regions, where more particles accumulate. TEM was performed to verify the presence of AgNP in the samples. Images were also collected from separate ‘test’ roots that were soaked in a very high concentration of AgNPs (2 mg/mL) for 2 hours before fixing, allowing more uptake of the particles and increased probability of finding AgNPs in the images, and to determine where they tend to accumulate. A total of 10 sections were examined.

## 2.6 Toxicity of Silver Nanoparticles to Soybeans

### 2.6.1 Phytotoxicity to Soybean

One day before harvest, the maximum potential quantum efficiency of photosystem II (variable fluorescence/maximum fluorescence;  $F_v/F_m$ ) was recorded for each plant treated with 30 nm AgNPs ( $n = 6$ ). Recordings were taken from only the second and third newest trifoliolate leaves, avoiding use of the newest trifoliolate, which was still developing and could affect results. Duplicate measurements were taken using a handheld fluorometer (Opti-Sciences, OS-30, USA), on leaves subjected to darkness for 30 minutes, with the median value being recorded per plant. The measurement of photosynthetic efficiency was not determined for plants subjected to 16 nm AgNPs, which also showed no visible effects of chlorosis and thus most likely also did not suffer any negative photosynthetic effects. On harvest day, leaf area was measured by removing leaves, flattening, and placing them on white paper alongside a ruler for scale, then taking a digital photograph. ImageJ (<https://imagej.nih.gov/ij/>) was used to process images. The colour scale was set to binomial to have the leaf a constant black colour while also allowing for selection of the leaf prior to using the program to calculate leaf area.

Leaves from each plant were placed in a brown paper bag and dried to constant mass in an oven at 60 °C, and total leaf mass was recorded for each plant. Aboveground stems and full root systems without nodules per plant were separately dried in brown paper bags, dried to constant mass in the oven at 60 °C and then weighed.

## 2.6.2 Carbon and Nitrogen Analysis

The concentrations of carbon and nitrogen in the soybean roots were measured to see if differences occurred when treated with AgNPs using a CHNS analysis machine, which combusts samples at (1800 °C) and uses ‘purge and trap’ chromatography, where a series of traps slows down the different elements allowing for differentiation. Nitrogen is not retained, thus comes out first, each other element is retained in their designated trap to allow the elements to separate in time. The elements are then detected by thermal conductivity, which is the reason why each element needs to be separated in time to quantify their presence within the sample.

## 2.7 Nodule Assessment

Nitrogen fixing activity of the nodules per inoculated plant (n = 6 per treatment) was assessed using an acetylene reduction assay (Bergersen, 1970) at Agriculture and Agri-Food Canada, London Research and Development Centre. Plants were clipped at the junction between the roots and the stem, roots were put into sealed vials, 10 µL of air was pulled from the vial with a syringe, and 10 µL of acetylene (C<sub>2</sub>H<sub>2</sub>) gas was added. Plants were processed in 5-minute intervals to ensure that each set of roots had equal time of exposure to acetylene. These intervals of 5 minutes were used as this was the time that it took for each sample to run. After 1 hour incubation with the acetylene gas, 10 µL of air from each sealed vial was injected into a GC-FID (Gas Chromatograph – Flame-Ionization Detection) to determine the amount of ethylene produced by nitrogenase reduction of the acetylene. Five non-inoculated plants were also processed, 3 with and 2 without silver treatment. Appendix B shows the standard curve that was used to estimate the nmol of nitrogen fixed by each set of roots. Nodule mass per plant was also recorded and used to quantify the nodule activity per gram of nodule, rather than just the total nodule activity per plant.

## 2.8 Data Analysis

Data analysis was conducted using Rstudio (Version 1.2.5042). The main packages used included ggplot2, tidyverse, dplyr, and MASS. Line graphs were completed in SigmaPlot, and box plots were completed on Rstudio. The significance level was set to  $p < 0.05$ , and all assumptions (i.e., normality and homogeneity of variance) were thoroughly checked through tests using plotted predictions and/or residuals on R. If variance was non-normal or non-homogeneous, then an ANOVA with Welch's adaptation not assuming equal variance was used. This was necessary for dry leaf biomass as well as desorption data. Student t-tests were done to confirm that weights (used to calculate concentrations of synthesized nanoparticle batches, as seen in section 2.2.2) were not significantly different from each other, thus were accurate measurements of the AgNP concentrations. One-way ANOVAs, followed by Holm-Sidak post hoc test when significant main effects were found, were performed for the other data sets, including biomass readings, carbon and nitrogen percentages, silver content (silver uptake), leaf area, nodule mass, nitrogen fixation rates and chlorophyll fluorescence.

## 3 Results and Discussion

In this section I will present the results of my experiment and the effects that AgNPs have on soybeans, its symbiont *B. japonicum* USDA 110 and their relationship. AgNPs were taken up mainly by the root and decreased both plant and bacterial growth at various concentrations and had detrimental effects on nodulation and nitrogen fixing.

### 3.1 Raman Measurements and Maps

Figure 3.1a shows a light microscopy image of a root section from a control plant that was assessed for Raman spectroscopy. The lack of clarity of the image is partially due to the resolution of the camera and partially due to zooming in to view a xylem cell within the stele of the root. Figure 3.1b shows three representative spectra taken from this region during mapping. These peaks correspond to vibrations of bonds within the sample and

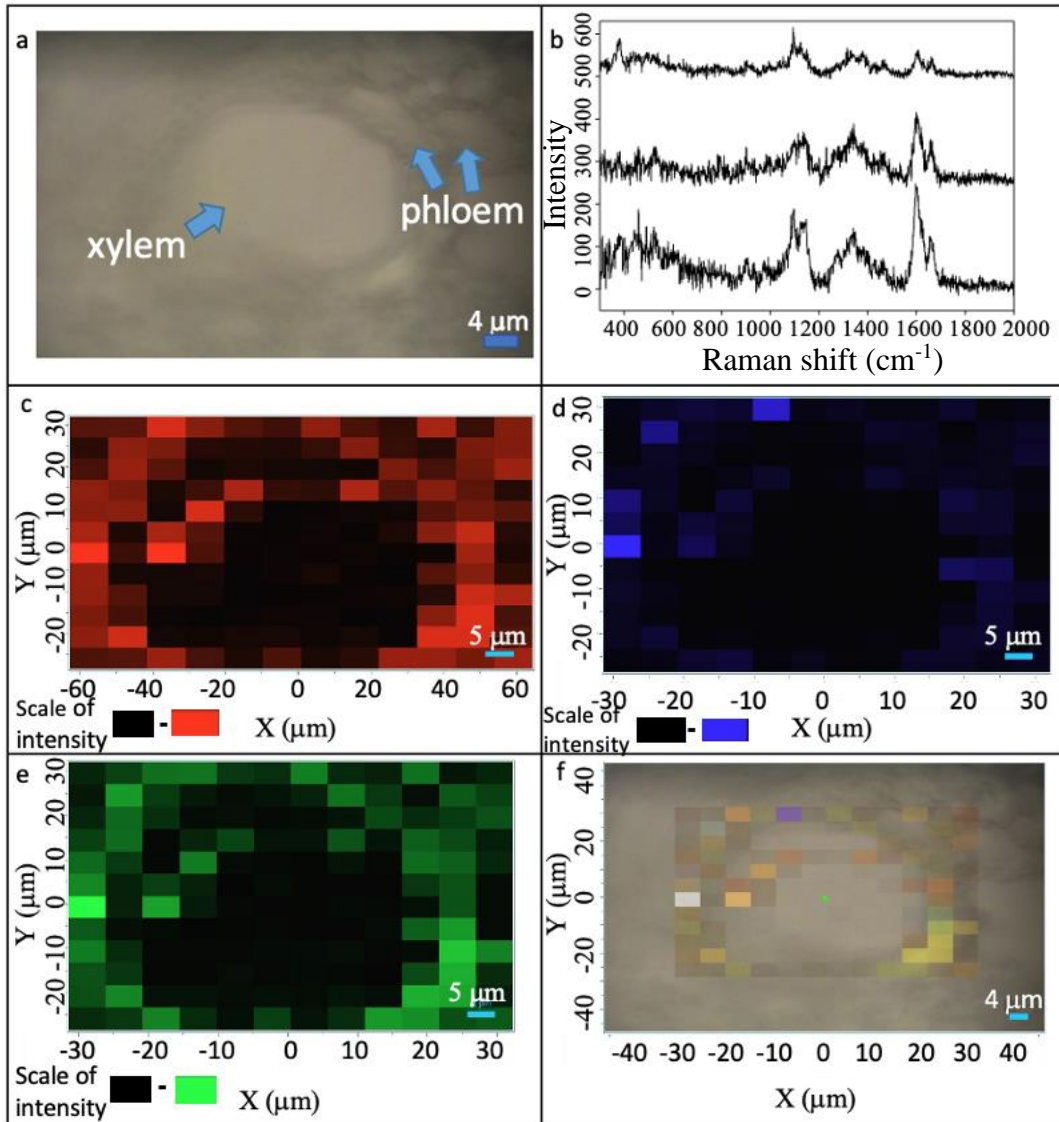


**Figure 3.1: Raman spectroscopy of control soybean root cross section showing a xylem cell within the stele.**

The top left panel (a) shows the light microscope video image of area assessed for Raman measurements of a root from a control plant. The top right panel (b) three representative spectra attained from Raman spectroscopy of control plants. The intensity is shifted for the two highest spectra so that space was inserted between each spectrum to achieve a vertical separation. The middle left panel (c) shows the red intensity map of the control plant from panel a, generated from the Raman peak between 1045 and 1165  $\text{cm}^{-1}$ , which represents cellulose, glucomannan and/or xylan. The middle right panel (d) shows blue intensity map of the control plant, generated from the Raman peak between 1238 – 1522  $\text{cm}^{-1}$ , which represents cellulose. The bottom left panel (e) shows the green intensity map of the control plant, generated from Raman peak between 1549 – 1702  $\text{cm}^{-1}$ , which represents lignin. The bottom right panel (f) shows the video image of control plant from panel a) with the corresponding overlapped red, blue, and green intensity maps. A scale of intensity could not be generated because the colour intensities are relative, not quantitative. The intensities range from zero (black) to the brightest spot (the brightest red, green or blue colour).



can be attributed to the molecular make-up of the sample. The peak ( $1096\text{ cm}^{-1}$ ) corresponds to cellulose, glucomannan and/or xylan (heavy atoms, any atom that is not hydrogen, for example CC and CO stretching). The peak at  $1333\text{ cm}^{-1}$  is attributed to cellulose (HCC and HCO bending) and the peak at  $1601\text{ cm}^{-1}$  is characteristic of lignin (aryl ring with symmetric stretching for bond vibrations) (Gierlinger and Schwanninger, 2006). The spectral intensity maps (Figure 3.1c-e) illustrate the locations and intensities for each type of signal in the cross section of the root. The intensity of the signal corresponds to the quantity of the bond that can be attributed to a particular molecule, but if gold or silver was close to any particular molecule it is possibly to have plasmonic resonance from these metal nanoparticles enhancing the signal by being near a bond. Being a control sample, this could not occur as there was no silver or gold present. Figure 3.1(c) shows the red intensity map for cellulose, glucomannan and/or xylan (the peak at  $1045 - 1165\text{ cm}^{-1}$  Raman shift) these molecules appear to be evenly distributed throughout the area sampled. Figure 3.1 (d) shows the blue intensity map for cellulose, which is the peak between  $1238 - 1522\text{ cm}^{-1}$  Raman shift. The cellulose signals are most likely coming from the cellulose signal indicated by the peak at  $1045 - 1165\text{ cm}^{-1}$  and not so much from the  $1238 - 1522\text{ cm}^{-1}$  signal. I came to this conclusion due to the blue intensity map having nearly no signals at all, meaning almost no cellulose detected. Figure 3.1 (e) shows the green intensity map for lignin, the signal between  $1549 - 1702\text{ cm}^{-1}$  Raman shift; it shows a ring of lignin surrounding the xylem cell. Figure 3.1f shows an overlay of all 3 intensity maps onto the video image for the control plant. Most of the signal comes from around the wall of the xylem cell, which is expected since the interior of xylem cells is open space (Zimmermann 1983) used to carry water and nutrients to the stems and leaves.

However, these images should be interpreted with caution. For example, although the red map for cellulose, glucomannan and/or xylan shows some signals from the interior of the xylem cell (Figure 3.1c) these signals could be attributed to the glass on which the sample was mounted.

A Raman spectrum for the glass is shown in Figure 3.2. Where the laser passes through the plant sample and picks up the glass signal, it produces a reading that cannot be

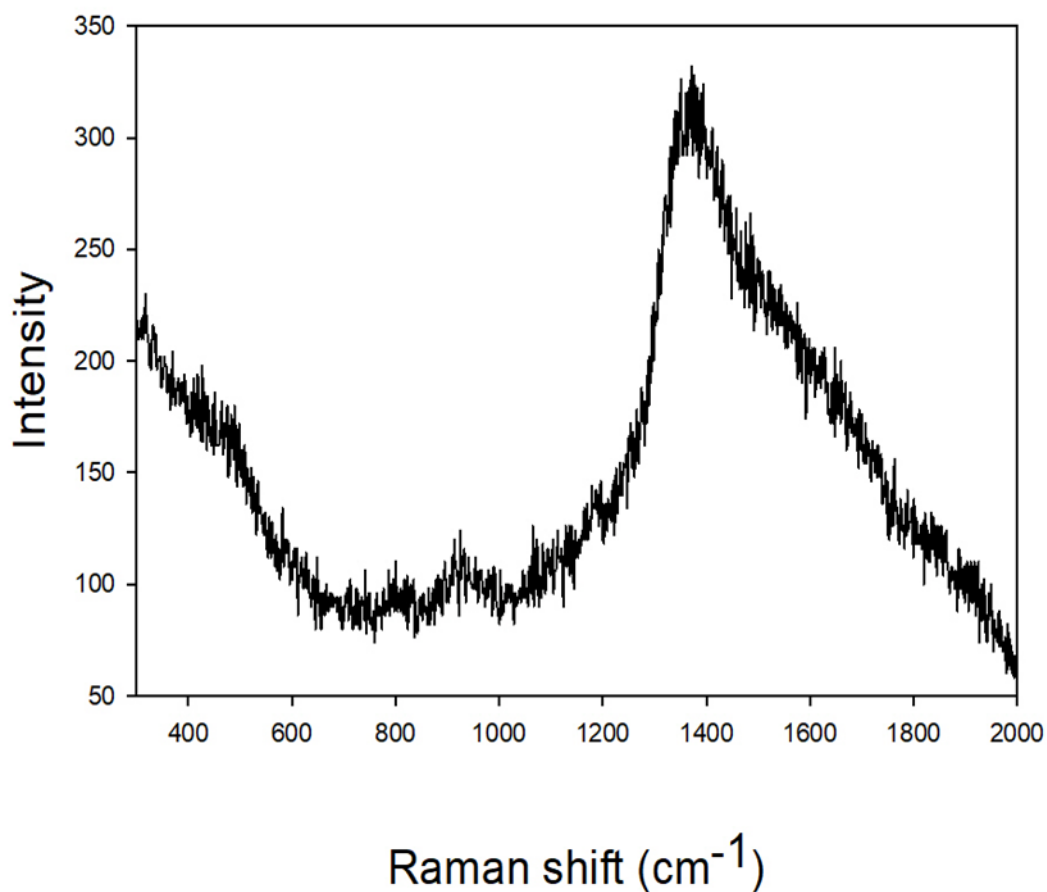


**Figure 3.2: Raman spectrum associated with glass.**

The peak at 1135-1800 cm<sup>-1</sup> represents glass. When the laser passes through a plant sample, the often-intense glass signal creates hot spots in the intensity maps. This interference reduces the ability to detect signals from peaks of interest in the plant sample.

distinguished from that of the plant sample. When the signal from the glass is intense, it is a problem for the lower intensity readings from the plant sample as it creates a 'bright' spot on the intensity map. The intensity scale is relative, meaning that a bright spot effectively 'dulls' the actual readings. This was specifically a problem for the blue and red maps, which had less overall intensity, thus were more affected by the high intensity of the glass signals.

Glucomannan is mainly found in seeds and wood and thus is most likely a molecule that is not represented in the red map, yet it is possible since it has been found in mung bean seedlings (Elbein 1969). The red map likely does indicate xylan and cellulose, as they are an integral part of plant cell walls and found associated together (Busse-Wicher et al. 2016; Simmons et al. 2016; Wang and Hong, 2016). Another main component of the cell wall is the molecule lignin, which is highly abundant in xylem cell walls (reviewed in Liu et al. 2018). It is likely all these molecules (with the exception of glucomannan) are within the sample. However, it is hard to tell if a glass signal has altered the red map as there should be no signals from the empty centre of the xylem cell.

Figure 3.3a shows an area of the of the AgNP-treated plants that was assessed for Raman spectroscopy, the approximate location is difficult to define due to inability to focus the image. Figure 3.3b shows three representative spectra taken from this area during mapping, these spectra show similar peaks compared to the control: peaks at 1096, 1333 and 1601  $\text{cm}^{-1}$  showing the distributions of cellulose, glucomannan and/or xylan, cellulose, and lignin, respectively. As with the control, intensity maps were created for these peaks. Figure 3.3c shows the red intensity map for cellulose, glucomannan or xylan, which has similar features to the control sample with signals detected throughout the cross section. Figure 3.3d shows the blue intensity map for cellulose, on which one bright spot can be seen, which resulted in failure to detect the localization of cellulose in the sample. Other root cross sections were examined, and each was problematic due to the laser picking up at least one intense signal from the glass under the sample. One would expect cellulose to be positioned around the xylem cell and not in the open space in the centre. The same problem occurred for the green intensity map of lignin (Figure 3.3e) and

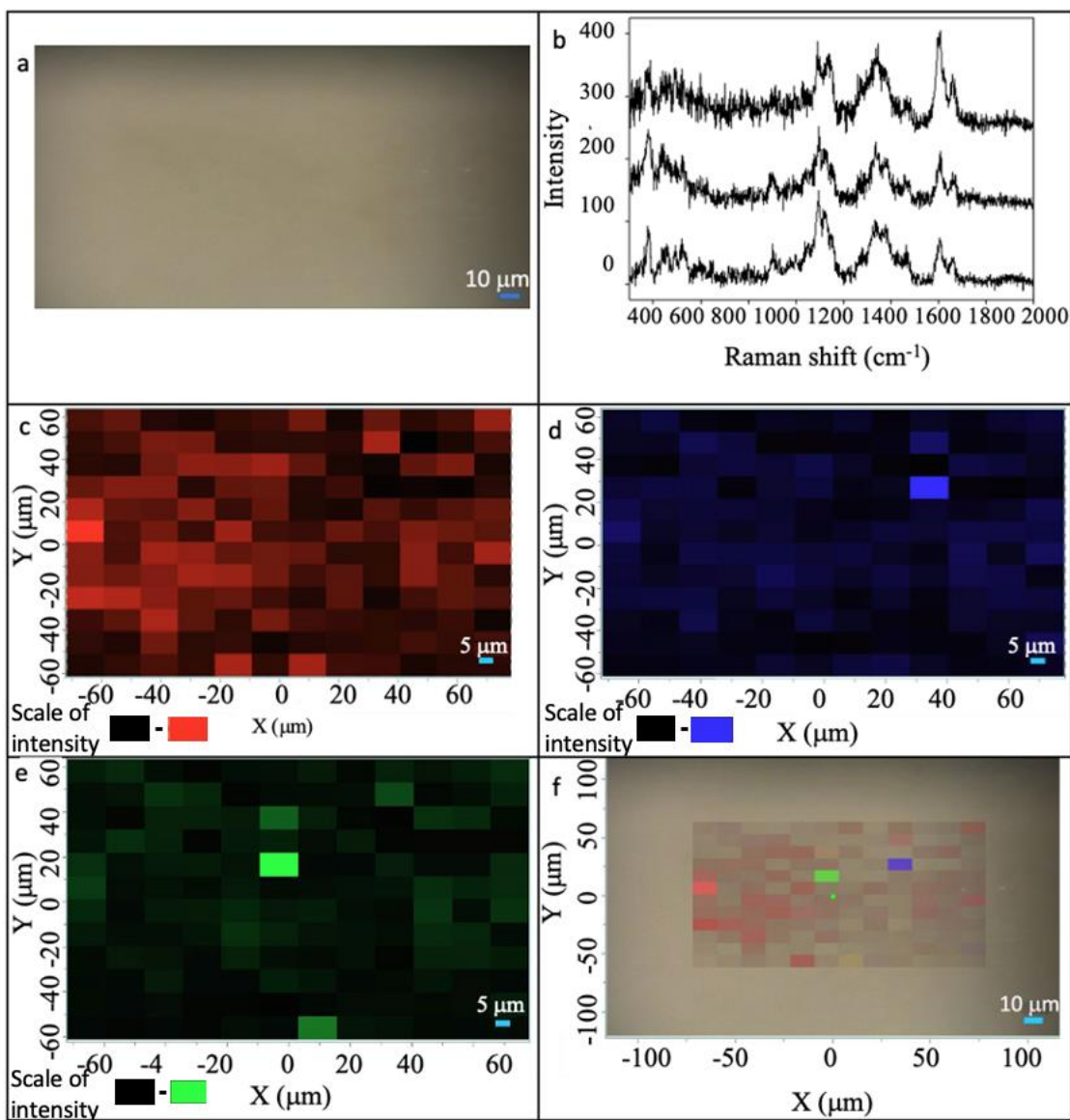


**Figure 3.3: Raman spectroscopy of an AgNP-treated soybean root cross section showing a xylem cell within the stele.**

The panel at the top left (a) shows the light microscope video image of area assessed (xylem) for Raman measurements of plants treated with 2.5  $\mu\text{g/mL}$  of 30 nm AgNPs. The panel at the top right (b) shows 3 examples of spectra attained from Raman spectroscopy of treated plant, intensity is shifted for two highest spectra so that space was achieved between each spectra, to achieve vertical separation. The panel middle left (c) shows red intensity map for treated plant, generated from Raman peak between 1045 and 1165  $\text{cm}^{-1}$ , cellulose, glucomannan and/or xylan. The middle right panel (d) shows blue intensity map for treated plant, generated from Raman peak between 1238 – 1522  $\text{cm}^{-1}$ , which corresponds with cellulose. The bottom left panel (e) shows green intensity map for treated plants, generated from Raman peak between 1549 – 1702  $\text{cm}^{-1}$ , which corresponds with lignin. The bottom right panel (f) shows the video image of control plant from panel a) with the corresponding overlapped red, blue, and green intensity maps. A scale of intensity could not be generated because the colour intensities are relative, not quantitative. The intensities range from zero (black) to the brightest spot (the brightest red, green or blue colour).

in the overlay of all 3 intensity maps onto the video image for the treated plant (Figure 3.3 f).

One other problem was that the video images for AgNP-treated roots were difficult to focus, which may have contributed to not being able to detect strong signals from the molecules within the sample. This is because blurriness of the image does not allow us to orientate ourselves in areas where we can assume we have the best chance to see AgNPs, such as the xylem. Having an uneven surface may also contribute to unclear sample readings with some spots not being detected as well as other areas.

Nonetheless, when comparing the spectra from control (Figure 3.1b) versus (Figure 3.3b) AgNP-treated roots, there was no perceptible difference in any peak's intensity between the control and treated samples. If anything, the control spectra had higher intensities than those from the treated plants. This is the opposite of what was expected since it was hypothesized that the plasmonic resonance of AgNPs would increase the signal of any bonds that they were near (reviewed in Long, 2002).

In conclusion, the Raman spectroscopy was useful for determining the position of lignin and cellulose/xylan (and possibly, but unlikely, glucomannan) within the root cross sections. One can also conclude that the amount of AgNPs within the sample was not concentrated enough to produce an enhanced signal for any of the molecules detected. Therefore, Raman spectroscopy was unable to detect the location or bonding environment of the AgNPs. More method development is needed to assess the potential of Raman spectroscopy to detect localization of AgNPs in plants. It is possible that with higher concentrations or larger particles and a wavelength that is closer to the resonance of the particles could generate a stronger signal. Testing plants exposed to larger AgNPs might result in larger signals because longer wavelengths could be used, and these generate less fluorescence because the sample is being hit with decreased energy (Yeshchenko et al. 2012). Higher concentrations of AgNPs would, however, not likely be environmentally relevant. The dose used was similar to concentrations of AgNPs in biosolids, which was anywhere from 1.94-856 mg/kg (USEPA, 2009). The treatment concentration was roughly 10 mg/kg, but being in hydroponic solution more of the nanoparticles would be bioavailable as they would not be affected by, or interact with, soil components.

## 3.2 Silver Nanoparticle Effects on *Bradyrhizobium japonicum* USDA 110

Bacterial growth was inhibited at 10  $\mu\text{g/mL}$  of 16 nm AgNPs (Figure 3.4). Treated cell cultures did not grow over 4 days' exposure to AgNPs, while control cultures grew exponentially over the same time period. They stayed in exponential growth for this period of time likely due to being at a lower than optimal temperature (22  $^{\circ}\text{C}$  as compared to 28  $^{\circ}\text{C}$ ). However, I used a relatively high concentration (10  $\mu\text{g/mL}$ ) of AgNPs; a level that would probably not be reached in the environment for many years at the current rate of accumulation. In contrast, Shah et al. (2014) reported no inhibitory effect of nanoparticles, including AgNPs, on the genus *Bradyrhizobium*. In their experiment, they treated potted field soil (23.6 cm  $\times$  26.7 cm pot with 20 cm of soil in pot) with 550 mg of various types of nanoparticles, depending on the weight of the soil. Their concentrations are quite high compared to my bacterial medium dose of 10 mg/L (roughly 10 mg/kg given the aqueous medium), and slightly higher than the highest levels of silver within biosolids (856 mg/kg) and they did not identify bacteria to the species level. I would expect AgNPs to be more toxic in hydroponics, due to AgNPs and silver ions being almost fully bioavailable to the plant, as compared to in soil where they would bond with soil organic compounds and other materials (Jones and Peterson, 1986; Jacobson et al. 2005). Although Shah et al. (2014) determined that the genus *Bradyrhizobium* is tolerant of AgNPs, it is possible that *B. japonicum* is more sensitive than other species in this genus. Since their study did not test individual species within the genus, increases and decreases for individual species in response to AgNPs might have led to no overall change at the genus level.

## 3.3 Location of Silver Within Soybeans

Transmission electron microscopy was used to detect nanoparticles in root cross sections. Figure 3.5a shows a section of a control root with no AgNPs present, and Figure 3.5b is an image of a section of a root from a plant given 2.5  $\mu\text{g/mL}$  of 30 nm AgNPs, which shows very small amounts of silver within it. The nanoparticles are better seen in plants given a high dose before imaging (Figure 3.5c), in which they can be seen in the cell

wall and also scattered throughout the cell. Some plasmodesmata in roots appeared clogged with AgNPs (Figure 3.5d). Giesler-Lee et al. (2014) found a similar pattern of AgNPs in *Arabidopsis*; the particles were throughout the cell wall and accumulated in the middle lamella or cell corner as well as within plasmodesmata.

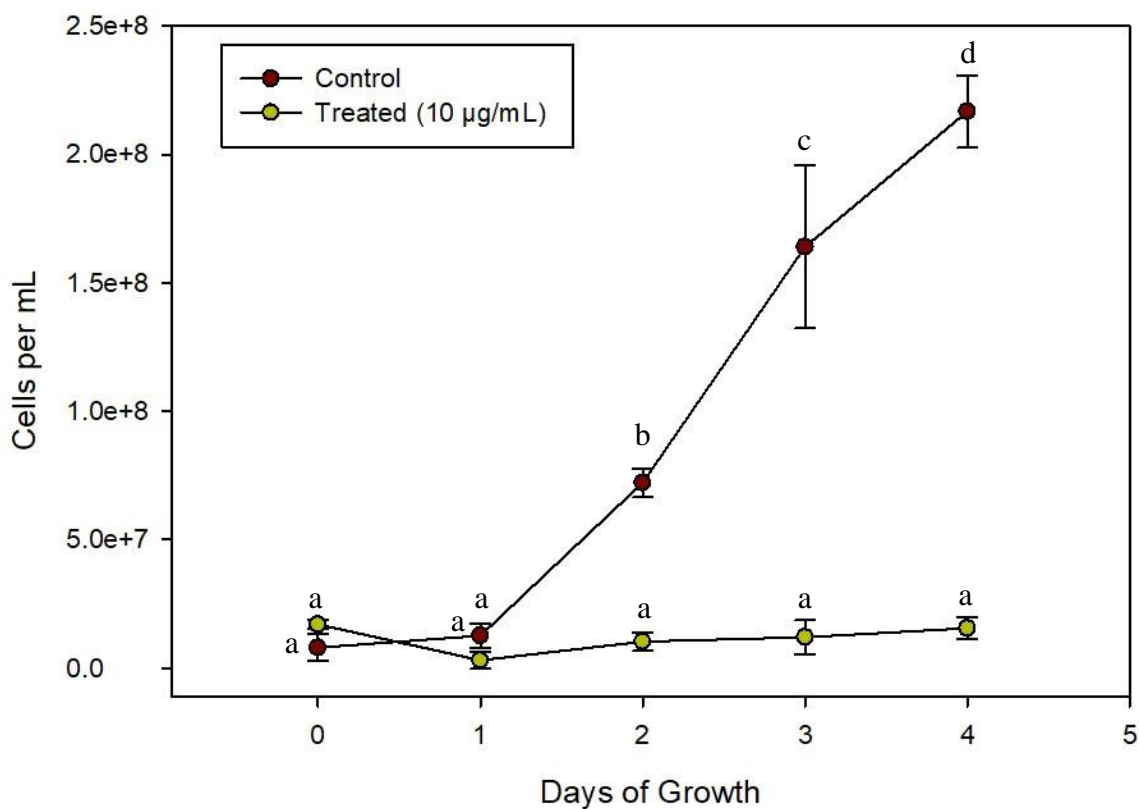


**Figure 3.3 Growth of *Bradyrhizobium japonicum* USDA 110 in response to AgNPs.**

Liquid cell cultures exposed to 16 nm AgNPs at a concentration of 10 µg/mL were grown in 96-well plates. The density of cells in liquid cultures was measured as optical density and converted to cells/mL (Appendix A).



### 3.4 Location of Silver Within Soybeans

Transmission electron microscopy was used to detect nanoparticles in root cross sections. Figure 3.5a shows a section of a control root with no AgNPs present, and Figure 3.5b is an image of a section of a root from a plant given 2.5  $\mu\text{g/mL}$  of 30 nm AgNPs, which shows very small amounts of silver within it. The nanoparticles are better seen in plants given a high dose before imaging (Figure 3.5c), in which they can be seen in the cell wall and also scattered throughout the cell. Some plasmodesmata in roots appeared clogged with AgNPs (Figure 3.5d). Giesler-Lee et al. (2014) found a similar pattern of AgNPs in Arabidopsis; the particles were throughout the cell wall and accumulated in the middle lamella or cell corner as well as within plasmodesmata.

The ICP-MS analysis verified that silver entered and moved throughout the plant. Figure 3.6a shows that the concentration of silver in roots increased with concentration of AgNPs in solution, except between 0.5 and 1  $\mu\text{g/mL}$ , with root tissue of treated plants appearing to have a proportional increase of silver, showing five times more silver within roots treated with five times more concentrated AgNP solution (0.5  $\mu\text{g/mL}$  compared to 2.5  $\mu\text{g/mL}$ ), and a 16-fold increase in root silver content in plants treated with 20 times more concentrated AgNP solution. The total amount of silver associated with the root, however, may not be a good indication that silver entered the plant; it could be in a root plaque on the root surface. This root plaque did contain 98-99% of the silver that was associated with the roots, as can be seen in Figure 3.6b, which would likely still occur in soil. As seen in iron (Fe) plaque formation there was 12 and 32 times more iron plaque on plants in solution as compared to plants within soil (Chen et al. 2008). Yet this was at 5 weeks of growth, after 11 weeks there was a 50% decrease of Fe root plaque (Chen et al. 2008), which indicates that root plaque formation may reach a maximum then decrease over time. Silver plaques may act differently than iron plaques and could potentially reach a maximum earlier and/or never decline. The plants grown for my experiment were exposed to silver for only 2 weeks. Given longer, this plaque could possibly develop to the point where it cannot hold any more silver and excess silver could be readily taken up by the plant. Likely the plaque depends on concentrations, pH, media and other factors.



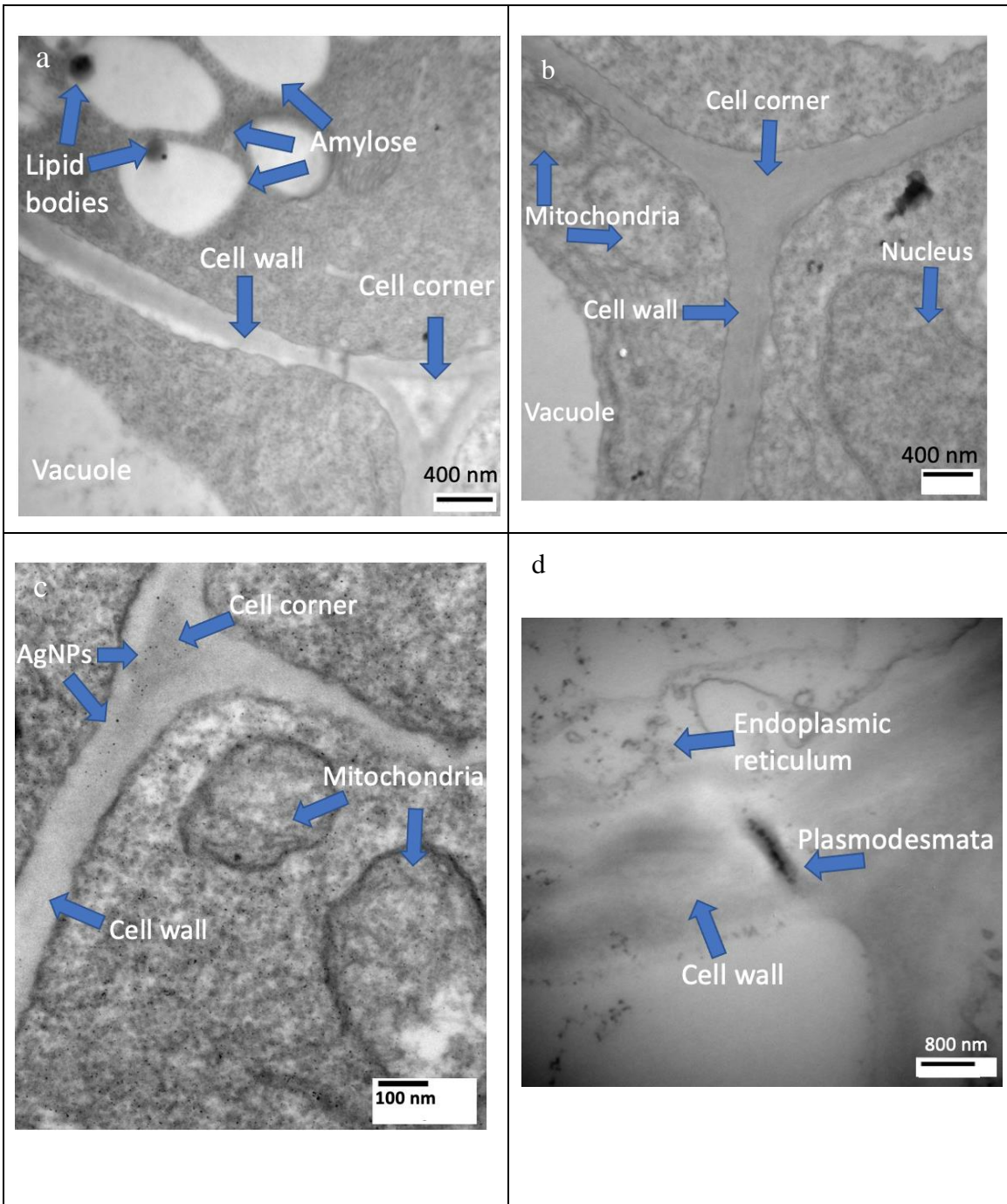


**Figure 3.4: Electron micrographs of root cross sections.**

Transmission electron microscope images of panel a) a control root with no AgNPs and panel b) a plant treated with 2.5  $\mu\text{g}/\text{mL}$  for 2 weeks, similar to all other experiment treatment times; no AgNPs are visible. Panel c) Transmission electron microscope image of a plant treated with 30 nm AgNP at 2.5  $\mu\text{g}/\text{mL}$  for two weeks with a super dose of 3.35 mg/mL for 2 hours previous to imaging. Panel d) Transmission electron microscope image of a plasmodesmata that is possibly clogged with 30 nm AgNPs, EDAX was not done to confirm particle composition.

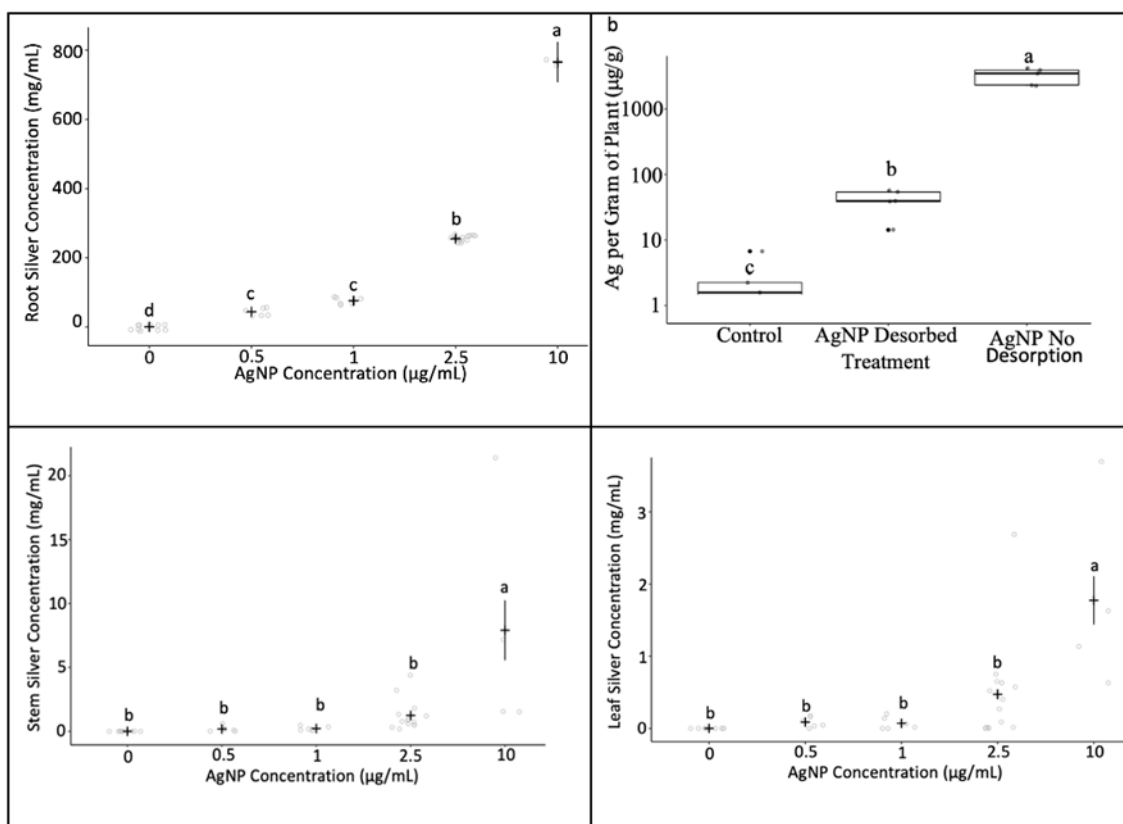


**Figure 3.5 Silver was taken up by and translocated within the plants.**

Concentrations of silver increase with AgNP doses in roots (a), stems (c) and leaves (d) with most of the silver being retained in the roots. Panel (b) concentration of silver in roots from control plants and AgNP-treated plants with and without chemical desorption of silver from the root surface.

Panel a)  $F = 260.7$ ,  $p < 0.0001$ ,  $n = 10$  for 0 – 2.5 µg/mL and  $n = 3$  for 10 µg/mL, this was done to conserve AgNPs. Panel b)  $F = 27.6$ ,  $p > 0.05$ ,  $n = 5$ , data plotted on log scale. Panel c)  $F = 3.323$ ,  $p < 0.05$ ,  $n = 10$  for 0 – 2.5 µg/mL and  $n = 3$  for 10 µg/mL, this was done to conserve AgNPs. Panel d)  $F = 6.373$ ,  $p < 0.001$ ,  $n = 10$  for 0 – 2.5 µg/mL and  $n = 3$  for 10 µg/mL, this was done to conserve AgNPs. The post-hoc used to determine difference between treatments was Holm-Sidak while for panel b a one-way ANOVA with Welch's adaptation not assuming equal variance was used, followed by Games-Howell post hoc test). All significant differences are denoted by lower case letters, and `geom_jitter()` (on R) was used to distribute data points horizontally for easier viewing.

The development of a root plaque has both advantages and disadvantages to a plant. If the plaque prevents silver (and other toxic elements) from entering the soybean root and being translocated aboveground, then the edible beans might not accumulate silver and remain safe to eat. However, elemental binding in the plaque is not specific and it might reduce the uptake of nutrients by the plant, as seen with iron plaque blocking zinc uptake (Otte et al. 1989). Most likely thicker root plaques will have even more of a detrimental effect on nutrient uptake and plant roots grown in high-silver environments for long periods of time may essentially become ‘clogged’.

Despite the high proportion of silver on the surface of the root, measurable concentrations were found in the stem and leaves. Figure 3.6c shows the higher silver concentrations in the stems from plants grown with 10  $\mu\text{g/mL}$  only. Significant accumulation also occurred in the leaves of plants from the 10  $\mu\text{g/mL}$  treatment (Figure 3.6d). Overall, the stem silver concentration increased roughly ten times with a 10-fold increased AgNP concentration (comparing 1  $\mu\text{g/mL}$  to 10  $\mu\text{g/mL}$ ). The leaf also had a proportional relationship in terms of silver uptake with roughly ten times higher leaf silver concentrations with a 10-fold increase in AgNP concentration (comparing 1  $\mu\text{g/mL}$  to 10  $\mu\text{g/mL}$ ).

Silver is entering the soybean plants and moving up through the plant despite the root plaque barrier. This was also seen by Giesler-Lee et al. (2014), who found that movement of silver depended on the size of the particle, and that smaller particles could readily enter plant roots at low concentrations, yet this was reversed at high concentrations. The authors did not speculate on the reason why this might occur, but they did find that with only  $\text{AgNO}_3$  not as much silver entered the plant compared to when plants were given AgNPs. It is possible that AgNPs facilitate the uptake of more silver ions into the plant roots and up the plant, possibly larger particles are entering due to creation of new or larger pores, yet this was only speculated in Navarro et al. (2008). Larger pores could allow for more movement of silver throughout the plant, leading to an appearance of more silver movement to the leaves and shoot with larger particles.

### 3.5 Silver Nanoparticle Effects on the Mass and Health of Soybeans

The dry mass of roots, stems and leaves of inoculated and non-inoculated plants are shown in Figure 3.7, while top growth (stem and leaf) and total biomass along with chlorophyll fluorescence and leaf area are seen in Figure 3.8. Root dry biomass for non-inoculated plants given 2.5  $\mu\text{g/mL}$  of 30 nm AgNPs was about 125% higher than that of the control, while the dry mass of inoculated plants did not vary with treatment (Figure 3.7a). The root mass increase might be due to the response of roots reaching out into new areas that are not afflicted by AgNPs, it is possible the inoculated plants do not have the same response because they are saving energy for the nodulation process, or genes related to root growth have been suppressed due to the nodulation process. For the 16 nm AgNP treated plants only inoculated plants were tested. The dry root biomass decreased by 40-55% compared to control when treated with 0.5, 1 and 2.5  $\mu\text{g/mL}$  AgNPs (Figure 3.7b). Compared to the 30 nm particles the 16 nm AgNPs are clearly more toxic for the plant and result in decreased root growth. Even at low concentrations these smaller particles inhibited root growth.

Stems appear to be more sensitive than roots to silver toxicity. The 30 nm AgNP-treated plants had a 55% decrease in dry stem biomass for non-inoculated plants and a 60% decrease for inoculated plants given 2.5  $\mu\text{g/mL}$  AgNPs (Figure 3.7c). For 16 nm AgNP, the stems of inoculated plants were 60-70% smaller than control for all treated plants (0.5, 1 and 2.5  $\mu\text{g/mL}$  AgNPs) (Figure 3.7d). Leaves were also more sensitive than roots. In non-inoculated plants, leaf dry biomass for 30 nm treated plants given 2.5  $\mu\text{g/mL}$  AgNPs were roughly 25% less than control, while the inoculated plants dry leaf biomass decreased by 50% (Figure 3.7e). For plants given 16 nm AgNPs, dry leaf biomass for treated plants was 60-70% of control (Figure 3.7f). Not surprisingly, for plants given 30 nm AgNPs, non-inoculated plants given 2.5  $\mu\text{g/mL}$  had a 10% decrease in top growth (stem plus leaf), and inoculated plants given 2.5  $\mu\text{g/mL}$  had a 50% decrease (Figure 3.8a). For 16 nm-treated plants, top growth was reduced by about 65% in plants from all AgNP treatments (Figure 3.8b).

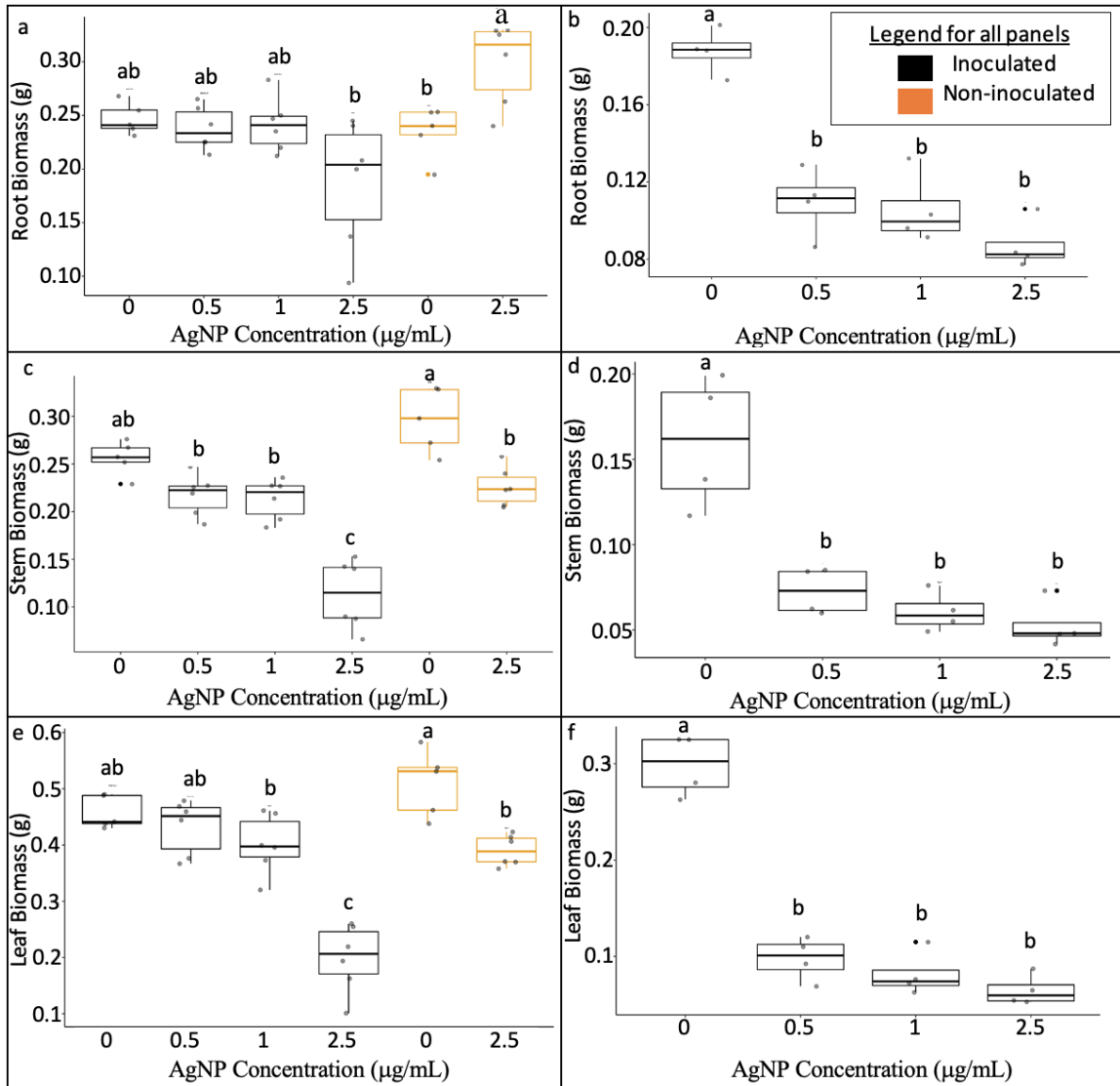




**Figure 3.8 Dry biomass of roots, stems and leaves for inoculated and non-inoculated plants treated with AgNPs.**

The panels on the left side are for plants treated with 30 nm AgNPs, the panels on the right are for plants treated with 16 nm AgNPs. Root biomass (top panels) did not vary with AgNP treatment for inoculated plants with 30 nm AgNPs, decreased when given 16 nm AgNPs, and decreased with dose in non-inoculated plants. Stem (middle panels) and leaf (bottom panels) dry biomass decreased with increased concentrations of AgNPs. The results of one-way ANOVA are as follows: Panel a)  $F = 5.552$ ,  $p < 0.01$ . Panel b)  $F = 33.54$ ,  $p < 0.001$ . Panel c)  $F = 30.98$ ,  $p < 0.001$ . Panel d)  $F = 19.55$ ,  $p < 0.001$ . Panel e)  $F = 28.02$ ,  $p < 0.001$ . Panel f)  $F = 83.76$ ,  $p < 0.001$ .  $N = 5$  for all treatments described. The post-hoc used to determine difference between treatments was Holm-Sidak. All significant differences are denoted by lower case letters, and `geom_jitter()` (on R) was used to distribute data points horizontally for easier viewing.

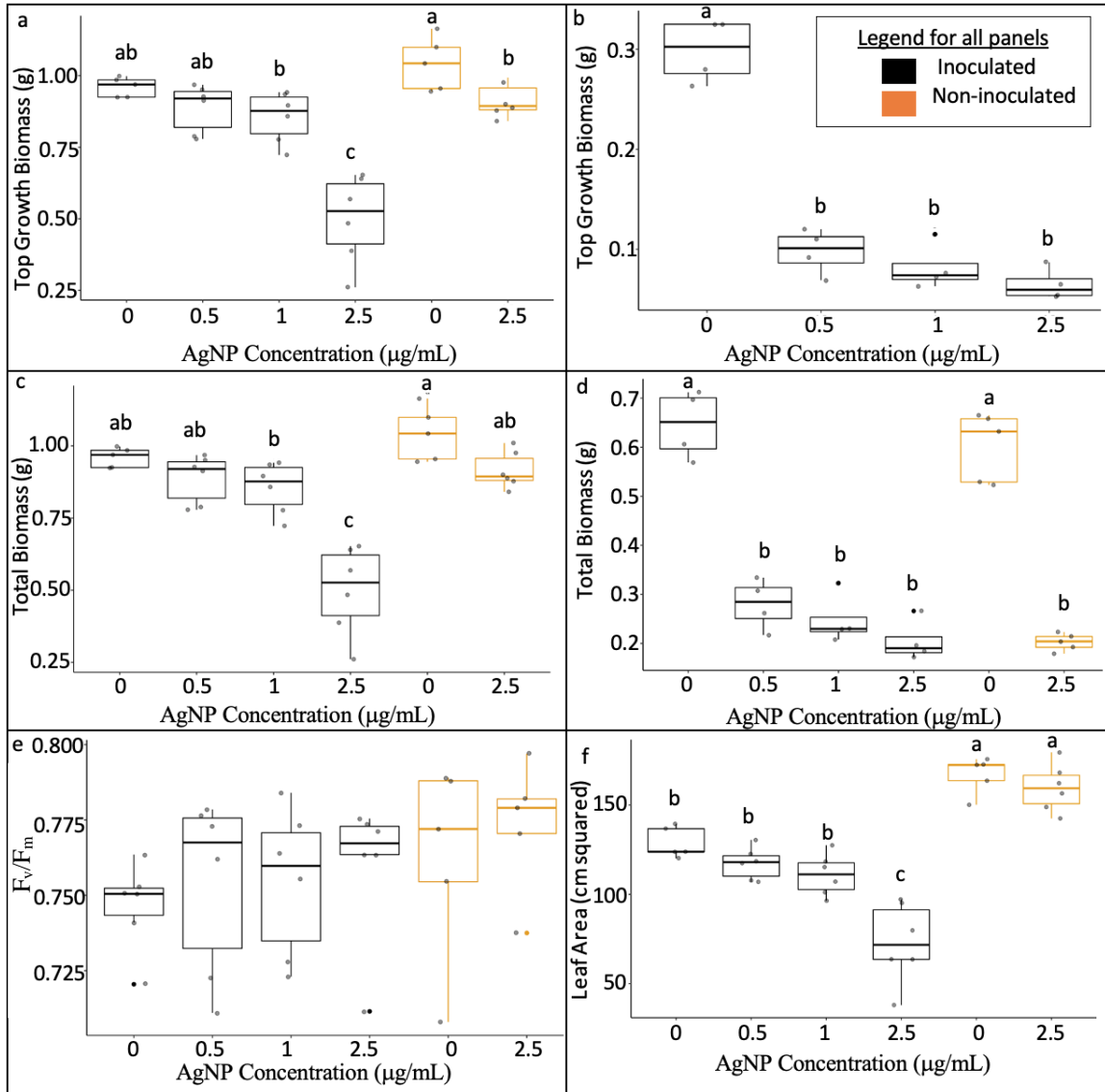


**Figure 3.9: Top growth, total biomass for inoculated and non-inoculated plants given both 16 nm and 30 nm AgNPs, as well as the chlorophyll fluorescence and leaf area for plants subjected to 30 nm AgNPs.**

The panels on the left side are for plants treated with 30 nm AgNPs, the panels on the right are for plants treated with 16 nm AgNPs, except for leaf area on the right which also had 30 nm AgNPs. Top growth (top panels) decreased with increasing AgNP dose for both inoculated and non-inoculated plants. Total biomass (middle panels) decreased with increased concentrations of AgNPs.  $F_v/F_m$  in leaves (bottom left panel) did not vary with treatment of AgNPs, yet leaf area (bottom right panel) showed decreases with increased concentration of AgNPs. The results of one-way ANOVA are as follows: Panel a)  $F = 32.15$ ,  $p < 0.001$ . Panel b)  $F = 49.27$ ,  $p < 0.001$ . Panel c)  $F = 22.62$ ,  $p < 0.001$ . Panel d)  $F = 55.66$ ,  $p < 0.001$ . Panel e)  $F = 0.701$ ,  $p = 0.627$ . Panel f)  $F = 36.39$ ,  $p < 0.001$ .  $N = 5$  for all treatments described. The post-hoc used to determine difference between treatments was Holm-Sidak. All significant differences are denoted by lower case letters, and `geom_jitter()` (on R) was used to distribute data points horizontally for easier viewing.

These findings make sense. The elongated roots of the non-inoculated plants given 30 nm AgNPs might be expected to be accompanied by decreases to their aboveground biomass due to an energetic trade-off for increased root growth.

The detrimental effects of AgNP treatment on aboveground biomass could be due to direct effects on growth or indirect effects on the nitrogen fixation process. Nitrogen is a necessary macronutrient for plant growth. Plant growth would not be possible without nitrogen, thus with limited nitrogen plant growth will also be limited. The non-inoculated plants have been given enough nitrogen to grow normally, therefore the negative effects to their growth can be attributed to factors other than nitrogen limitation unless the transport and uptake of nitrogen was affected by the AgNPs, although VISUAL MINTEQ did not indicate any unavailable nutrients across the experimental pH range. Yet the inoculated plants' decreased growth could be attributed to the problems with nodulation, along with growth problems.

For plants given 30 nm AgNPs, total biomass did not differ between the non-inoculated plants treated with 0 and 2.5  $\mu\text{g}/\text{mL}$  AgNPs, but there was a 40-50% decrease for inoculated plants given 2.5  $\mu\text{g}/\text{mL}$  compared to all other treatments (Figure 3.8c). This could indicate problems with nitrogen fixation since similar concentrations did not have any effect on the growth of non-inoculated plants. Yet when the nanoparticle size was decreased to 16 nm, growth was reduced for both inoculated and non-inoculated plants by similar amounts at the same concentrations of AgNPs. These results also help confirm that smaller particles are more phytotoxic, as was found by Giesler-Lee et al. (2014) and Martínez-Castañón (2008).

For control plants from the set given 16 nm AgNPs, there was no significant difference in total biomass between inoculated and non-inoculated plants. Yet there was a 50-70% decrease in total biomass for all treated plants (2.5  $\mu\text{g}/\text{mL}$ ), whether inoculated or non-inoculated, compared to controls (Figure 3.8d). Since not only the inoculated but also the non-inoculated plants were negatively affected by AgNPs, the smaller nanoparticles have clear and obvious direct negative effects on plant growth that cannot just be attributed to indirect effects on the nitrogen fixation of these plants. Although the nature of these

effects is unknown and outside the scope of this project, this may have something to do with the root plaque, or to some of the damaging effects that AgNPs have on membranes and proteins (see section 1.6). One thing that can most likely be ruled out is the effects of AgNPs on photosystem II, since the photochemical efficiency of photosystem II ( $F_v/F_m$ ) was the same for inoculated or non-inoculated plants at any concentration given (up to 2.5  $\mu\text{g/mL}$ ) (Figure 3.8e). The value of  $F_v/F_m$  was lower than 0.8, which is indicative of a healthy typical plant. However, healthy soybeans have been documented to have an  $F_v/F_m$  of roughly 0.7-0.75 at their first trifoliolate stage (Hong et al. 2019). There is likely no effect of AgNPs on photochemical efficiency. Although leaf area of plants treated with 30 nm AgNPs decreased by 5-50% for only the inoculated plants (Figure 3.8f). Although photosynthetic efficiency was unaffected by AgNPs, the reduced leaf area of inoculated plants would explain their smaller aboveground biomass.

### 3.6 Nodulation, Nitrogen Fixation and Bacteroid Health

Total nodule biomass decreased by 45% and 70% when inoculated plants were given 30 nm AgNPs at 1 and 2.5  $\mu\text{g/mL}$ , respectively (Figure 3.9a). This also happened with 16 nm AgNPs but, like overall plant growth, the plants given smaller particles were more affected by lower concentrations of AgNPs. Nodule biomass for plants from every AgNP treatment (0.5, 1 and 2.5  $\mu\text{g/mL}$ ) was very close to zero, with masses equal to 1-2% of the control (Figure 3.9b). Since AgNPs are antimicrobial, this decrease in both size and nodule biomass does not come as a surprise. Even if the soil-form of *B. japonicum* is relatively tolerant of environmental levels of AgNPs (Shah et al. 2014), I did find that 10  $\mu\text{g/mL}$  completely inhibited bacterial growth). I also suspect the bacteroid form within nodules could be more sensitive than the soil form, due to the metabolic changes when switching from consuming carbon sources in soil to fixing nitrogen for the plant, nitrogen fixing is easily disrupted by oxygen and other elements that are more electronegative than nitrogen. Smaller particles are known to penetrate plant roots more easily at lower concentrations (Giesler-Lee et al. 2014), and smaller particles are likely to induce higher ROS formation and oxidative stress due to higher release of silver ions (Manke et al. 2013), both of which would induce more damage. These smaller particles enter easier

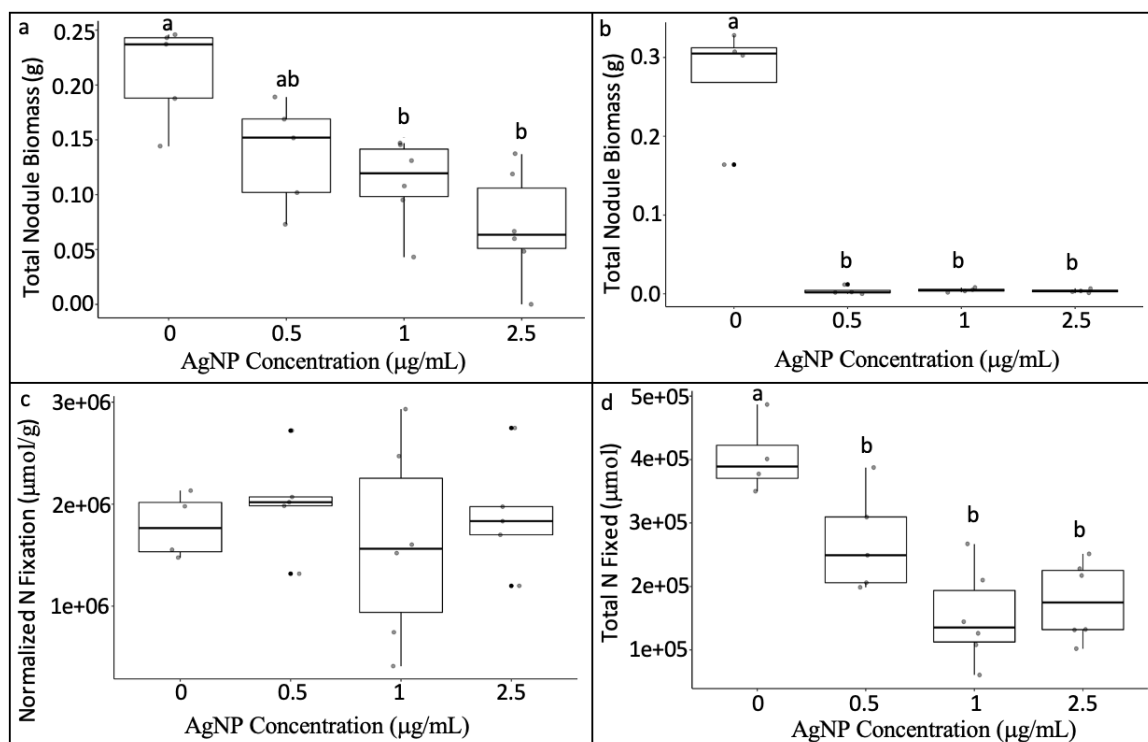


**Figure 3.10: Total nodule biomass of inoculated plants given both 16 nm and 30 nm AgNPs, along with normalized nitrogen fixation and total fixation of nitrogen.**

The top left panel (a) shows plants subjected to 30 nm AgNPs with decreasing nodule biomass with increasing AgNPs, while the right-hand top corner (b) is subjected to 16 nm AgNPs which shows a much lower nodule biomass at even lower concentrations. Both bottom panels are subjected to 30 nm AgNPs, bottom left (c) is normalized nitrogen fixation, while bottom right (d) is total nitrogen fixed. Normalized nitrogen fixation shows no changes the total amount of nitrogen fixed declines when given AgNPs. Panel a)  $F = 8.984$ ,  $p < 0.001$ . Panel b)  $F = 71.78$ ,  $p < 0.001$ . Panel c)  $F = 0.361$ ,  $p = 0.782$ . Panel d)  $F = 12.43$ ,  $p < 0.001$ .  $N = 5$  for all treatments described. The post-hoc used to determine difference between treatments was Holm-Sidak. All significant differences are denoted by lower case letters, and `geom_jitter()` (on R) was used to distribute data points horizontally for easier viewing.

simply due to being the same size as pores in the cell wall, whereas larger ones are filtered out essentially as most pores in cell walls are 3.5 – 5.5 nm (Carpita et al. 1979; Chesson et al. 1997). Yet AgNPs can still enter as seen in Giesler-Lee et al. 2014 with 40 nm AgNPs confirmed within the plant's roots, which most likely entered through nanoparticle induced enlarged pores which can reach up to 40 nm in size as reviewed in Navarro et al. (2008).

My results on nodulation and nitrogen fixation suggest that there is damage caused to the nodulation process or to the bacteroids themselves.. The nodules of AgNP-treated plants (concentrations 1 and 2.5  $\mu\text{g/mL}$ ) had 50-90% less biomass compared to control plants (Figure 3.9a and 3.9b), the bacteroids of AgNP-treated plants also produced 50-70% less total nitrogen fixation as compared to control plants (Figure 3.9c and 3.9d), and TEM images show healthy control nodules filled with bacteroids and treated nodules absent of bacteroids (Fig 3.10). All of this provides evidence that the soybean bacteroid could be damaged by AgNPs, yet it is very difficult to test the bacteroid form directly; they cannot be cultured outside the nodule. More studies would be required to determine if the AgNPs were directly toxic to the bacteroids or if AgNP-induced damage to the nodule membrane was responsible for the lack of bacteroids in treated nodules.

The metabolism and form of the bacteria change when they become bacteroids that fix nitrogen within the nodule. As discussed in section 1.7, bacteroids in the nodule might be more susceptible to silver toxicity, which could lead to sanctioning of the nodules by the plant. Sanctioning is where plants recognize that the nodule is not producing any nitrogen and be more likely to hold back on resources given to these nodules (reviewed in Simms et al. 2002). This might lead to lower levels of rhizobia in the soil over time as productive symbiotic relationships facilitate higher levels of the rhizobial strain in the soil (reviewed in Simms et al. 2002). Overall, one can conclude that addition of AgNPs into soil will most likely have direct effects on the health and abundance of *B. japonicum* bacteria within soil. However, this does not mean that AgNPs will not have negative effects on the symbiotic relationship between rhizobium species and legumes, specifically between *B. japonicum* and soybeans (see section 3.5).

Smaller nanoparticles are likely damaging the symbiosome membrane that holds the bacteroids within the nodule and maintains an almost completely anoxic environment. An anoxic environment is important for nitrogen fixation (Mus et al. 2016). Any damage to this membrane could result in bacteroids not functioning properly and could lead to the plant directing resources away from nodules and into other parts of the plant, such as roots to try to obtain nitrogen that way. As mentioned before plants can sanction their nodules if they are not fixing nitrogen, a defense mechanism to avoid symbiotic ‘cheaters’, and soybeans have been proven to be capable of this (Simms, 2006).

The normalized (nitrogen fixed per gram of nodule) nitrogen fixation of plants given 30 nm AgNPs did not vary among the treatments, including the control (Figure 3.9c). Yet the overall nitrogen fixation for control plants was 150-200% larger than that of the treated plants (Figure 3.9d). This indicates that all the plants given AgNPs had less nitrogen fixation compared to the control plants, which mirrors the observed decrease in nodule biomass. The AgNP-induced decrease in total nodule biomass in turn decreased the total nitrogen fixed by the plant. This resulted in decreased plant growth compared to non-inoculated plants. If I were to measure nitrogen fixation for plants given 16 nm AgNPs, I expect that the fixation results would be correlated to the nodule biomass and likely be very near to zero. Using Transmission Electron Microscopy, I saw that treated plants (given 2.5  $\mu\text{g/mL}$  of 30 nm AgNPs) had no bacteroids in their nodules (Figure 3.10a). However, these plants did fix nitrogen. Therefore, the images may not have been taken in the right locations to see the bacteroids. It is also possible that senescence occurred earlier in their nodule development for AgNP treated plants, leading to their larger nodules being absent of bacteroids. In contrast, control plants had nodules filled with bacteroids (Figure 3.10b). All this data clearly shows that AgNPs cause damage to the nodules, resulting in decreased nodule mass and fixation, and indirectly decreasing plant biomass.

Having decreased or inhibited nitrogen fixation would be a large problem for the agricultural sector, leading to increased cost of growing as soybeans. Not only would the crop need supplemental nitrogen, but it would be less useful as a rotational crop, which is expected to add nitrogen to the soil through the process of fixation. Not only will this



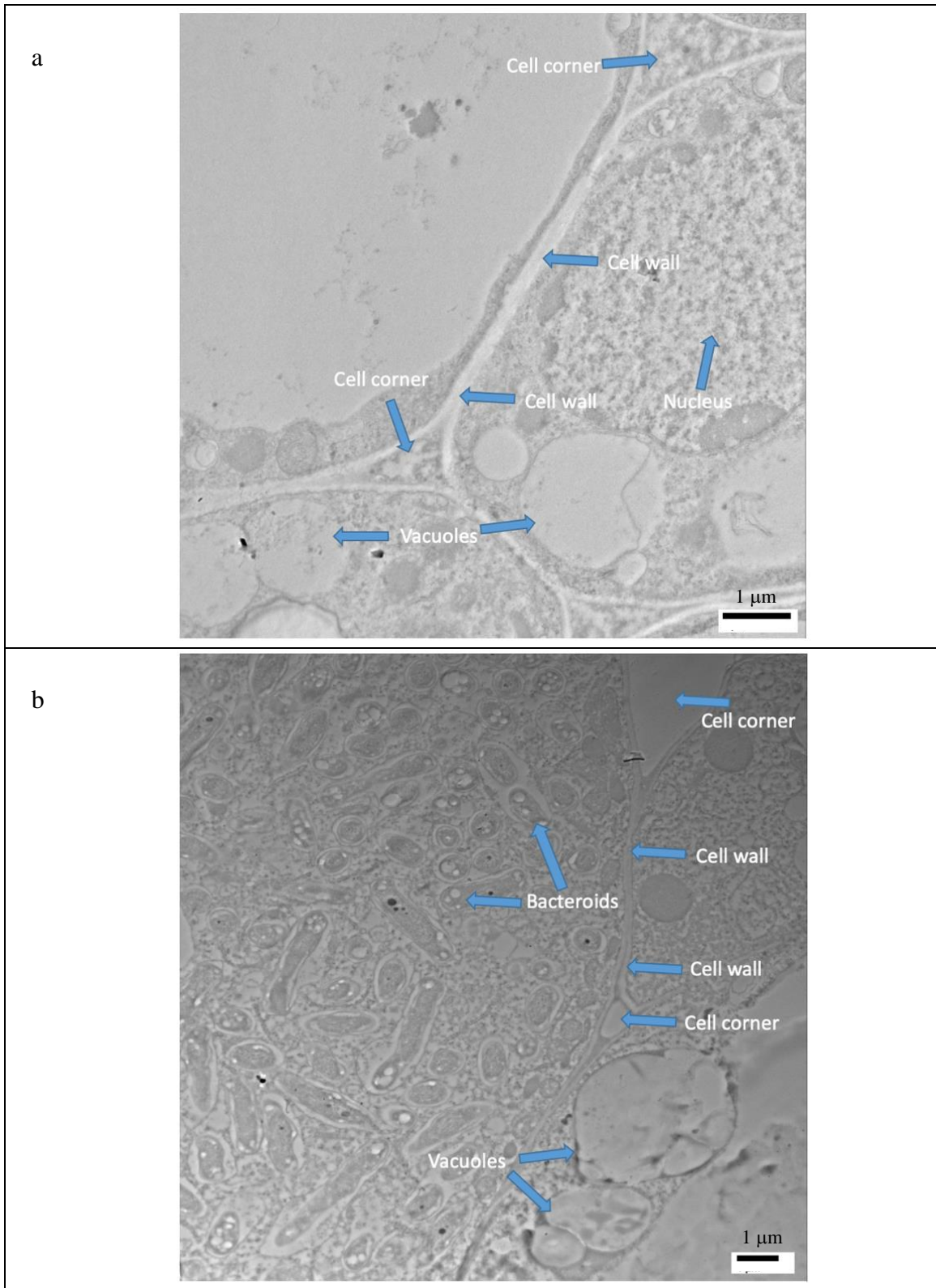


**Figure 3.11: TEM images of healthy and AgNP-treated nodules.**

Transmission electron microscope images of a) treated nodules absent of bacteroids and b) healthy bacteroids from within nodules of control plants.

affect soybean yield, but in turn this will lead to farmers using more nitrate fertilizers, which will then be washed into water systems and released as  $\text{NO}_2$  gas into the atmosphere (Park et al. 2012). Also, higher costs to the farmer could possibly lead to a higher cost for food, increasing prices of livestock being fed high soybean diets and for soybean (edamame) prices as well.

### 3.7 Changes to Nitrogen and Carbon

Decreased fixation in nodules would be expected to result in lower nitrogen concentration in the plants. However, I found some interesting results when looking at the percentage nitrogen per gram tissue. As seen in Figure 3.11a, N% (% of nitrogen in plant mass) was 125-145% higher for inoculated plants and 250% higher for non-inoculated plants treated with 16 nm AgNPs. Although this may seem strange, it is most likely a result of the decreased growth (as seen in section 3.5) that resulted from the AgNP treatments; the nitrogen in smaller plants may represent a higher percentage of total plant mass, this trend also occurs in non-inoculated plants, providing further confirmation. Good evidence for this is that the pattern for percentage nitrogen mirrors the pattern for biomass: plants with higher biomass have lower percentage nitrogen. The total nitrogen mass of plants given 16 nm AgNPs was about 200% higher in the inoculated control plants compared to plants from all other treatments (all non-inoculated plants and all inoculated plants treated with AgNPs) (Figure 3.11b). This result is exactly what was expected, plants with healthy nodules obtained more nitrogen and had more overall nitrogen mass as compared to plants that were non-inoculated, or inoculated plants subjected to AgNPs. Some nitrogen could have come from the cotyledons since these plants were grown for only 21 days and cotyledons fell off around day 15-17.

As was found for percentage nitrogen, carbon as a percentage of plant mass increased with concentrations of 16 nm AgNPs with non-inoculated plants having 107% more percentage carbon compared to control, and inoculated plants having about 105% higher percentage carbon in plants from all AgNP treatments (Figure 3.11d). The changes to percentage carbon are likely caused by the same phenomenon that explained relative

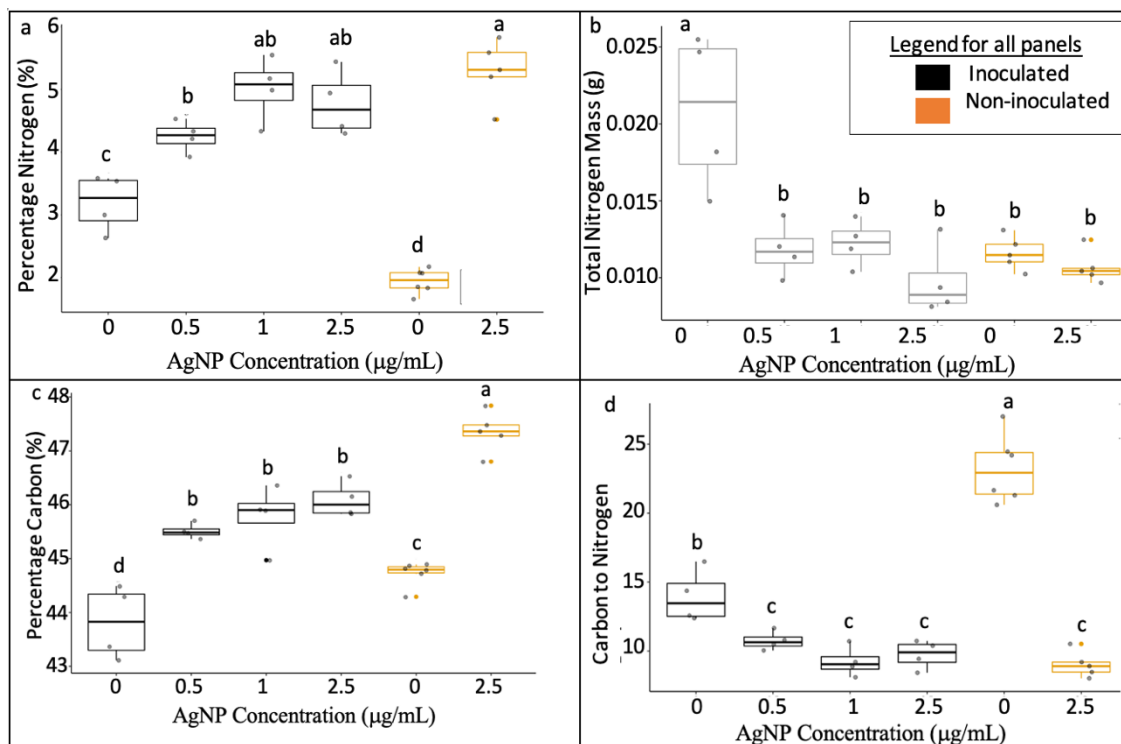


**Figure 3.12: Nitrogen and carbon percentages along with nitrogen total mass and carbon to nitrogen ratios.**

Plants were subjected to 16 nm AgNPs. The top left panel (a) shows an increase of percentage nitrogen with increases in AgNPs for inoculated and non-inoculated plants, the top right panel (b) shows that nitrogen totals are decreased when plants are subjected to AgNPs or when non-inoculated. The middle panel left (c) shows a carbon increase similar to nitrogen. (d) shows decreases for carbon to nitrogen ratios on the right. Panel a)  $F = 12.97$ ,  $p < 0.001$ . Panel b)  $F = 10.46$ ,  $p < 0.01$ . Panel c)  $F = 17.85$ ,  $p < 0.001$ . Panel d)  $F = 11.17$ ,  $p < 0.001$ .  $N = 4$  for all treatments described here. The post-hoc used to determine difference between treatments was Holm-Sidak. All significant differences are denoted by lower case letters, and `geom_jitter()` (on R) was used to distribute data points horizontally for easier viewing.

nitrogen percentages: the amount of the element taken up is effectively ‘diluted’ in the mass of larger plants.

The carbon to nitrogen ratio for non-inoculated control plants was 200% higher than for inoculated control plants, and inoculated control plants were 25-30% higher compared to all other plants treated with 16 nm AgNPs (Figure 3.11f). An increasing carbon to nitrogen ratio indicates a greater increase of carbon relative to nitrogen in those samples. This may be because it is easier for the AgNP-treated plants to obtain carbon than nitrogen.

## 4 Limitations, Future Directions and Conclusions

### 4.1 Limitations and Future Directions

I manufactured AgNPs due to the high cost of commercially produced AgNPs and the sheer amount that was needed to test a sufficient number of plants. Even when AgNPs were made locally, the amount that could be produced was limited due to the size of the equipment that was available. Because AgNPs and their associated silver ions would be expected to interact with organic matter and clay particles in soil (Jones and Peterson, 1986; Jacobson et al. 2005), even greater amounts of AgNPs would have been required to run the experiments using soil. This was the primary reason for using a hydroponic culture system. Nonetheless, treatment of soil with AgNPs will be required in order to establish their phytotoxicity to soybean and antimicrobial activity to *B. japonicum* under natural conditions. Other limitations include the inability to get thin and precise cross-section for easier readings and viewing of the samples. A new method for precise cutting of live plants allowing smoother and thinner cross-sections without need of fixation is needed. I tried using a vibratome but attempts to hold the plant tissue within water using superglue did not work.

The technique of TEM-EDAX (transmission electron microscopy with energy dispersive X-Ray analysis) to locate silver in plant samples was not attempted due to lack of a functional EDAX on the TEM that I was using. I did attempt SEM-EDAX (scanning

electron microscopy with EDAX) yet failed to get readings. However, the plant samples were mounted on copper grids. Carbon-coated copper grids may have been better due to carbon not having metallic properties, masking the copper and allowing us to see other metallic elements, such as silver, in the sample easier. Electron microscopy with EDAX should be done to confirm accurate locations of the AgNPs within the plant cells because there are multiple lipid bodies that appear as nanoparticles when the samples are stained. Staining is essential to see the structures of the cell and affirm where these nanoparticles go, especially in areas such as the plasmodesmata and cell corners. One can see nanoparticle-like bodies using SEM or TEM, but EDAX would confirm that they are composed of silver and not lipids. Looking at the fixed samples of stems and leaves may also be a viable option for future projects, although this is of less priority since ICP-MS shows minute amounts of silver entering the stem and leaves, as compared to the root.

Another important project would entail growing soybeans to maturity. One could then test the beans for silver content in addition to measuring bean yield to evaluate the effects of AgNPs on mature plants, harvest yields and safety of food for human or animal consumption. Soybean plants could be grown in either soil or hydroponics, although soil would likely be easier, the number of nanoparticles needed would likely push the project towards hydroponics. If this project was done, we would learn if these particles were transported into the edible portions of the plant and another study could examine if they accumulate in livestock or otherwise travel up the food chain.

Nitrogen-fixing bacteria, including *B. japonicum*, could be further tested to determine the minimal inhibitory concentration (MIC) for agronomic species. In my study, a relatively high concentration was tested to see clear toxic effect, and thus lower concentrations were not tested. Quantifying the MIC would be important to policy makers for setting guidelines on the levels of silver permitted in agriculture soils so as to avoid killing important rhizobial bacteria. Bacteria could also be tested this way in soil to see if the soil has any specific effects on the interaction of AgNPs and *B. japonicum*. The genus has been tested in soil with AgNPs (Shah et al. 2014), but the specific species has not been, and it is likely there will be different results than those found in my liquid medium. As

soil is where all actual crops are grown, the soil is likely more important, yet it may be difficult to achieve axenic cultures within soil.

Raman spectroscopy of the root plaque may also be an informative project to complete. Examining the root surface may be a smarter option than cutting cross-sections of the plant. The root plaque was proven to hold copious amounts of silver, it is possible that with this much silver present that Raman would indicate to the user that silver is bound within the plaque. Possibly using handheld Raman devices, and some root material from the area could serve as a diagnostic tool for silver contamination if differences were present within the treated and control roots.

Another technique that may have more success for looking at lignin, cellulose and other cell wall materials is FTIR-spectroscopy, which is similar to Raman spectroscopy but uses the infrared spectrum. This has longer wavelengths (in the 1100 nm range) and thus less energy is applied to the sample, which results in less fluorescence and stronger signals. Although the FTIR-spectroscopy would likely not be able to detect AgNPs as they have resonances closer to green light (which is around 500 nm), thus this option is not any more reliable to determine the positioning or bonding of the AgNPs within the plant.

## 4.2 Conclusions

Silver is known to be taken up by plants (Giesler-Lee et al. 2014; Li et al. 2017) and so it is no surprise that silver was taken up by soybeans in my experiment. However, I was the first to discover that at least 95% of the silver associated with the plant was contained within a root plaque. The retention of silver in a root plaque could be exploited for removal of silver from soil and remediation purposes.

Raman spectroscopy is known to be able to detect lignin and cellulose, I confirmed that this is also possible within soybeans. I believe I am the first who attempted to see AgNPs within plants using Raman spectroscopy without adding tags to the nanoparticles to help show their location and boost their signals. However, the concentrations of AgNPs within

soybeans in my experiment was below the detection limit and I therefore did not detect amplified signals that would indicate bonds with other molecules.

I did not find any publications in which researchers directly tested AgNPs on *B. japonicum* cultures. While previous papers have shown that the genus of *Bradyrhizobia* was unaffected by AgNPs in soil (Shah et al. 2014), I am the first to evaluate the response of *B. japonicum* USDA 110 and to discover their sensitivity to AgNPs.

I determined that AgNPs have detrimental effects on nodulation and nitrogen fixation within soybeans, this is a novel finding that has not yet been reported. The only other plant species for which this has been found is faba beans (Abd-Alla et al. 2016). I found that smaller nanoparticles and higher concentrations are more toxic to plant growth, which was previously known, yet none of those publications mentioned that smaller nanoparticles are also more detrimental to nodule health. I found that nodule biomass dropped to almost zero when plants were subjected to smaller AgNPs, and nitrogen fixation was subsequently reduced.

I am also the first to study changes in nitrogen and carbon percentages when plants are subjected to AgNPs. Changes in nitrogen and carbon were likely due to the decrease in size and growth of the plant, leading to increased relative percentages of these important elements. It will be important to determine if the effects of AgNPs on relative proportions of carbon and nitrogen in turn affect crop productivity and yield.

In summary, I determined AgNPs not only interfere with plant-microbe relations but also with general plant and bacterial growth. Given the increasing use of AgNPs, and other metal-NPs, we should be mindful of not releasing them to the environment and agricultural land. I recommend that concentrations of AgNPs in wastewater and biosolids be monitored and that environmental and agricultural guidelines be established to help protect wild and agricultural plants and microbes.



## References

- Abd-Alla, M.H., Nafady, N.A., Khalaf, D.M., 2016. Assessment of silver nanoparticles contamination on faba bean-*Rhizobium leguminosarum* bv. *viciae-Glomus aggregatum* symbiosis: Implications for induction of autophagy process in root nodule. *Agric. Ecosyst. Environ.* 218, 163–177. <https://doi.org/10.1016/j.agee.2015.11.022>
- Abdelsalam, N.R., Abdel-Megeed, A., Ali, H.M., Salem, M.Z.M., Al-Hayali, M.F.A., Elshikh, M.S., 2018. Genotoxicity effects of silver nanoparticles on wheat (*Triticum aestivum* L.) root tip cells. *Ecotoxicol. Environ. Saf.* 155, 76–85. <https://doi.org/10.1016/j.ecoenv.2018.02.069>
- Akaighe, N., MacCusprie, R., Navarro, D.A., Aga, D.S., Banerjee, S., Sohn, M., and Sharma, V.K., 2011. Humic acid-induced silver nanoparticle formation under environmental relevant conditions. *Environ. Sci. Technol.* 45, 3895–3901
- Al-Huqail, A.A., Hatata, M.M., Al-Huqail, A.A., Ibrahim, M.M., 2018. Preparation, characterization of silver phyto nanoparticles and their impact on growth potential of *Lupinus termis* L. seedlings. *Saudi J. Biol. Sci.* 25, 313–319
- Anghelone, M., Jembrih-Simbürger, D., Schreiner, M., 2015. Identification of copper phthalocyanine blue polymorphs in unaged and aged paint systems by means of micro-Raman spectroscopy and Random Forest. *Spectrochim. Acta - Part A Mol. Biomol. Spectrosc.* 149, 419–425. <https://doi.org/10.1016/j.saa.2015.04.094>
- Aslani, F., Bagheri, S., Muhd Julkapli, N., Juraimi, A.S., Hashemi, F.S.G., Baghdadi, A., 2014. Effects of engineered nanomaterials on plants growth: An overview. *Sci. World J.* 641759 <https://doi.org/10.1155/2014/641759>
- Asli, S., Neumann, P.M., 2009. Colloidal suspensions of clay or titanium dioxide nanoparticles can inhibit leaf growth and transpiration via physical effects on root water transport. *Plant, Cell Environ.* 32(5), 577-584. <https://doi.org/10.1111/j.1365-3040.2009.01952.x>
- Bagherzadeh Homae, M., Ehsanpour, A.A., 2016. Silver nanoparticles and silver ions: Oxidative stress responses and toxicity in potato (*Solanum tuberosum* L.) grown in vitro. *Hortic. Environ. Biotechnol.* 57, 544–553. <https://doi.org/10.1007/s13580-016-0083-z>
- Bastús, N.G., Merkoçi, F., Piella, J., Puentes, V., 2014. Synthesis of highly monodisperse citrate-stabilized silver nanoparticles of up to 200 nm: Kinetic control and catalytic properties. *Chem. Mater.* 26, 2836–2846. <https://doi.org/10.1021/cm500316k>

- Benn, T.M., Westerhoff, P., 2008. Nanoparticle silver released into water from commercially available sock fabrics. *Environ. Sci. Technol.* 42, 7025–7026. <https://doi.org/10.1021/es801501j>
- Bergersen, J., 1970. The quantitative relationship between nitrogen and the acetylene reduction assay. *Aust. J. Biol. Sci.* 23, 1015-1025
- Blaser, S.A., Scheringer, M., MacLeod, M., Hungerbühler, K., 2008. Estimation of cumulative aquatic exposure and risk due to silver: Contribution of nano-functionalized plastics and textiles. *Sci. Total Environ.* 390, 396–409. <https://doi.org/10.1016/j.scitotenv.2007.10.010>
- Boersma, P., 2019. Effects of Silver Nanoparticles on Soybeans (*Glycine max*) Growth and Nodulation. Undergraduate Thesis, Biology, University of Western Ontario
- Busse-Wicher, M., Li, A., Silveira, R.L., Pereira, C.S., Tryfona, T., Gomes, T.C.F., Skaf, M.S., Dupree, P., 2016. Evolution of xylan substitution patterns in gymnosperms and angiosperms: Implications for xylan interaction with cellulose. *Plant Physiol.* 171, 2418–2431. <https://doi.org/10.1104/pp.16.00539>
- Calderón-Jiménez, B., Johnson, M.E., Montoro Bustos, A.R., Murphy, K.E., Winchester, M.R., Baudrit, J.R.V., 2017. Silver nanoparticles: Technological advances, societal impacts, and metrological challenges. *Front. Chem.* 5, 1–26. <https://doi.org/10.3389/fchem.2017.00006>
- Calì, E., Qi, J., Preedy, O., Chen, S., Boldrin, D., Branford, W.R., Vandeperre, L., Ryan, M.P., 2018. Functionalised magnetic nanoparticles for uranium adsorption with ultra-high capacity and selectivity. *J. Mater. Chem. A* 6, 3063–3073. <https://doi.org/10.1039/c7ta09240g>
- Callejas, J.F., McEnaney, J.M., Read, C.G., Crompton, J.C., Biacchi, A.J., Popczun, E.J., Gordon, T.R., Lewis, N.S., Schaak, R.E., 2014. Electrocatalytic and photocatalytic hydrogen production from acidic and neutral-pH aqueous solutions using iron phosphide nanoparticles. *ACS Nano* 8, 11101–11107. <https://doi.org/10.1021/nn5048553>
- Cañas, J.E., Long, M., Nations, S., Vadan, R., Dai, L., Luo, M., Ambikapathi, R., Lee, E.H., Olszyk, D., 2008. Effects of functionalized and nonfunctionalized single-walled carbon nanotubes on root elongation of select crop species. *Environ. Toxicol. Chem.* 27, 1922-1931. <https://doi.org/10.1897/08-117.1>
- Carlson, C., Hussein, S.M., Schrand, A.M., Braydich-Stolle, L.K., Hess, K.L., Jones, R.L., Schlager, J.J., 2008. Unique cellular interaction of silver nanoparticles: Size-dependent generation of reactive oxygen species. *J. Phys. Chem. B* 112, 13608–13619. <https://doi.org/10.1021/jp712087m>

- Carpita, N., Sabularse, D., Montezinos D., Delimer D., 1979. Determination of the pore size of cell walls of living plant cells. *Science* 205:1144–1147.
- Chen, X.P., Kong, W.D., He, J.Z., Liu, W.J., Smith, S.E., Smith, F.A., Zhu, Y.G., 2008. Do water regimes affect iron-plaque formation and microbial communities in the rhizosphere of paddy rice? *J. Plant Nutr. Soil Sci.* 171, 193–199. <https://doi.org/10.1002/jpln.200700018>
- Chesson, A., Gardner, P.T., Wood, T.J., 1997. Cell wall porosity and available surface area of wheat straw and wheat gram fractions. *J. Sci. Food Agric.* 75(3), 289-295. [https://doi.org/10.1002/\(SICI\)1097-0010\(199711\)75:3<289::AID-JSFA879>3.0.CO;2-R](https://doi.org/10.1002/(SICI)1097-0010(199711)75:3<289::AID-JSFA879>3.0.CO;2-R)
- Cohn, J., Bradley Day, R., Stacey, G., 1998. Legume nodule organogenesis. *Trends Plant Sci.* 3, 105–110. [https://doi.org/10.1016/S1360-1385\(97\)01185-0](https://doi.org/10.1016/S1360-1385(97)01185-0)
- Cole, M.A., Elkan, G.H., 1973. Transmissible resistance to penicillin G, neomycin, and chloramphenicol in *Rhizobium japonicum*. *Antimicrob. Agents Chemother.* 4, 248–253. <https://doi.org/10.1128/AAC.4.3.248>
- Committee on Climate Change., 2017. Report to parliament - meeting carbon budgets: Closing the policy gap. *Microbiol. Mol. Biol. Rev.* 68, 203. <https://doi.org/10.1128/MMBR.68.2.280>
- Corradini, E., de Moura, M.R., Mattoso, L.H.C., 2010. A preliminary study of the incorporation of NPK fertilizer into chitosan nanoparticles. *Express Polym. Lett.* 4, 509–515. <https://doi.org/10.3144/expresspolymlett.2010.64>
- Cvjetko, P., Milošić, A., Domijan, A.M., Vinković Vrček, I., Tolić, S., Peharec Štefanić, P., Letofsky-Papst, I., Tkalec, M., Balen, B., 2017. Toxicity of silver ions and differently coated silver nanoparticles in *Allium cepa* roots. *Ecotoxicol. Environ. Saf.* 137, 18–28. <https://doi.org/10.1016/j.ecoenv.2016.11.009>
- Danish Ecological Consumer Council, Accessed July 7<sup>th</sup> 2021. The Nanodatabase. URL <http://nanodb.dk/en/search-database/>
- Das, A., Kamle, M., Bharti, A., Kumar, P., 2019. Nanotechnology and its applications in environmental remediation: An overview. *Vegetos* 32, 227–237. <https://doi.org/10.1007/s42535-019-00040-5>
- Delhaye, M., and Dhamelinourt, P., 1975. Raman microprobe and microscope with laser excitation. *J. Raman. Spectrosc.* 3, 33–43
- Devi, J.S., Bhimba, B.V., 2014. Antibacterial and antifungal activity of silver nanoparticles synthesized using *Hypnea muciformis*. *Biosci. Biotechnol. Res. Asia* 11, 235–238. <https://doi.org/10.13005/bbra/1260>

- Dieing, T., Hollricher, O., Toporski, J., 2010. Springer Series in Optical Sciences, Springer Science & Business Media, Berlin, Germany
- Dietz, K.J., Herth, S., 2011. Plant nanotoxicology. *Trends Plant Sci.* 16, 582–589. <https://doi.org/10.1016/j.tplants.2011.08.003>
- Elbein, A.D., 1969. Biosynthesis of a cell wall glucomannan in mung bean seedlings. *J. Biol. Chem.* 244, 1608–1616. [https://doi.org/10.1016/s0021-9258\(18\)91803-x](https://doi.org/10.1016/s0021-9258(18)91803-x)
- EPCD (European Parliament and Council Directive) 94/36/EC of 30 June 1994 on colours for use in foodstuffs. 1994. Official Journal of the European Union.
- Eustis, S., El-Sayed, M., 2006. Why gold nanoparticles are more precious than pretty gold: Noble metal surface plasmon resonance and its enhancement of the radiative and nonradiative properties of nanocrystals of different shapes. *Chem. Soc. Rev.* 35, 209-217
- Finnish Institute of Occupational Health (2017) NANOSOLUTIONS Final Report: Final publishable summary report 30. editors K. Savolainen and A. Vartio, <http://nanosolutionsfp7.com/final-report-and-publishable-summary/>
- Gage, D.J., 2004. Infection and invasion of roots by symbiotic, nitrogen-fixing rhizobia during nodulation of temperate legumes. *Microbiol. Mol. Biol. Rev.* 68, 280-300
- Gallon, J.R., 1981. The oxygen sensitivity of nitrogenase: a problem for biochemists and micro-organisms. *Trends Biochem. Sci.* 6, 19–23. [https://doi.org/10.1016/0968-0004\(81\)90008-6](https://doi.org/10.1016/0968-0004(81)90008-6)
- Geisler-Lee, J., Brooks, M., Gerfen, J., Wang, Q., Fotis, C., Sparer, A., Ma, X., Berg, R., Geisler, M., 2014. Reproductive toxicity and life history study of silver nanoparticle effect, uptake and transport in *Arabidopsis thaliana*. *Nanomater.* 4, 301–318. <https://doi.org/10.3390/nano4020301>
- Geurts, R., Bisseling, T., 2013. *Rhizobium* Nod factor perception and signalling. *Plant Cell* 14 Suppl, S239-249. <https://doi.org/10.1105/tpc.002451>.
- Gierlinger, N., Schwanninger, M., 2006. Chemical imaging of poplar wood cell walls by confocal Raman microscopy. *Plant Physiol.* 140, 1246–1254. <https://doi.org/10.1104/pp.105.066993>
- Research and Markets (2018) Global nanotechnology market (by component and applications), funding and investment, patent analysis and 27 companies profile and recent developments – Forecast 2024. Id number 4520812. <https://www.researchandmarkets.com/research/zc7qgf/global?w=5>

- Glover, R.D., Miller, J.M., Hutchison, J.E., 2011. Generation of metal nanoparticles from silver and copper objects: Nanoparticle dynamics on surfaces and potential sources of nanoparticles in the environment. *ACS Nano* 5, 8950–8957. <https://doi.org/10.1021/nn2031319>
- González-Melendi, P., Fernández-Pacheco, R., Coronado, M.J., Corredor, E., Testillano, P.S., Risueño, M.C., Marquina, C., Ibarra, M.R., Rubiales, D., Pérez-De-Luque, A., 2008. Nanoparticles as smart treatment-delivery systems in plants: Assessment of different techniques of microscopy for their visualization in plant tissues. *Ann. Bot.* 101, 187–195. <https://doi.org/10.1093/aob/mcm283>
- González, A.L., Noguez, C., Beránek, J., Barnard, A.S., 2014. Size, shape, stability, and color of plasmonic silver nanoparticles. *J. Phys. Chem. C* 118, 9128–9136. <https://doi.org/10.1021/jp5018168>
- Gordienko, M.G., Palchikova, V. V., Kalenov, S. V., Belov, A.A., Lyasnikova, V.N., Poberezhniy, D.Y., Chibisova, A. V., Sorokin, V. V., Skladnev, D.A., 2019. Antimicrobial activity of silver salt and silver nanoparticles in different forms against microorganisms of different taxonomic groups. *J. Hazard. Mater.* 378, 120754. <https://doi.org/10.1016/j.jhazmat.2019.120754>
- Gottschalk, F., Sonderer, T., Scholz, R.W., Nowack, B., 2009. Modeled environmental concentrations of engineered nanomaterials (TiO<sub>2</sub>, ZnO, Ag, CNT, fullerenes) for different regions. *Environ. Sci. Technol.* 43, 9216–9222. <https://doi.org/10.1021/es9015553>
- Government of Canada, 2017. Canada-United States Regulatory Cooperation Council Initiative on Chemicals Management. URL <https://www.canada.ca/en/health-canada/services/chemical-substances/chemicals-management-plan/canada-united-states-regulatory-cooperation-council.html>. Accessed June 13th 2021.
- Grün, A.L., Manz, W., Kohl, Y.L., Meier, F., Straskraba, S., Jost, C., Drexel, R., Emmerling, C., 2019. Impact of silver nanoparticles (AgNP) on soil microbial community depending on functionalization, concentration, exposure time, and soil texture. *Environ. Sci. Eur.* 31, 15. <https://doi.org/10.1186/s12302-019-0196-y>
- Hamad, S., Podagatlapalli, G.K., Tewari, S.P., Rao, S.V., 2013. Influence of picosecond multiple/single line ablation on copper nanoparticles fabricated for surface enhanced Raman spectroscopy and photonics applications. *J. Phys. D. Appl. Phys.* 46, 485501. <https://doi.org/10.1088/0022-3727/46/48/485501>
- Hänsch, M., Emmerling, H., 2010. Effects of silver nanoparticles on the microbiota and enzyme activity in soil. *J. Plant Nutr. Soil Sci.* 173(4), 554–558. <https://doi.org/10.1002/jpln.200900358>

- Hao, E., Schatz, G.C., 2004. Electromagnetic fields around silver nanoparticles and dimers. *J. Chem. Phys.* 120, 357–366. <https://doi.org/10.1063/1.1629280>
- Hao, E., Schatz, G.C., Hupp, J.T., 2004. Synthesis and optical properties of anisotropic metal nanoparticles. *J. Fluoresc.* 14, 331–341. <https://doi.org/10.1023/B:JOFL.0000031815.71450.74>
- Hao, Y., Xu, B., Ma, C., Shang, J., Gu, W., Li, W., Hou, T., Xiang, Y., Cao, W., Xing, B., Rui, Y., 2019. Synthesis of novel mesoporous carbon nanoparticles and their phytotoxicity to rice (*Oryza sativa L.*). *J. Saudi Chem. Soc.* 23, 75–82. <https://doi.org/10.1016/j.jscs.2018.05.003>
- Heath, K.D., Tiffin, P., 2009. Stabilizing mechanisms in a legume-rhizobium mutualism. *Evolution.* 63, 652–662. <https://doi.org/10.1111/j.1558-5646.2008.00582.x>
- Hischemöller, A., Nordmann, J., Ptacek, P., Mummenhoff, K., Haase, M., 2009. In-vivo imaging of the uptake of upconversion nanoparticles by plant roots. *J. Biomed. Nanotechnol.* 5, 278–284. doi: 10.1166/jbn.2009.1032.
- Hoagland, D. R., Arnon, D. I., 1950. The water-culture method for growing plants without soil. *Calif. Agric. Exp. Stn.* 347, 32.
- Hong, D.D., Anh., H.T.L., Tam, L.T., 2019. Effects of nanoscale zerovalent cobalt on growth and photosynthetic parameters of soybean *Glycine max (L.) Merr.* DT26 at different stages. *BMC Energy* 1, 6. <https://doi.org/10.1186/s42500-019-0007-4>
- Jacobson, A.R., McBride, M.B., Baveye, P., Steenhuis, T.S., 2005. Environmental factors determining the trace-level sorption of silver and thallium to soils. *Sci. Total Environ.* 345, 191–205. <https://doi.org/10.1016/j.scitotenv.2004.10.027>
- Jasim, B., Thomas, R., Mathew, J., Radhakrishnan, E.K., 2017. Plant growth and diosgenin enhancement effect of silver nanoparticles in Fenugreek (*Trigonella foenum-graecum L.*). *Saudi Pharm. J.* 25, 443–447. <https://doi.org/10.1016/j.jsps.2016.09.012>
- Jones, A.M., Garg, S., He, D., Pham, A.N., Waite, T.D., 2011. Superoxide-mediated formation and charging of silver nanoparticles. *Environ. Sci. Technol.* 45, 1428–1434. <https://doi.org/10.1021/es103757c>
- Jones, K.C., Peterson, P.J., 1986. The influence of humic and fulvic acids on silver uptake by perennial ryegrass, and its relevance to the cycling of silver in soils. *Plant Soil* 95, 3–8. <https://doi.org/10.1007/BF02378846>
- Kampe, S., Kaegi, R., Schlich, K., Wasmuth, C., Hollert, H., Schlechtriem, C., 2018. Silver nanoparticles in sewage sludge: Bioavailability of sulfidized silver to the terrestrial isopod *Porcellio scaber*. *Environ. Toxicol. Chem.* 37, 1608–1613.

- Kanchi, S., 2014. Environmental Analytical chemistry nanotechnology for water treatment. *J Env. Anal Chem* 1, 10–12.
- Kim, B., Park, C.S., Murayama, M., Hochella, M.F., 2010. Discovery and characterization of silver sulfide nanoparticles in final sewage sludge products. *Environ. Sci. Technol.* 44, 7509–7514. <https://doi.org/10.1021/es101565j>
- Kim, J.S., Kuk, E., Yu, K.N., Kim, J.H., Park, S.J., Lee, H.J., Kim, S.H., Park, Y.K., Park, Y.H., Hwang, C.Y., Kim, Y.K., Lee, Y.S., Jeong, D.H., Cho, M.H., 2007. Antimicrobial effects of silver nanoparticles. *Nanomed. Nanotechnol.* 3, 95–101. <https://doi.org/10.1016/j.nano.2006.12.001>
- Kocak, A., Karasu, B., 2018. General evaluations of nanoparticles. *J. Plant. Nutr. Soil. Sci.* 5, 191–236. <https://doi.org/10.31202/ecjse.361663>
- Kozachuk, M.S., Avilés, M.O., Martin, R.R., Potts, B., Sham, T.K., Lagurné-Labarthe, F., 2018. Imaging the surface of a hand-colored 19th century daguerreotype. *Appl. Spectrosc.* 72, 1215–1224. <https://doi.org/10.1177/0003702818773760>
- Kumar, N., Shah, V., Walker, V.K., 2011. Perturbation of an arctic soil microbial community by metal nanoparticles. *J. Hazard. Mater.* 190, 816–822. <https://doi.org/10.1016/j.jhazmat.2011.04.005>
- Kumari, M., Mukherjee, A., Chandrasekaran, N., 2009. Genotoxicity of silver nanoparticles in *Allium cepa*. *Sci. Total Environ.* 407, 5243–5246. <https://doi.org/10.1016/j.scitotenv.2009.06.024>
- Li, C.C., Dang, F., Li, M., Zhu, M., Zhong, H., Hintelmann, H., Zhou, D.M., 2017. Effects of exposure pathways on the accumulation and phytotoxicity of silver nanoparticles in soybean and rice. *Nanotoxicology* 11, 699–709. <https://doi.org/10.1080/17435390.2017.1344740>
- Li, W.R., Xie, X.B., Shi, Q.S., Zeng, H.Y., Ou-Yang, Y.S., Chen, Y. Ben, 2010. Antibacterial activity and mechanism of silver nanoparticles on *Escherichia coli*. *Appl. Microbiol. Biotechnol.* 85, 1115–1122. <https://doi.org/10.1007/s00253-009-2159-5>
- Liu, Q., Luo, L., Zheng, L., 2018. Lignins: Biosynthesis and biological functions in plants. *Int. J. Mol. Sci.* 19, 335–351. <https://doi.org/10.3390/ijms19020335>
- Lombardo, D., Kiselev, M.A., Caccamo, M.T., 2019. Smart nanoparticles for drug delivery application: Development of versatile nanocarrier platforms in biotechnology and nanomedicine. *J. Nanomater.* 2019, 3702518. <https://doi.org/10.1155/2019/3702518>

- Long, D.A., 2002. The Raman Effect: a Unified Treatment of the Theory of Raman Scattering by Molecules. John Wiley & Sons Ltd. West Sussex, England.
- Luoma, S.N., 2008. Silver nanotechnologies and the environment: Old problems or new challenges? Project on Emerging Nanotechnologies, Woodrow Wilson Centre, Washington, DC, USA.
- Ma, S., He, F., Tian, D., Zou, D., Yan, Z., Yang, Y., Zhou, T., Huang, K., Shen, H., Fang, J., 2018. Variations and determinants of carbon content in plants: A global synthesis. *Biogeosciences* 15, 693–702. <https://doi.org/10.5194/bg-15-693-2018>
- Ma, X., Geiser-Lee, J., Deng, Y., Kolmakov, A., 2010. Interactions between engineered nanoparticles (ENPs) and plants: Phytotoxicity, uptake and accumulation. *Sci. Total Environ.* 408, 3053–3061. <https://doi.org/10.1016/j.scitotenv.2010.03.031>
- Mahler, R.L., 2004. Nutrients Plants Require. University of Idaho CIS 1124. 20–23.
- Manke, A., Wang, L., Rojanasakul, Y., 2013. Mechanisms of nanoparticle-induced oxidative stress and toxicity. *Biomed Res. Int.* 2013. <https://doi.org/10.1155/2013/942916>
- Martínez-Castañón, G.A., Niño-Martínez, N., Martínez-Gutierrez, F., Martínez-Mendoza, J.R., Ruiz, F., 2008. Synthesis and antibacterial activity of silver nanoparticles with different sizes. *J. Nanoparticle Res.* 10, 1343–1348. <https://doi.org/10.1007/s11051-008-9428-6>
- Maurer, F., Christl, I., Hoffmann, M., Kretzschmar, R., 2012. Reduction and reoxidation of humic acid: Influence on speciation of cadmium and silver. *Environ. Sci. Technol.* 46, 8808–8816. <https://doi.org/10.1021/es301520s>
- Maynard, A.D., Michelson, E., 2005. The Project on Emerging Nanotechnologies. The Nanotechnology Consumer Products Inventory. URL <https://www.nanotechproject.tech/cpi/>
- McAnuff, M.A., Omoruyi, F.O., Morrison, E.Y.S.A., Asemota, H.N., 2002. Plasma and liver lipid distributions in streptozotocin-induced diabetic rats fed sapogenin extract of the Jamaican bitter yam (*Dioscorea polygonoides*). *Nutr. Res.* 22, 1427–1434. [https://doi.org/10.1016/S0271-5317\(02\)00457-8](https://doi.org/10.1016/S0271-5317(02)00457-8)
- Mitrano, D.M., Rimmele, E., Wichser, A., Erni, R., Height, M., Nowack, B., 2014. Presence of nanoparticles in wash water from conventional silver and nano-silver textiles. *ACS Nano* 8, 7208–7219. <https://doi.org/10.1021/nn502228w>
- Moreno-Garrido, I., Pérez, S., Blasco, J., 2015. Toxicity of silver and gold nanoparticles on marine microalgae. *Mar. Environ. Res.* 111, 60–73. <https://doi.org/10.1016/j.marenvres.2015.05.008>



- Mus, F., Crook, M.B., Garcia, K., Costas, A.G., Geddes, B.A., Kouri, E.D., Paramasivan, P., Ryu, M.H., Oldroyd, G.E.D., Poole, P.S., Udvardi, M.K., Voigt, C.A., Ané, J.M., Peters, J.W., 2016. Symbiotic nitrogen fixation and the challenges to its extension to nonlegumes. *Appl. Environ. Microbiol.* 82, 3698–3710.  
<https://doi.org/10.1128/AEM.01055-16>
- Navarro, E., Baun, A., Behra, R., Hartmann, N.B., Filser, J., Miao, A.J., Quigg, A., Santschi, P.H., Sigg, L., 2008. Environmental behavior and ecotoxicity of engineered nanoparticles to algae, plants, and fungi. *Ecotoxicology* 17, 372–386.  
<https://doi.org/10.1007/s10646-008-0214-0>
- Otte, M.L., Rozema, J., Koster, L., Haarsma, M.S., Broekman, R.A., 1989. Iron plaque on roots of *Aster tripolium* L.: Interaction with zinc uptake. *New Phytol.* 111, 309–317. <https://doi.org/10.1111/j.1469-8137.1989.tb00694.x>
- Pallavi, Mehta, C.M., Srivastava, R., Arora, S., Sharma, A.K., 2016. Impact assessment of silver nanoparticles on plant growth and soil bacterial diversity. *Biotech.* 6, 1–10.  
<https://doi.org/10.1007/s13205-016-0567-7>
- Panda, K.K., Achary, V.M.M., Krishnaveni, R., Padhi, B.K., Sarangi, S.N., Sahu, S.N., Panda, B.B., 2011. In vitro biosynthesis and genotoxicity bioassay of silver nanoparticles using plants. *Toxicol. Vitro.* 25, 1097–1105.  
<https://doi.org/10.1016/j.tiv.2011.03.008>
- Park, H-J., Kim, S.H., and Choi, S-H., 2006. A new composition of nanosized silica-silver for control of various plant diseases. *Plant Pathol. J.* 22, 295-302.
- Park, S., Croteau, P., Boering, K.A., Etheridge, D.M., Ferretti, D., Fraser, P.J., Kim, K.R., Krummel, P.B., Langenfelds, R.L., Van Ommen, T.D., Steele, L.P., Trudinger, C.M., 2012. Trends and seasonal cycles in the isotopic composition of nitrous oxide since 1940. *Nat. Geosci.* 5, 261–265. <https://doi.org/10.1038/ngeo1421>
- Patlolla, A.K., Berry, A., May, L., Tchounwou, P.B., 2012. Genotoxicity of silver nanoparticles in *Vicia faba*: A pilot study on the environmental monitoring of nanoparticles. *Int. J. Environ. Res. Pu.* 9, 1649–1662.  
<https://doi.org/10.3390/ijerph9051649>
- Peoples, M.B., Craswell, E.T., 1992. Biological nitrogen fixation: Investments, expectations and actual contributions to agriculture. *Plant Soil* 141, 13–39.  
<https://doi.org/10.1007/BF00011308>
- Pereira, S.P.P., Jesus, F., Aguiar, S., de Oliveira, R., Fernandes, M., Ranville, J., Nogueira, A.J.A., 2018. Phytotoxicity of silver nanoparticles to *Lemna minor*: Surface coating and exposure period-related effects. *Sci. Total Environ.* 618, 1389–1399. <https://doi.org/10.1016/j.scitotenv.2017.09.275>

- Peters, R.J.B., Van Bommel, G., Herrera-Rivera, Z., Helsper, H.P.F.G., Marvin, H.J.P., Weigel, S., Tromp, P.C., Oomen, A.G., Rietveld, A.G., Bouwmeester, H., 2014. Characterization of titanium dioxide nanoparticles in food products: Analytical methods to define nanoparticles. *J. Agric. Food Chem.* 62, 6285–6293. <https://doi.org/10.1021/jf5011885>
- Priester, J.H., Ge, Y., Mielke, R.E., Horst, A.M., Moritz, S.C., Espinosa, K., Gelb, J., Walker, S.L., Nisbet, R.M., An, Y.J., Schimel, J.P., Palmer, R.G., Hernandez-Viezcas, J.A., Zhao, L., Gardea-Torresdey, J.L., Holden, P.A., 2012. Soybean susceptibility to manufactured nanomaterials with evidence for food quality and soil fertility interruption. *Proc. Natl. Acad. Sci. U. S. A.* 109, 2451–2456. <https://doi.org/10.1073/pnas.1205431109>
- Pulci, G., Paglia, L., Genova, V., Bartuli, C., Valente, T., Marra, F., 2018. Low density ablative materials modified by nanoparticles addition: Manufacturing and characterization. *Compos. Part A Appl. Sci. Manuf.* 109, 330–337. <https://doi.org/10.1016/j.compositesa.2018.03.025>
- Ralston, E., and Imsande, J., 1983. Nodulation of hydroponically grown soybean plants and inhibition of nodule development by nitrate. *Phyton-Int. J. Exp. Bot.* 34, 1371–1378.
- Robards, A.W., Clarkson, D.T., 1976. The role of plasmodesmata in the transport of water and nutrients across roots. *Intercell. Commun. Plants Stud. Plasmodesmata.* 181–201. [https://doi.org/10.1007/978-3-642-66294-2\\_10](https://doi.org/10.1007/978-3-642-66294-2_10)
- Robson, R.L., Postgate, J.R., 1980. Oxygen and hydrogen. *Annu. Rev. Microbiol.* 34, 183–207.
- Ruenraroengsak, P., Kiryushko, D., Theodorou, I.G., Klosowski, M.M., Taylor, E.R., Niriella, T., Palmieri, C., Yagüe, E., Ryan, M.P., Coombes, R.C., Xie, F., Porter, A.E., 2019. Frizzled-7-targeted delivery of zinc oxide nanoparticles to drug-resistant breast cancer cells. *Nanoscale* 11, 12858–12870. <https://doi.org/10.1039/c9nr01277j>
- Ryu, S.W., Kim, C.H., Han, J.W., Kim, C.J., Jung, C., Park, H.G., Choi, Y.K., 2010. Gold nanoparticle embedded silicon nanowire biosensor for applications of label-free DNA detection. *Biosens. Bioelectron.* 25, 2182–2185. <https://doi.org/10.1016/j.bios.2010.02.010>
- Saha, N., Dutta Gupta, S., 2017. Low-dose toxicity of biogenic silver nanoparticles fabricated by *Swertia chirata* on root tips and flower buds of *Allium cepa*. *J. Hazard. Mater.* 330, 18–28. <https://doi.org/10.1016/j.jhazmat.2017.01.021>
- Schlich, K., Hund-Rinke, K., 2015. Influence of soil properties on the effect of silver nanomaterials on microbial activity in five soils. *Environ. Pollut.* 196, 321–330. <https://doi.org/10.1016/j.envpol.2014.10.021>

- Schlich, K., Klawonn, T., Terytze, K., Hund-Rinke, K., 2013. Hazard assessment of a silver nanoparticle in soil applied via sewage sludge. *Environ. Sci. Eur.* 25, 1–14. <https://doi.org/10.1186/2190-4715-25-17>
- Seregin, I. V., Ivanov, V.B., 2001. Physiological Aspects of Cadmium and Lead Toxic Effects. *Russ. J. Plant. Physiol.* 48, 523–544.
- Shackleton, C., 2002. Growth and fruit production of *Sclerocarya birrea* in the South African lowveld. *Agrofor. Syst.* 55, 175–180. <https://doi.org/10.1023/A:1020579213024>
- Shah, V., Collins, D., Walker, V.K., Shah, S., 2014. The impact of engineered cobalt, iron, nickel and silver nanoparticles on soil bacterial diversity under field conditions. *Environ. Res. Lett.* 9. <https://doi.org/10.1088/1748-9326/9/2/024001>
- Shang, J., Gao, X., 2015. Nanoparticle counting: Towards accurate determination of the molar concentration. *Chem. Soc. Rev.* 43, 7267–7278. <https://doi.org/10.1039/c4cs00128a.Nanoparticle>
- Shute, T., Macfie, S.M., 2006. Cadmium and zinc accumulation in soybean: A threat to food safety? *Sci. Total Environ.* 371, 63–73. <https://doi.org/10.1016/j.scitotenv.2006.07.034>
- Simmons, T.J., Mortimer, J.C., Bernardinelli, O.D., Pöppler, A.C., Brown, S.P., DeAzevedo, E.R., Dupree, R., Dupree, P., 2016. Folding of xylan onto cellulose fibrils in plant cell walls revealed by solid-state NMR. *Nat. Commun.* 7, 1–9. <https://doi.org/10.1038/ncomms13902>
- Simms, E. L., Taylor, D.L., Povich, J., Shefferson, R.P., Sachs, J.L., Urbina, M., and Tausczik, 2006. An empirical test of partner choice mechanisms in a wild legume-rhizobium interaction. *Proc. R. Soc. Lond. B* 273, 77–81.
- Simms, E. L., and Taylor, D.L., 2002. Partner choice in nitrogen-fixation mutualism of legumes and rhizobia. *Integr. Comp. Biol.* 42, 369–380.
- Slomberg, D.L., Schoenfisch, M.H., 2012. Silica nanoparticle phytotoxicity to *Arabidopsis thaliana*. *Environ. Sci. Technol.* 46, 10247–10254. <https://doi.org/10.1021/es300949f>
- Sondi, I., Salopek-Sondi, B., 2004. Silver nanoparticles as antimicrobial agent: A case study on *E. coli* as a model for Gram-negative bacteria. *J. Colloid Interface Sci.* 275, 177–182. <https://doi.org/10.1016/j.jcis.2004.02.012>
- Stockman, M.I., 2006. Electromagnetic theory of SERS. *Top. Appl. Phys.* 103, 47–66. [https://doi.org/10.1007/11663898\\_3](https://doi.org/10.1007/11663898_3)

- Streeter, J.G., 1985. Nitrate inhibition of legume nodule growth and activity. *Plant Physiol.* 77, 325–328. <https://doi.org/10.1104/pp.77.2.325>
- Strobbia, P., Crawford, B.M., Wang, H.-N., Zentella, R., Kemner, K.M., Sun, T.-P., Vo-Dinh, T., Pei, Z.-M., Boyanov, M.I., 2019. Application of plasmonic nanoprobe for SERS sensing and imaging of biotargets in plant systems. *Proceedings Volume 10894, Plasmonics in Biology and Medicine XVI, SPIE BiOS 2019, San Francisco, California, USA* <https://doi.org/10.1117/12.2512010>
- Tartaj, P., Morales, M.P., González-Carreño, T., Veintemillas-Verdaguer, S., Serna, C.J., 2005. Advances in magnetic nanoparticles for biotechnology applications. *J. Magn. Mater.* 290-291, 28–34. <https://doi.org/10.1016/j.jmmm.2004.11.155>
- The Project on Emerging Nanoparticles, 2013. Consumer Product Inventory. URL <https://www.nanotechproject.tech/cpi/>
- Tripathi, D.K., Tripathi, A., Shweta, Singh, S., Singh, Y., Vishwakarma, K., Yadav, G., Sharma, S., Singh, V.K., Mishra, R.K., Upadhyay, R.G., Dubey, N.K., Lee, Y., Chauhan, D.K., 2017a. Uptake, accumulation and toxicity of silver nanoparticle in autotrophic plants, and heterotrophic microbes: A concentric review. *Front. Microbiol.* 8, 1–16. <https://doi.org/10.3389/fmicb.2017.00007>
- Tripathi, D.K., Singh, Swati, Singh, Shweta, Srivastava, P.K., Singh, V.P., Singh, Samiksha, Prasad, S.M., Singh, P.K., Dubey, N.K., Pandey, A.C., Chauhan, D.K., 2017b. Nitric oxide alleviates silver nanoparticles (AgNPs)-induced phytotoxicity in *Pisum sativum* seedlings. *Plant Physiol. Biochem.* 110, 167–177. <https://doi.org/10.1016/j.plaphy.2016.06.015>
- USEPA (U.S. Environmental Protection Agency), 2018a. EPA unable to assess the impact of hundreds of unregulated pollutants in land-applied biosolids on human health and the environment. Office of Inspector General, United States Environmental Protection Agency Report No. 19-P-0002.

USDA, Caldas de Castro, M., Singer, B.H., Abbas, T., Younus, M., Muhammad, S., Kulldorff, M., Tango, T., Park, P.J., Porter, W.F., Fleming, K.K., Porter, W.F., Kirchgessner, M.S., Dubovi, E.J., Whipps, C.M., Levine, N., Kulldorf, M., Ord, J.K., Getis, A., Anselin, L., Chainey, S., Tompson, L., Uhlig, S., Gatrell, A.C., Bailey, T.C., Diggle, P.J., Rowlingson, B.S., Elliott, P., Wartenberg, D., Biggs, P.M., McDougall, J.S., Frazier, J. a, Milne, B.S., Biggs, P.M., Shilleto, R.W., Milne, B.S., USDA, A. and P.H.I.S.V.S., Harris, M., Miles, A., Pearce, J., Prosser, D., Sleeman, J., Whalen, M., Decker, D.J., Wild, M. a., Riley, S.J., Siemer, W.F., Miller, M.M., Leong, K.M., Powers, J.G., Rhyhan, J.C., Ostfeld, R.S., Glass, G.E., Keesing, F., Ward, M.P., Carpenter, T.E., Wei, K., Sun, Z., Zhu, S., Guo, W., Sheng, P., Wang, Z., Zhao, C., Zhao, Q., Zhu, R., Guo, H., Li, H., Cheng, Z., Liu, J., Cui, Z., Gingerich, E., Porter, R.E., Lupiani, B., Fadly, A.M., Porter, A.R.E., Fadly, A.M., Thomas, J.M., Allison, A.B., Holmes, E.C., Phillips, J.E., Bunting, E.M., Yabsley, M.J., Brown, J.D., Kevin Keel, M., Philips, J.E., Cartoceti, A.N., Munk, B. a., Nemeth, N.M., Welsh, T.I., Thomas, J.M., Crum, J.M., Lichtenwalner, A.B., Fadly, A.M., Zavala, G., Holmes, E.C., Brown, J.D., 2007. 2007 Census of Agriculture, United States Summary and State Data. Volume 1. Geographic Area Series, Part 51. Geogr. Anal. 7, 2 p.

USEPA, 2018b. Targeted National Sewage Sludge Survey Statistical Analysis Report (Appendix A of report).

USEPA, 2009. Targeted National Sewage Sludge Survey Sampling and Analysis Technical Report. EPA 88.

USEPA, 2017. Control of Nanoscale Materials under the Toxic Substances Control Act. URL <https://www.epa.gov/reviewing-new-chemicals-under-toxic-substances-control-act-tsca/control-nanoscale-materials-under>

Vance, M.E., Kuiken, T., Vejerano, E.P., McGinnis, S.P., Hochella, M.F., Hull, D.R., 2015. Nanotechnology in the real world: Redeveloping the nanomaterial consumer products inventory. Beilstein J. Nanotechnol. 6, 1769–1780. <https://doi.org/10.3762/bjnano.6.181>

Velavan, R., Myvizhi, P., 2015. Nano technology in electronic devices and computer. Int. j. innov. res. sci. eng. technol. 4, 6492–6495. <https://doi.org/10.15680/IJRSET.2015.0407292>

Vinković, T., Novák, O., Strnad, M., Goessler, W., Jurašin, D.D., Parađiković, N., Vrček, I.V., 2017. Cytokinin response in pepper plants (*Capsicum annuum* L.) exposed to silver nanoparticles. Environ. Res. 156, 10–18. <https://doi.org/10.1016/j.envres.2017.03.015>

- Vishwakarma, K., Shweta, Upadhyay, N., Singh, J., Liu, S., Singh, V.P., Prasad, S.M., Chauhan, D.K., Tripathi, D.K., Sharma, S., 2017. Differential phytotoxic impact of plant mediated silver nanoparticles (AgNPs) and silver nitrate (AgNO<sub>3</sub>) on *Brassica sp.* *Front. Plant Sci.* 8, 1–12. <https://doi.org/10.3389/fpls.2017.01501>
- Wang, P., Lombi, E., Sun, S., Scheckel, K.G., Malysheva, A., McKenna, B.A., Menzies, N.W., Zhao, F.J., Kopittke, P.M., 2017. Characterizing the uptake, accumulation and toxicity of silver sulfide nanoparticles in plants. *Environ. Sci. Nano* 4, 448–460. <https://doi.org/10.1039/c6en00489j>
- Wang, P., Menzies, N.W., Lombi, E., Sekine, R., Blamey, F.P.C., Hernandez-Soriano, M.C., Cheng, M., Kappen, P., Peijnenburg, W.J.G.M., Tang, C., Kopittke, P.M., 2015. Silver sulfide nanoparticles (Ag<sub>2</sub>S-NPs) are taken up by plants and are phytotoxic. *Nanotoxicology* 9, 1041–1049. <https://doi.org/10.3109/17435390.2014.999139>
- Wang, T., Hong, M., 2016. Solid-state NMR investigations of cellulose structure and interactions with matrix polysaccharides in plant primary cell walls. *J. Exp. Bot.* 67, 503–514. <https://doi.org/10.1093/jxb/erv416>
- Wayne, R., 2019. Plasmodesmata. *Plant Cell Biol.* 3, 55–65. <https://doi.org/10.1016/b978-0-12-814371-1.00003-5>
- Wen, Y., Zhang, L., Chen, Z., Sheng, X., Qiu, J., Xu, D., 2016. Co-exposure of silver nanoparticles and chiral herbicide imazethapyr to *Arabidopsis thaliana*: Enantioselective effects. *Chemosphere* 145, 207–214. <https://doi.org/10.1016/j.chemosphere.2015.11.035>
- Whiteley, C.M., Valle, M.D., Jones, K.C., Sweetman, A.J., 2013. Challenges in assessing release, exposure and fate of silver nanoparticles within the UK environment. *Environ. Sci. Process. Impacts* 15, 2050–2058. <https://doi.org/10.1039/c3em00226h>
- Wippermann, S., Vörös, M., Rocca, D., Gali, A., Zimanyi, G., Galli, G., 2013. High-pressure core structures of Si nanoparticles for solar energy conversion. *Phys. Rev. Lett.* 110, 1–5. <https://doi.org/10.1103/PhysRevLett.110.046804>
- Yan, A., Chen, Z., 2019. Impacts of silver nanoparticles on plants: A focus on the phytotoxicity and underlying mechanism. *Int. J. Mol. Sci.* 20, 23–25. <https://doi.org/10.3390/ijms20051003>
- Yang, J., Jiang, F., Ma, C., Rui, Y., Rui, M., Adeel, M., Cao, W., Xing, B. 2018. Alteration of crop yield and quality of wheat upon exposure to silver nanoparticles in a life cycle study. *J. Agric. Food Chem.* 66, 2589–2597.

- Yeshchenko, O.A., Dmitruk, I.M., Alexeenko, A.A., Kotko, A. V., Verdal, J., Pinchuk, A.O., 2012. Size and temperature effects on the surface plasmon resonance in silver nanoparticles. *Plasmonics* 7, 685–694. <https://doi.org/10.1007/s11468-012-9359-z>
- Yin, Y., Liu, J., Jiang, G., 2012. Sunlight-induced reduction of ionic Ag and Au to metallic nanoparticles by dissolved organic matter. *ACS Nano* 6, 7910–7919. <https://doi.org/10.1021/nn302293r>
- Zhai, Y., Hunting, E.R., Wouters, M., Peijnenburg, W.J.G.M., Vijver, M.G., 2016. Silver nanoparticles, ions, and shape governing soil microbial functional diversity: Nano shapes micro. *Front. Microbiol.* 7, 1–9. <https://doi.org/10.3389/fmicb.2016.01123>
- Zhang, H., Huang, M., Zhang, W., Gardea-Torresdey, J.L., White, J.C., Ji, R., Zhao, L., 2020. Silver nanoparticles alter soil microbial community compositions and metabolite profiles in unplanted and cucumber-planted soils. *Environ. Sci. Technol.* 54, 3334–3342. <https://doi.org/10.1021/acs.est.9b07562>
- Zhang, J., Wang, X.J, Wang, J.P, Wang, W.X, 2014. Carbon and nitrogen contents in typical plants and soil profiles in Yanqi basin of Northwest China. *J. Integr. Agric.* 13, 648–656. [https://doi.org/10.1016/S2095-3119\(13\)60723-6](https://doi.org/10.1016/S2095-3119(13)60723-6)
- Zhang, Z., Guo, H., Ma, C., Xia, M., White, J.C., Xing, B., He, L., 2019. Rapid and efficient removal of silver nanoparticles from plant surfaces using sodium hypochlorite and ammonium hydroxide solution. *Food Control* 98, 68–73. <https://doi.org/10.1016/j.foodcont.2018.11.005>
- Zimmerman, M.H. 1983. *Xylem Structure and the Ascent of Sap*. Springer Series in Wood Science. Springer Science & Business Media, Berlin, Germany
- Zoubir, A., 2012. *Raman imaging*. Springer Science & Business Media, Berlin, Germany

## Appendices

Appendix A: Standard curve for *Bradyrhizobium japonicum* USDA 110 cell density.

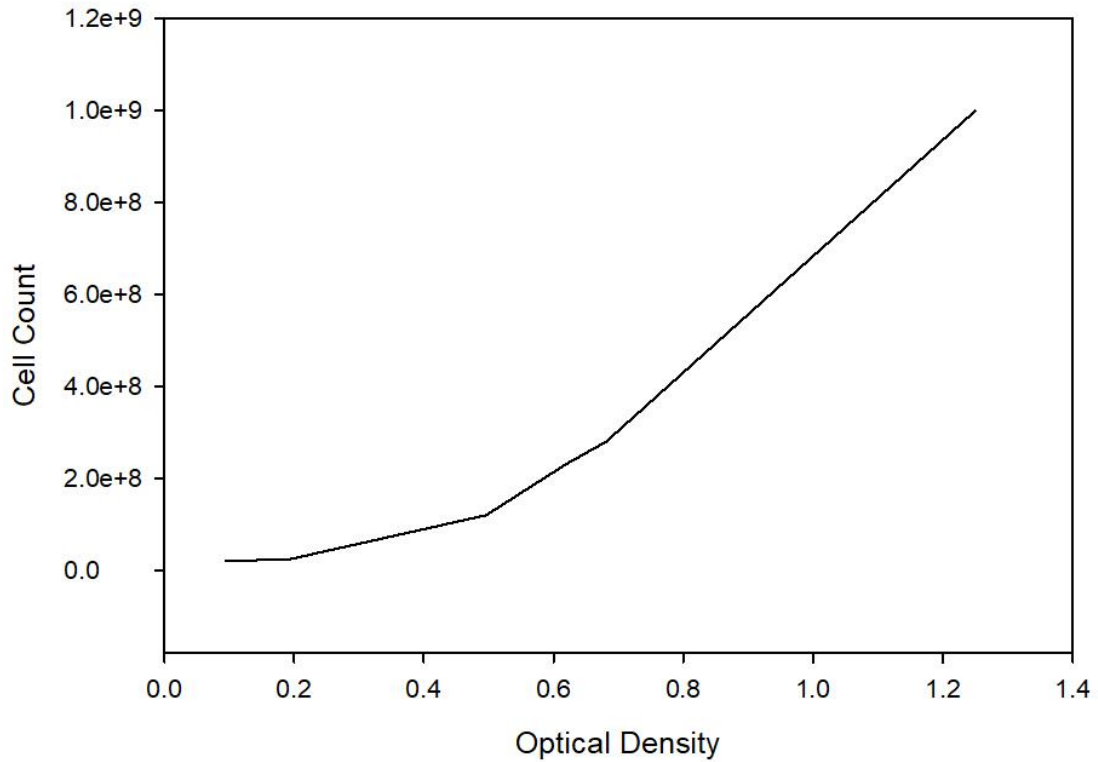


Figure A.1 Standard curve to estimate cell density given optical density.

Cells were in HM medium, and taken at different times to be able to assess the growth at different times, in order to find the log growth phase. Cells were counted using a hemocytometer.



Appendix B: VISUAL MINTEQ model of availability of selected nutrients within the full-N solution.

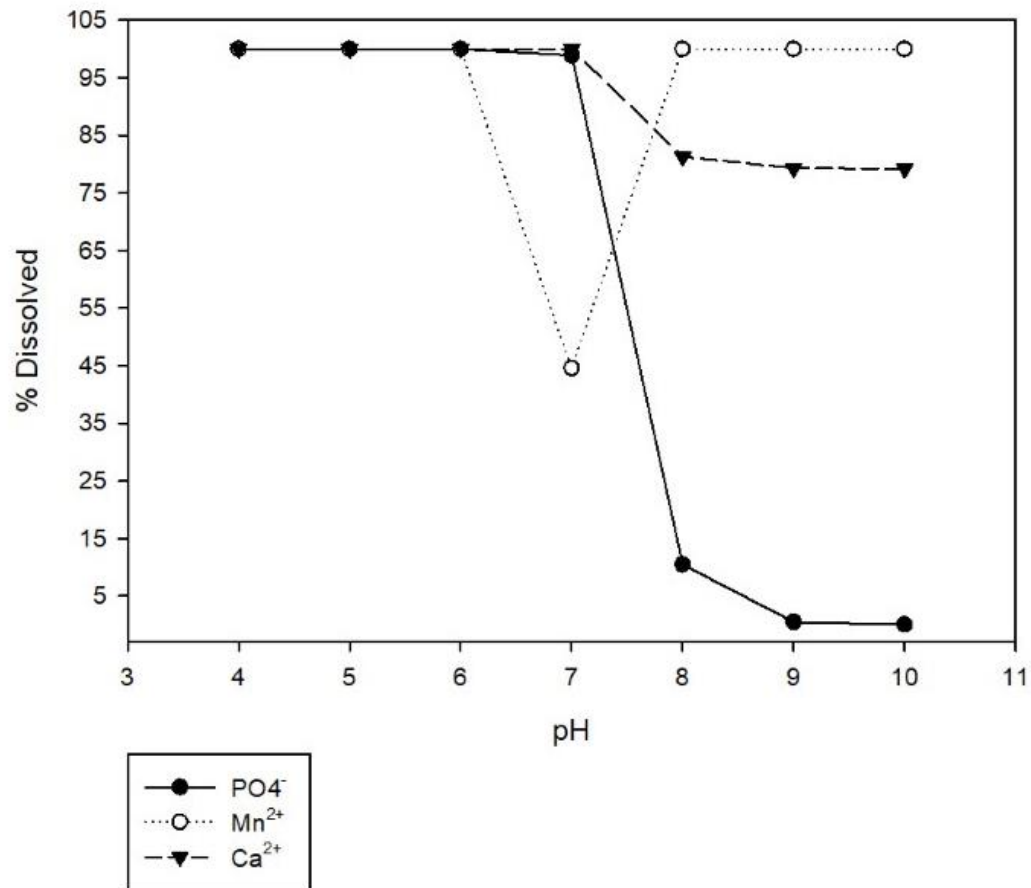


Figure B.1 Modelling the effect of pH on dissolved nutrients.

The whole biological pH range for the nutrient solution, low-N shows very similar chemical equilibria (not shown). Precipitant is hydroxyapatite, which was also modelled to dissociate into ions when pH was adjusted to < 7.4 pH, after equilibrium. Soybean growth acidified the solution, making all nutrients bioavailable during the experiment.

## Curriculum Vitae

**Name:** Paul Boersma

**Post-secondary Education and Degrees:** University of Western Ontario  
London, Ontario, Canada  
2015-2019 B.Sc. Honours. Spec. in Biology  
2019- In-progress - M.Sc in Biology

**Honours and Awards:** Deans honour roll  
2017-2018, 2018-2019

**Related Work Experience:** Teaching Assistant  
Department of Biology, the University of Western Ontario  
2019 – 2021

**Conference Presentations:** Ontario Biology Day Conference Poster and 5-min Talk  
2019 – Effects of Silver Nanoparticles on Soybean Growth and Nodulation

Canadian Society of Plant Biologists Conference Poster  
2021 - Silver and Symbiosis: Detrimental Effect of Silver Nanoparticles on Soybean (*Glycine max*) Symbiosis with *B. japonicum*

Canadian Society of Plant Biologists Conference 3-min Talk  
2021- Silver and Symbiosis: Detrimental Effect of Silver Nanoparticles on Soybean (*Glycine max*) Symbiosis with *B. japonicum*